

**The flux of ozone to a maize crop and the underlying
soil during a growing season**

CENTRALE LANDBOUWCATALOGUS



0000 0478 5966

Promotor: Dr. ir. L. Wartena
hoogleraar in de Meteorologie,

Co-promotor: Dr. ir. A.F.G. Jacobs
universitair hoofddocent Meteorologie

NN08201, 1479.

W.A.J. van Pul

The flux of ozone to a maize crop and the underlying soil during a growing season

Proefschrift

ter verkrijging van de graad van doctor
in de landbouw- en milieuwetenschappen,
op gezag van de rector magnificus,
dr. H.C. van der Plas,
in het openbaar te verdedigen
op woensdag 18 maart 1992
des namiddags te vier uur in de aula
van de Landbouwuniversiteit te Wageningen.

ian = 555812

40951

Voorwoord

Het onderzoek waarvan hier verslag wordt gedaan, is tot stand gekomen door een samenwerking tussen de vakgroep Meteorologie en de afdeling Milieuonderzoek van de KEMA. Bij de KEMA vormde dit onderzoek een onderdeel van een project dat als doel had, de effecten van luchtverontreinigende stoffen (met name ozon) op landbouwgewassen, te bestuderen. De eerste twee jaren maakte dit onderzoek deel uit van de eerste fase van het Nationaal Programma Verzuringsonderzoek (Project 72).

Vele mensen hebben bijgedragen tot het tot stand komen van dit proefschrift en ik wil hen hier dan ook graag bedanken.

Bert Wartena, mijn promotor, wil ik bedanken voor zijn energieke manier van begeleiden die mij zowel enthousiasmeerde als ook vaak aanleiding gaf tot fundamentele overpeinzingen aangaande de materie.

Adrie, A3, Jacobs, mijn co-promotor wil ik bedanken voor zijn amicale manier van begeleiden en ondersteunen. Vrijwel altijd vond ik bij jou een gewillig oor voor mijn theoretische en praktische problemen. Deze afronding neemt niet weg dat er nog een aantal zaken af te ronden zijn; nu de verhalen nog!

Ik wil de KEMA, met name Maria Janssen en Bert Elshout, bedanken voor de mogelijkheid die zij mij geboden hebben om dit onderzoek uit te voeren.

Zonder het maïsveld, geen onderzoek; het ICW (Winand Staring Centrum) bedankt voor het beschikbaar stellen van hun proefterrein 'de Sinderhoeve'.

Met name voor een relatief groot opgezet experimenteel onderzoek, zoals hier uitgevoerd is, geldt dat dit nooit zonder een immense praktische ondersteuning had kunnen plaatsvinden.

De Fijn-mechanische en Electronische werkplaatsen van de oude Vakgroep Natuur en Weerkunde van de LU ben ik zeer dankbaar voor hun inzet en waren altijd bereid iets op te zetten, af te breken, te repareren etc., met name Anton Jansen, Teun Jansen, Peter Jansen, Willy Hillen, Dick Welgraven, Kees van Asselt, Kees van den Dries.

Van de KEMA-zijde wou ik graag Peter Gamelkoorn, Rein de Vries (MMD) en Han van Duuren, Bertus van den Beld, Hans Jaspers en Wim de Bruin (MO), bedanken voor hun essentiële hulp bij het uitvoeren van de luchtverontreinigingsmetingen.

Een zeer belangrijk onderdeel van de hulp die ik tijdens de experimenten heb gehad werd gevormd door doctoraal studenten. Jeannette Beck, Alex Vermeulen, Ariën Stolk en Mark

- 1) Overdag kan de flux van ozon naar de droge bodem zo'n 20-50% uitmaken van de totale flux van ozon, gemeten boven een maïsgewas. (Leuning et al., Agricultural Meteorology 20, 1979, 115-135, Wesely et al., Boundary Layer Meteorology 15, 1978, 361-373, dit proefschrift.)
- 2) De toename van de oppervlakteweerstand voor ozon, bepaald uit metingen boven een maïsgewas aan het eind van de dag, wordt naast het sluiten van de huidmondjes mede bepaald door een verminderd transport van ozon naar de onderliggende bodem ten gevolge van de toenemende stabiliteit van de atmosfeer. (Dit proefschrift.)
- 3) De seizoensvariatie in de dagelijkse depositie van ozon naar een maïsgewas en de onderliggende bodem wordt voornamelijk veroorzaakt door de variatie in de concentratie van ozon. (Dit proefschrift.)
- 4) Voor de bepaling van de dagelijkse depositie van een luchtverontreinigende component met meteorologische technieken kan uit praktische overwegingen beter een profieltechniek dan de eddy-correlatietechniek worden gebruikt.
- 5) Bij het gebruik van de eddy-correlatietechniek voor het meten van de flux van een luchtverontreinigende component dient als controle de sluiting van de energiebalans, betrekking hebbende op de met de eddy-correlatietechniek gemeten voelbare en latente warmtestroom en de afzonderlijke gemeten beschikbare energie hiervoor, uitgevoerd te worden.
- 6) Doordat de niet-lokale uitwisselingsterm in het gewasstromingsmodel van Li et al. (Boundary Layer Meteorology 33, 1985, 77-83) onafhankelijk is van turbulentie, kunnen de experimenteel gevonden gelijkvormige windprofielen in het gewas bij verschillende windsnelheden niet worden gesimuleerd. (Van Pul en Van Boxel, Boundary Layer Meteorology 51, 1990, 313-315.)
- 7) Het effect van de verhoogde depositie van een luchtverontreinigende component aan de loefzijde van een bosrand is groter voor een langzaam deponerende component dan voor een snel deponerende component.

8) Het gebruik van het begrip menghoogte onder alle atmosferische omstandigheden in plaats van grenslaaghoogte leidt tot de misvatting dat alle grootheden tot deze hoogte ook goed gemengd zijn.

9) De door Businger (Journal of Climate and Applied Meteorology, 25, 1986, 1100-1124) getrokken conclusie, dat voor droge depositie metingen een completere beschrijving van de oppervlakte laag en de aangrenzende planetaire grenslaag nodig is, geeft aan dat het gebruik van de term micrometeorologische techniek in principe onjuist is.

10) De zon geeft vaak aanleiding tot schijn-verbanden.

11) De toxiciteit van een stof is positief gecorreleerd met de prijs van de analysemethode.

12) De op de Derde Internationale Noordzeeconferentie gemaakte afspraken aangaande de emissiebeperkende maatregelen van wel 50% of meer zonder een referentiepunt te noemen, geeft aan dat het milieuprobleem vaak nog niet au sérieux wordt genomen.

13) Het overvloedig gebruik van stoplichten leidt tot een slaafser weggebruik en uiteindelijk tot een onveiligere verkeerssituatie.

14) Voor het snel aangeven van gevoelens en stemmingen bieden BWV-nummers van vele Bach-cantates een ruime keuze.

Stellingen behorende bij het proefschrift van W.A.J. van Pul:

"The flux of ozone to a maize crop and the underlying soil during a growing season".

Wageningen, 18 maart 1992.

Kosters bedankt voor jullie werk!

En dan de man die niet bedankt wou worden, Paul van Espelo, BEDANKT!, voor je nimmer aflatende inzet de plaatjes en krabbeltjes van mij om te zetten in zeer fraai figuren die dit proefschrift sieren en niet te vergeten voor de omslag.

Ik bedank alle medewerkers van de vakgroep voor de zeer gezellige en leerzame periode die ik op de vakgroep heb doorgebracht. Met name mijn kamergenoten van het eerste uur, Niek Jan Bink en John van Boxel, bedank ik voor de vele tips en hulp die ik bij het opzetten van de experimenten van hen heb gehad; de latere kamergenoten: Hans Hakvoort waar ik vele discussies, meestal 'groen van aard' (wanneer is het oogstfeest ook alweer?), mee heb gehad and Rushdi El-Kilani, lets discuss some more crop modelling again!

A special thanks to Jordi Vilà-Guerau de Arellano (IMAU) who made modelruns with his model to support me with information about the influence of chemical reactions.

Frank de Leeuw (RIVM), bedankt voor je opmerkingen op het manuscript en het geduld.

Mevrouw de Wijs en Anje Andriessen (RIVM) wil ik bedanken voor hun correcties op het Engels en Nederlands, respectievelijk.

Ik mag me verheugen dat ik tijdens mijn promotietijd in een zeer gezellig huis heb gewoond, al aan de Hoogstraat in Wageningen. Zonder 'Centre Pom Pompidou' zou het leven een stuk onaangener zijn geweest!

Nou, Silke, het zit er op; wat een start; dank je wel!

Table of contents

List of symbols

<u>Chapter 1 Introduction</u>	1
<u>Chapter 2 Techniques used to determine the flux of ozone</u>	7
2.1 Scaling the equations that describe the concentration and flux of ozone	7
2.1.1 Mass conservation equation applied to reference volume 1	7
2.1.2 Mass conservation equation applied to reference volume 2	14
2.1.3 The local time derivative of the flux of ozone applied in reference volume 1	21
2.2 Conclusions	24
2.3 Measuring techniques	24
2.3.1 Eddy correlation technique	26
2.3.2 Gradient technique or profile technique	28
2.3.3 Bowen ratio technique	32
<u>Chapter 3 Experimental outline</u>	35
3.1 Site description	36
3.2 Sensors used in the experiments	39
3.2.1 Continuous measurements	39
3.2.2 Incidental measurements	46
3.3 Data acquisition and processing	48
3.3.1 Continuous measurements (slow-response signals)	48
3.3.2 Incidental measurements (fast-response signals)	51
3.3.3 Practical implications of using the eddy correlation technique	52
3.3.4 Corrections due to density fluctuations	55

3.4 Some environmental conditions and plant parameters	55
3.4.1 Plant parameters	55
3.4.2 Description of the soil	57
3.4.3 Water balance	57
<u>Chapter 4 Accuracy of the fluxes and comparison of the techniques</u>	63
4.1 Accuracy of the fluxes derived with the meteorological techniques	63
4.1.1 Profile and modified Bowen ratio technique	63
4.1.2 Eddy correlation technique	66
4.2 Uncertainty of the flux of ozone due to chemical reactions	67
4.3 Comparison of the meteorological techniques used	67
4.4 Conclusions	75
<u>Chapter 5 The resistance and conductance of a maize crop and bare soil to ozone</u>	77
5.1 Theoretical background of the resistance model used	77
5.2 The resistance of bare soil to ozone	84
5.2.1 Method of calculation	84
5.2.2 Results and discussion	84
5.3 The resistance and conductance of a maize crop and the underlying soil to ozone	86
5.3.1 Method of calculation	86
5.3.2 Data used and results	88
5.3.3 Discussion	90
5.3.4 Conclusions	94
<u>Chapter 6 Overview of the deposition of ozone and its governing factors during the growing season of maize in 1988</u>	105
6.1 Method of calculation	105
6.2 Results and discussion	107
6.3 Conclusions	113
<u>Chapter 7 Summary and recommendations</u>	115

<u>Samenvatting</u>	119
<u>References</u>	125
<u>Appendices</u>	133
Appendix A Stability functions used in the flux profile relationships	133
Appendix B Estimates and corrections of some terms in the energy balance of a maize crop and the underlying soil	134
Appendix C The damping of the concentration fluctuations due to sampling through a tube	136
Appendix D Laboratory experiments on the soil resistance to ozone	138
Appendix E The influence of chemical reactions on the flux of ozone	139
Appendix F The probable error method	143
Appendix G Estimates of the daytime deposition of ozone using idealized daily patterns of deposition velocity and concentration	145
<u>Curriculum vitae</u>	147

List of symbols

Symbol	description	units
A	available energy	W m^{-2}
B	resistance ratio	-
C_c	drag coefficient for the flux of O_3	-
C_d	drag coefficient for momentum	-
c_p	specific heat of air at constant pressure	$\text{J kg}^{-1} \text{K}^{-1}$
d	displacement height for momentum	m
d_s	displacement height for a scalar quantity	m
$D(x)$	molecular diffusion coefficient for x	$\text{m}^2 \text{s}^{-1}$
e_a	water vapour pressure of the air	mb
e_w	saturated water vapour pressure	mb
F_S	flux of O_3	$\mu\text{g m}^{-2} \text{s}^{-1}$
g	acceleration due to gravity	m s^{-1}
H_s	sensible heat flux	W m^{-2}
H_{cr}	crop height	m
h	boundary layer height	m
h_0	initial boundary layer height	m
$I_{t,d,m}$	integrals of the flux of O_3 over the total day, during daytime ($R_g > 0$) and between 1200-1600 GMT	mg m^{-2}
I_c	daily uptake of O_3 by the crop or dose during daytime	mg m^{-2}
I_{so}	daily destruction of O_3 at the soil during daytime	mg m^{-2}
K_x	eddy diffusion coefficient for x	$\text{m}^2 \text{s}^{-1}$
L	Obukhov stability length scale	m

LAI	one-sided leaf area index	$\text{m}^2 \text{ m}^{-2}$
LAD	one-sided leaf area distribution	$\text{m}^2 \text{ m}^{-3}$
LE	latent heat flux density	W m^{-2}
L_v	latent heat of vaporization	J kg^{-1}
p'	pressure fluctuations	N m^{-2}
P	atmospheric pressure	mb
Ph	energy used in the photosynthesis of maize crop per time unit per ground area	W m^{-2}
q	specific humidity	kg kg^{-1}
Q	chemical production and destruction of O_3	$\mu\text{g m}^{-3} \text{ s}^{-1}$
Q_n	net radiation density	W m^{-2}
r_{ac}	excess resistance due to difference in stability functions between momentum and a scalar	s m^{-1}
r_{as}	total resistance at z_{ref} to O_3	s m^{-1}
r_{am}	aerodynamic resistance at z_{ref}	s m^{-1}
r_b	resistance of the quasi laminar boundary layer	s m^{-1}
r_c	crop resistance to O_3	s m^{-1}
r_{exc}	excess surface resistance	s m^{-1}
r_{inc}	in-crop aerodynamic resistance	s m^{-1}
r_s	surface resistance to O_3	s m^{-1}
r_{sc}	resistance to O_3 in the layer from z_{ref} to d	s m^{-1}
r_{soil}	soil resistance to O_3	s m^{-1}
r_{stom}	stomatal resistance to O_3	s m^{-1}
$R_{1,2,3}$	reaction rates in the photochemical reactions of O_3	$\mu\text{g m}^{-3} \text{ s}^{-1}$
R_g	global radiation	W m^{-2}
R_v	specific gas constant for moist air	$\text{J kg}^{-1} \text{ K}^{-1}$

RC	time constant of the fast-response ozone monitor	s
s_*	turbulent scale of a scalar in units of that scalar	-
$S_{1,2,3}$	concentration of O_3 , NO_2 and NO	$\mu g\ m^{-3}$
$s'_{1,2,3}$	concentration fluctuations of O_3 , NO_2 and NO	$\mu g\ m^{-3}$
S^+_1	concentration of O_3 in the reservoir layer	$\mu g\ m^{-3}$
S_x	concentration of O_x	$\mu g\ m^{-3}$
$S_x(0)$	concentration of O_x in the boundary layer when $h = h_0$	$\mu g\ m^{-3}$
S_b	heat storage in the biomass per time unit per ground area	$W\ m^{-2}$
S_{so}	heat storage of the soil per time unit per ground area	$W\ m^{-2}$
t	time	s
T_d	dry bulb temperature	$^{\circ}C$
T_{leaf}	leaf temperature	$^{\circ}C$
T_w	wet bulb temperature	$^{\circ}C$
u_*	friction velocity	$m\ s^{-1}$
u', v', w'	wind velocity fluctuations in x,y,z direction	$m\ s^{-1}$
$\bar{U}, \bar{V}, \bar{W}$	mean wind velocity in x,y,z direction	$m\ s^{-1}$
V_c	crop conductance to O_3	$m\ s^{-1}$
V_d	deposition velocity of O_3	$m\ s^{-1}$
V_s	surface conductance to O_3	$m\ s^{-1}$
V_w	crop conductance to water vapour	$m\ s^{-1}$
$V_c(4)$	crop conductance to O_3 averaged between 1200-1600 GMT	$m\ s^{-1}$
$V_s(4)$	surface conductance to O_3 averaged between 1200-1600 GMT	$m\ s^{-1}$
V_{exc}	excess surface conductance to O_3	$m\ s^{-1}$
w_e	entrainment velocity	$m\ s^{-1}$

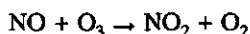
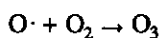
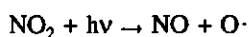
z_0	roughness length of the crop for momentum	m
z_s	roughness length of the crop for a scalar	m
z_{ref}	reference height in the resistance model	m
z_m	measurement height	m

Greek symbols

α	constant used in the Bowen ratio	$\text{kg m}^{-3} \text{K}^{-1}$
β	Bowen ratio	-
γ	temperature lapse rate in the reservoir layer	K m^{-1}
η	constant between λ and τ_a	mol m^{-3}
$\Phi_{m,s}$	dimensionless gradients of wind speed and scalars	-
Φ'	modified Φ function in the roughness layer	-
$\chi_{1,2,3}$	x,y,z direction	m
κ	von Karman's constant	-
λ	constant in the chemical reaction between NO and O ₃	$\text{mol m}^{-3} \text{s}$
ρ_a	density of dry air	kg m^{-3}
ρ_v	absolute humidity	kg m^{-3}
$\Psi_{m,s}$	integrated stability functions for wind speed and scalars	-
τ_a	time scale of the photolysis of NO ₂	s
τ_w	turbulence time scale	s
θ	potential temperature	K

Chapter 1 Introduction

Ozone (O_3) is a chemical component present in the troposphere and stratosphere. Ozone is formed both by natural processes and by processes influenced by anthropogenic activities. Within the troposphere ozone is formed during the photo-oxidation reactions of volatile organic compounds (VOC) in the presence of nitrogen dioxide (NO_2). The key reactions are summarized below.



The critical step in the ozone formation is the photolysis of nitrogen dioxide by sunlight at 300-410 nm. In this reaction a nitrogen oxide (NO) and an oxygen ($O\cdot$) atom are formed. The oxygen-atom recombines with molecular oxygen which results in the formation of ozone. The main chemical destruction route of ozone is the reaction with nitrogen oxide. In this reaction nitrogen dioxide is regenerated. The photolysis reaction and the reaction of nitrogen oxide with ozone are all very fast. Therefore, these three components are in equilibrium with each other, the so-called photostationary equilibrium. The reactions of the photostationary equilibrium do not lead to a net production of ozone. Production of ozone will occur when nitrogen oxide is oxidized to nitrogen dioxide without the consumption of ozone. These types of reactions are involved in the atmospheric oxidation cycle of VOC. The temporal and spatial scale on which VOC contributes to ozone production depends on their reactivity. Less reactive compounds such as carbon oxide (CO) and methane (CH_4) play a role on the global scale and contribute to the long-term average background concentration of ozone. On the continental scale the more reactive VOC lead rapidly to ozone formation. Under special meteorological conditions (sunny days, high temperature, stagnating weather type) so-called smog episodes with very high ozone concentrations can occur.

Processes determining ozone at ground level are photochemical production within the boundary layer, dry deposition (destruction at the earth's surface) and vertical exchange with

layers above the boundary layer. Ozone is a very strong oxidizer and as such is destroyed rapidly at various surfaces, for example, vegetation and materials. Dry deposition accounts for about 30% of the loss of ozone in the total tropospheric ozone budget (Sloof et al., 1987). Caused by the development of the boundary layer during the day an exchange of ozone takes place at the top of that layer with the so-called aged smog or reservoir layer. Also, other meteorological phenomena (such as frontal systems, transport in convective cells) on a larger scale cause exchange of ozone between the boundary layer and the free troposphere. Builtjes (1989) gives a review of these processes.

The increase in anthropogenic emissions of nitrogen oxides, carbon oxide, methane and VOCs have caused an increase of the concentration of ozone of 1% per year in the last two decades in large parts of the Northern Hemisphere (Bojkov, 1988).

The damage to plants by ozone is described extensively in the literature (Heck et al., 1982; Krupa and Manning, 1988; Van der Eerden et al., 1988). Ozone enters the leaves mainly via the stomata where it causes the greatest effects (Rich et al., 1970; Heath et al., 1975).

At high levels, ozone can have acute effects such as necrosis and chlorosis (Tingey and Taylor, 1982). At ambient levels, ozone can in the long term, cause a reduction in the yield of agricultural crops (Heck et al., 1982; Tonneijck, 1988; Van der Eerden et al., 1988). Assessments made for agricultural crops in the Netherlands by Van der Eerden et al. showed a reduction in the crop volume of 5%, of which 70% was caused by ozone.

To observe the effects of ozone on plants several types of experimental set-ups are used in which plants are exposed for a certain time to a certain quantity of ozone (e.g. open-top chambers (Mandl et al., 1973) and open-air fumigation systems (McLeod et al., 1985)). These experiments are mostly carried out for short exposure or fumigation periods, varying from several hours to several weeks at relatively high levels of ozone. The experimental facilities differ mainly in the level of control of the environmental growth parameters.

The effects of ozone in these studies are coupled with the dose which the plants receive, defined as the concentration times the fumigation time, leading to so-called dose-response relationships (Tonneijck, 1988). Because the plants are grown under controlled conditions, this dose is correlated with a certain uptake of ozone by the stomata of the plants. In some laboratory experiments, the mass balance of ozone is calculated to obtain the real uptake of ozone by the plants (Aben, 1990).

It is difficult to translate the results of these experiments towards crops growing under field conditions. Generally, crops are grown during much longer periods in which the environmental conditions and the concentration of ozone are strongly varying (Kruppa and Nosal, 1989). Under these field conditions it is not *a priori* possible to couple the uptake of ozone by the crop or the effects of ozone on the crop to the concentration or dose of ozone. To assess this uptake one has to measure or model the transport or flux of ozone to the crop.

The flux of ozone towards the crop under field conditions can be measured using meteorological techniques (Leuning et al., 1979a,b; Wesely et al., 1978; Delany et al., 1986). These techniques are used to quantify the turbulent fluxes of momentum, heat or air pollution above a surface. As such they are widely used in dry deposition studies of air pollution components (e.g. Hicks, 1986). These techniques can only be applied under certain meteorological conditions. Many authors have pointed out that these measuring techniques can produce fluxes with large errors if these conditions are not fulfilled (Garratt, 1980; Businger, 1986; Wyngaard, 1988). An advantage of these techniques is that a value is obtained which is representative for a rather large area.

Using these meteorological techniques the total flux of ozone towards the surface, i.e. the crop and the underlying soil is measured. Information on the partitioning of the flux into a flux to the crop and a flux to the soil is not obtained. Because of the complex turbulent flow in the crop and the special sensor requirements needed, the meteorological techniques are rarely used in the crop to measure the flux towards the soil or lower plant parts.

Often resistance models are used to evaluate these meteorological flux measurements above a surface (e.g. Thom, 1975). In these models the transport process of the component from a certain height to a surface is parameterized with a chain of resistances. The resistances are defined as the driving force divided by the flux (density) of the component, as in an electrical circuit. Here the driving force is the difference of the component over this height. By measuring the vertical profile and the flux of the component, the resistances to the transport can be revealed.

A very simple resistance model is the so-called Big leaf model (e.g. Fowler, 1978; Baldocchi et al., 1987). In this model the vertical dimension of the crop is neglected and the model does not distinguish between a flux to the crop or the soil. From this type of model, the so-called

surface resistance can be deduced, which is, in principle, only dependent on the properties of the surface and the component. However, due to the simplification of the surface, this resistance is also dependent on the flow features in the vegetation.

An estimate on the above-mentioned partitioning of the flux of ozone derived from concurrent measurements of the concentration and flux of ozone and water vapour can be made using such a resistance model (Wesely et al., 1978). In this estimate the analogy is used between the transport of ozone and water vapour towards and in the stomata. Following this approach Wesely et al. concluded that on two days 20-50% of the total flux of ozone measured above a maize crop was to the soil and lower plant parts. Leuning et al.(1979a) made assessments for the uptake of ozone by a maize crop during a growing season using flux and porometer measurements and found that 50-70% of the flux of ozone had entered the leaves via the stomata.

No large data sets exist on flux measurements of ozone and water vapour throughout a growing season of a crop and consequently, no indications of this partitioning throughout the growing season are known.

In air pollution models describing or forecasting the concentration of ozone over an area the deposition of ozone as well is described using such a Big leaf resistance model (Wesely, 1989; Hicks et al., 1991). Here, the resistance of the surface is needed as input in the model. To model this surface resistance correctly both the resistance of the crop and the soil to ozone have to be incorporated in the total surface resistance.

The goals of this study

1) To measure the flux of ozone towards a maize crop during a growing season using meteorological techniques. Three techniques were used to check on the performance of the techniques and to decide which technique was the most suitable for the continuous measurement of the flux of ozone.

2) To determine the partitioning of the measured flux of ozone into a flux to the crop and the soil.

3) To assess the total daily integrals of the fluxes or daily deposition of ozone and its partitioning into a flux to the crop and the soil during the growing season.

In order to reach these goals measurements were carried out during the growing season of maize in 1988. Maize is the second most important agricultural crop in the Netherlands, covering about 10% of the agricultural area (CBS, 1991).

Outline of the thesis

A description of the meteorological techniques and the atmospheric conditions under which they have to be used, are given in chapter 2. Chapter 3 presents the experimental outline in which the sensors used in the measurements and the experimental set-up are given. Moreover, several environmental and crop conditions are summarized. Chapter 4 describes the accuracy of and a comparison among the three meteorological techniques. In chapter 5 the surface resistances to ozone are determined for the crop and soil. A comparison is made between the surface conductance to ozone and the crop conductance to ozone, based on the transpiration of the crop. This results in a partitioning of the flux of ozone to the crop and the soil. Chapter 6 presents an overview of the daily deposition of ozone and its governing factors. As well, assessments of the deposition based on these factors are given. The method described in chapter 5 is used to determine the partitioning of the flux of ozone to the crop and soil. Finally, chapter 7 summarizes the thesis and presents some recommendations.

Chapter 2 Techniques used to determine the flux of ozone

In this chapter the measuring techniques used to quantify the flux of ozone under field conditions are described. These techniques are commonly used in dry deposition studies (e.g. Businger, 1986; Hicks, 1986) and are based on the theory of the turbulent flow of the atmospheric boundary layer. They are originally used to calculate flux densities of momentum, heat and water vapour. This theory can be applied to any scalar quantity in the analogy of heat and water vapour (e.g. Monin and Yaglom, 1971; Thom, 1975). From various experiments evidence has been obtained that this theory is also valid for scalar quantities, like ozone i.e. they are transported in roughly the same way by turbulence as temperature (sensible heat) or humidity is (e.g. Droppo 1985; Zeller et al., 1989).

In applying these techniques one should keep in mind that they are based on theory, which is only valid under certain conditions. If these conditions are not met this will lead to serious errors in the estimated flux or deposition. For this reason some theoretical considerations are given in section 2.1 on the processes determining the concentration and the flux of ozone in the atmospheric boundary layer. From these considerations it can be seen under which circumstances the measurements of the flux are in error. Besides this, estimations on the deviation from the real flux are given. This is done by scaling the mass conservation equation for ozone for two reference volumes (section 2.1.1 and 2.1.2 respectively). In section 2.1.3 the time evolution of the flux of ozone is analysed in one reference volume and some qualitative results are given. In section 2.2 the conclusions which are relevant for these experiments are given.

Finally, section 2.3 describes the measuring techniques used in this study.

2.1 Scaling the equations that describe the concentration and flux of ozone

2.1.1 Mass conservation equation applied to reference volume 1

The conservation of the concentration of ozone in a certain volume, taking the mean wind

flow along the x direction, is given by:

$$\frac{\partial \bar{S}_1}{\partial t} + \bar{U} \frac{\partial \bar{S}_1}{\partial x} + \frac{\partial \bar{u}'s_1'}{\partial x} + \frac{\partial \bar{v}'s_1'}{\partial y} + \bar{W} \frac{\partial \bar{S}_1}{\partial z} + \frac{\partial \bar{w}'s_1'}{\partial z} - D \frac{\partial^2 \bar{S}_1}{\partial x_i \partial x_i} = \bar{Q} \quad 2.1.1$$

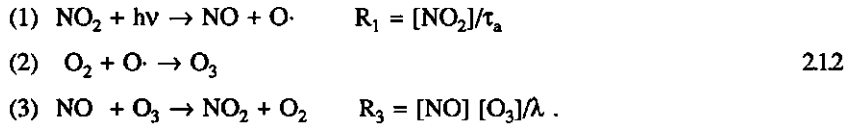
Here we have used Reynolds decomposition of the variables, which means that a variable, x , can be written as the sum of the mean of the variable, \bar{X} , and the fluctuations around this mean, x' , in a certain averaging time or : $x = \bar{X} + x'$. The bar indicates the averaging in time. The 'i' indicates the directions x,y,z of a Cartesian coordinate system, where $i=1,2,3$. U,V,W are the wind speeds in these three directions in $m s^{-1}$, and where we have taken $\bar{V} = 0$.

$S_{1,2,3}$ is the concentration of $[O_3]$, $[NO_2]$ and $[NO]$, ($\mu g m^{-3}$),

D is the molecular diffusion coefficient for ozone ($m^2 s^{-1}$) and

Q is the sum of the sources and sinks of ozone ($\mu g m^{-3} s^{-1}$).

As sources or sinks of ozone we will consider here the main chemical reactions that produce or destroy ozone :



R_1 is the reaction rate of reaction 1 with a reaction constant of $1/\tau_a$. The reaction constant $1/\tau_a$ depends on the solar radiation density and is, among other things dependent on the turbidity of the air, the zenith angle and the presence of clouds. Bahe (1980) derived a simple parameterization for this reaction constant, which is solely dependent on the global radiation. Here we use a typical value for $\tau_a = 250$ s. R_3 is the reaction rate of reaction 3 with a reaction constant of $1/\lambda$ and is rather well-known, $\lambda = 6.75 \cdot 10^{13} \text{ molec } m^{-3} s$ or 2500 ppb s (Fitzjarrald and Lenschow, 1983).

Reaction 2 is much more rapid than the other reactions and so the net production or destruction of ozone can be written as:

$$\bar{Q} = \bar{R}_1 - \bar{R}_3 \quad 2.1.3$$

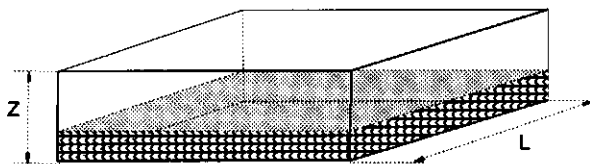


Figure 2.1 Reference volume 1. Box over a field of maize extending to the height, Z.

If the three components form the so-called photostationary equilibrium, $\bar{Q} = 0$.

Splitting the concentrations into a mean and a fluctuating part, term \bar{Q} can be written as:

$$\bar{Q} = \frac{[\overline{NO_2}]}{\tau_a} - \frac{[\overline{NO}][\overline{O_3}]}{\lambda} - \frac{[\overline{NO}][\overline{O_3}]}{\lambda} . \quad 2.1.4$$

Let us consider equation 2.1 in a volume as shown in figure 2.1 and define some characteristic scales along with typical values (see Table 2.1).

Table 2.1 Characteristic scales and typical values used in scaling of the conservation equation of the concentration of ozone.

Characteristic scale	Symbol	Typical value
Concentration scales for O_3 , NO_2 and NO , respectively	C_1, C_2, C_3	100, 40, 10 $\mu g m^{-3}$
Concentration fluctuation scales for O_3 , NO_2 and NO , respectively	c_1, c_2, c_3	4 $\mu g m^{-3}$
Concentration difference scales for O_3 in x and z direction	$\Delta c_x, \Delta c_z$	2, 100 $\mu g m^{-3}$
Time scale of the mean concentration changes of O_3	t	10000 s
Mean wind speed scales of U and W	V_1, V_3	5 $m s^{-1}$, 0.1 $cm s^{-1}$
Wind fluctuation scales in x,y and z direction	v_1, v_2, v_3	2, 2, 1 $m s^{-1}$
Length scales in the x,y and z direction	L, B, Z	200, 200, 4 m
Molecular diffusion coefficient for O_3	D	1.4 $10^{-5} m^2 s^{-1}$

For every variable, a, of equation 2.1 we can write:

$\hat{a} = a/A$, where A is the scale of variable a.

Equation 2.1.1 combined with 2.1.4 can then be rewritten as:

$$\begin{aligned}
 & \underbrace{\frac{C_1}{t} \left[\frac{\partial \bar{s}_1}{\partial \bar{t}} \right]}_{\text{I}} + \underbrace{\frac{\Delta c_x V_1}{L} \left[\bar{U} \frac{\partial \bar{s}_1}{\partial \bar{x}} \right]}_{\text{II}} + \underbrace{\frac{\Delta c_z V_3}{Z} \left[\bar{W} \frac{\partial \bar{s}_1}{\partial \bar{z}} \right]}_{\text{III}} + \underbrace{\frac{v_1 c_1}{L} \left[\frac{\partial \bar{a}' s_1'}{\partial \bar{x}} \right]}_{\text{IV}} + \underbrace{\frac{v_2 c_1}{B} \left[\frac{\partial \bar{y}' s_1'}{\partial \bar{y}} \right]}_{\text{V}} + \\
 & \underbrace{\frac{v_3 c_1}{Z} \left[\frac{\partial \bar{w}' s_1'}{\partial \bar{z}} \right]}_{\text{VI}} + \underbrace{\frac{C_1 D}{Z^2} \left[\frac{\partial^2 \bar{s}_1}{\partial \bar{x}_i^2} \right]}_{\text{VII}} = \underbrace{\frac{C_2}{\tau_a} [\bar{s}_2]}_{\text{VIII}} - \frac{C_1 C_3}{\lambda} [\bar{s}_1 \bar{s}_3] - \frac{c_1 c_3}{\lambda} [\bar{s}_1' \bar{s}_3'] . \quad 2.1.5
 \end{aligned}$$

Note that all factors in brackets are dimensionless and have values in the order of unity.

Because we want to know whether our measurements of the flux of ozone at a certain measurement level differ from the flux of ozone at the surface, we will investigate the relative importance of the terms in equation 2.1.5 compared to the turbulence convection term, the sixth term of the equation. Equation 2.1.5 is divided by the 'turbulence mass convection scale' $v_3 c_1 / Z$, this leads to an equation in which all terms are dimensionless. If we use the typical values from table 2.1, typical values for the dimensionless factors can be derived for our problem:

I local time derivative

$$\frac{Z C_1}{t v_3 c_1} = 0.01$$

II advection by mean flow

$$\frac{ZV_1 \Delta c_x}{Lv_3 c_1} = 0.05$$

III convection by mean flow

$$\frac{V_3 \Delta c_z}{v_3 c_1} = 0.025$$

IV+V advection by turbulence

$$\frac{Zv_1}{Lv_3} = 0.04 \quad , \quad \frac{Zv_2}{Bv_3} = 0.04$$

VI convection by turbulence

1

VII molecular diffusion

$$\frac{C_1 D}{v_3 c_1 Z} = 0.0001$$

Term VIII a,b,c chemical reactions

$$\frac{ZC_2}{\tau_a v_3 c_1} - \frac{ZC_1 C_3}{\lambda v_3 c_1} - \frac{Zc_3}{\lambda v_3} = 0.16 - 0.32 - 0.0051 = -0.16 \quad .$$

The magnitude of the chemical reaction term is very sensitive to the choice of the concentration levels of the three components and whether they are in photostationary equilibrium or not. As a maximal estimate of this term we will take here the production term

$$R_1 = [\text{NO}_2]/\tau_a.$$

We see that besides the chemical reactions, all other terms are at least one order of magnitude smaller than the convection by turbulence. Therefore, as an approximation equation 2.1.1 is reduced to:

$$\frac{\partial \overline{w's_1'}}{\partial z} = \frac{\overline{[NO_2]}}{\tau_a} \quad 2.1.6$$

Equation 2.1.6 can be integrated with respect to height from the surface, $z = 0$, to the measurement level, z_m :

$$\left[\overline{w's_1'} \right]_{z_m} - \left[\overline{w's_1'} \right]_0 = \int_0^{z_m} \overline{Q} \, dz \quad 2.1.7$$

Positive as well as negative gradients of the vertical profiles of the concentration of nitrogen dioxide were observed above the soil and maize crop. As a worst-case analysis we will consider a concentration profile of nitrogen dioxide which is constant with height (In fact, generally a net deposition of nitrogen dioxide was observed and so a small mean positive gradient was present, but was less pronounced than for ozone). If we use this constant profile in equation 2.1.7, we get:

$$\int_0^{z_m} \overline{Q} \, dz = \frac{1}{\tau_a} \int_0^{z_m} \overline{[NO_2]} \, dz = \frac{1}{\tau_a} \overline{[NO_2]}_{z_m} z_m \quad 2.1.8$$

If the deposition velocity at z_m is used, as defined by (Chamberlain, 1953):

$$V_d(z_m) = \frac{\overline{w's_1'}}{\overline{S_1}(z_m)} \quad 2.1.9$$

equation 2.1.7 can be written as:

$$V_d(z_m) - \frac{\left[\overline{w's_1'} \right]_0}{\overline{S_1}(z_m)} = 0.13 z_m \frac{1}{\tau_a} \frac{\overline{[NO_2]}(z_m)}{\overline{S_1}(z_m)} \quad 2.1.10$$

which indicates the difference between the measured deposition velocity and the deposition velocity without the influence of chemical reactions.

Now some quantitative estimates can be made about the difference between the measured flux of ozone at height, z_m , and the flux of ozone at the surface. For ozone a deposition velocity of 0.5 cm s^{-1} is often observed. The error in the measured flux would be smaller than 10%

if $[\text{NO}_2] < 0.03 [\text{O}_3]$. The latter restriction is hardly fulfilled, even in rural areas, without local sources of nitrogen oxides and so chemical reactions could, at first hand, not be neglected in the analysis of the measurements of the flux of ozone. For an exact consideration of the influence of the chemical reactions on the flux of ozone, the set of equations describing the flux divergence of ozone and nitrogen oxides, and the chemical reactions, have to be solved numerically (Fitzjarrald and Lenschow, 1983; Kramm, 1989).

The advection and convection of ozone by the mean flow are relatively small in this scaling exercise; however, some remarks on these terms have to be made.

A small mean vertical wind velocity, \bar{W} at z_m , occurs due to density fluctuations of the air caused by a sensible and latent heat flux at the surface. Because of these fluxes less dense air rises from the surface while colder or more dense air descends. Under the assumption that no vertical mass flow of air is present a mean positive vertical wind velocity must exist. This \bar{W} is typically about 0.1 cm s^{-1} and cannot be derived from the measurements. Webb et al. (1980), give an extensive discussion on this matter and give practical formulations to calculate this \bar{W} (see also chapter 3). No correction for this phenomenon has to be made if the quantity is measured as a specific quantity. This means that if the quantity is measured at a constant temperature and in dry air or in air with a constant specific humidity, the density fluctuations are excluded from the measurements of that quantity.

The significance of the dimensionless horizontal advection term can be elaborated by rewriting it as:

$$\frac{Z}{L} \left[\frac{v_3}{V_1} \right]^{-1} \frac{\Delta c_x}{c_1} = \frac{Z}{L} \frac{1}{\sqrt{C_d}} \frac{\Delta c_x}{c_1} = \frac{Z}{L} \frac{1}{C_c} \frac{\Delta c_x}{\Delta c_z} ; \quad 2.1.11$$

where we have used bulk formulations for C_d and C_c as follows:

$$C_d = \left[\frac{v_3}{V_1} \right]^2 , \quad C_c = \frac{v_3 c_1}{V_1 \Delta c_z} .$$

The first dimensionless ratio of the third term in 2.1.11, Z/L , is the reciprocal of the often used fetch-to-(measurement) height ratio. The fetch-to-height ratio in this scaling was 50:1.

The second dimensionless term, $1/C_d$, is the reciprocal of a drag coefficient for the flux of ozone. This drag coefficient is dependent on properties of the surface such as the level at which the ozone is destroyed in which the aerodynamic roughness is incorporated. This drag coefficient is also dependent on the thermal stratification of the air flow.

The third dimensionless term indicates the ratio of typical horizontal and vertical concentration gradients. This ratio is, among other things, dependent on the strength of the sink of ozone of the surface above which the measurements are carried out and that of the upwind surface.

From this exercise it can be inferred that if the horizontal advection does not seriously affect the measurements of the flux, not only should the fetch-to-height ratio be large, but other properties of the surface and the upwind surface should be taken into account as well. This is one of the reasons why there is confusing information in the literature about an appropriate fetch-to-height ratio under which circumstances no influence of advection would occur.

Pasquill (1972) showed that the fetch should be at least 100 times the measurement height, this is an often used restriction.

When the upwind terrain is smoother than the observed terrain the flow adjusts more rapidly, and the fetch-to-height ratio requirement can be relaxed to 30:1 (Gash, 1986). Lindroth (1984) and Heilman et al. (1989) found in their experiments that this ratio could be reduced to even 20:1.

Also, the stability of the air flow is of importance to the adjustment of the exchange processes above the surface. This is expressed in the reverse dependency of the dimensionless horizontal advection term on the drag coefficients. When, for instance, the stability of the air flow increases the drag coefficients will decrease and the importance of the advection will increase.

2.1.2 Mass conservation equation applied to reference volume 2

The same reasoning as in section 2.1.1 can be applied to a reference volume which represents the whole atmospheric boundary layer in order to get some insight into the relative importance of the various processes which determine the concentration and flux of ozone. The reference volume is illustrated in figure 2.2. The same characteristic scales are used as in the previous section but some other typical values of these scales are used as indicated below:

L, B, the horizontal length scales: typical value 10000 m,

H, the vertical „ „ „ „ 1000 m, i.e. the boundary layer height,

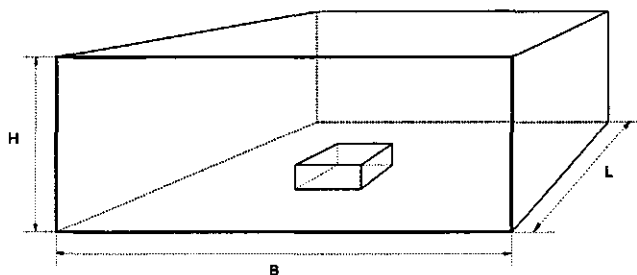


Figure 2.2 Reference volume 2. Box over an area of 10x10 km extending to the boundary layer height. Reference volume 1 is also drawn in this box.

Δc_x , the horizontal concentration gradient scale: typical value $4 \mu\text{g m}^{-3}$.

For this reference volume the same approach is followed as in the previous section, resulting in the following dimensionless numbers and their values:

I local time derivative

$$\frac{C_1 H}{t v_3 c_1} = 2.5$$

II advection by mean flow

$$\frac{\Delta c_x V_1 H}{L v_3 c_1} = 0.5$$

III convection by mean flow

$$\frac{\Delta c_z V_3}{v_3 c_1} = 0.025$$

IV+V advection by turbulence

$$\frac{H v_1}{L v_3} = 0.2 \quad , \quad \frac{H v_2}{B v_3} = 0.2$$

VI convection by turbulence

VII molecular diffusion

$$\frac{C_1 D}{H v_3 c_1} = 3.5 \cdot 10^{-7}$$

VIII a,b,c chemical reactions

$$\frac{C_2 H}{\tau_a v_3 c_1} - \frac{C_1 C_3 H}{\lambda v_3 c_1} - \frac{H c_3}{\lambda v_3} = 40 - 80 - 1.8 = -42$$

Again it should be emphasized that the scaling of the chemical reaction term is arbitrary, however, it remains a very important term. This can be illustrated by the fact that if only the accuracy in the concentration of nitrogen dioxide is considered in VII, i.e. about $1 \mu\text{g m}^{-3}$, as the deviation from its photostationary equilibrium value, it still remains one of the most important terms, being in the order of 1.

In the scaling only the molecular diffusion term is very small compared to the other terms. Furthermore it can be seen that convection by turbulence, local time derivative and the chemical reactions are the most important terms.

As an example let us consider equation 2.1.1 in the reference volume with the assumption that these three terms are dominant. Equation 2.1.1 is then reduced to:

$$\frac{\partial \bar{S}_1}{\partial t} + \frac{\partial \bar{w}'s_1'}{\partial z} = \bar{Q} \quad 2.1.12$$

The solution to this equation depends heavily on the choice of the vertical profiles of the concentration of ozone and nitrogen oxides and cannot easily be solved analytically.

A solution of 2.1.12 for the special case of a non-reactive component is given. As a non-reactive component the sum of the concentration of ozone and nitrogen dioxide, the total oxidant, O_x , (in the equations denoted with S_x) is taken. Let us consider a boundary layer driven mainly by convection. This means that all variables are rather well mixed throughout the boundary layer, resulting in profiles independent of height, z .

Integration of 2.1.12 over the boundary layer height, h , leads to:

$$\bar{h} \frac{\partial \bar{S}_x}{\partial t} + \left[\overline{w' s_x'} \right]_{\bar{h}} - \left[\overline{w' s_x'} \right]_0 = 0 \quad . \quad 2.1.13$$

A solution to 2.1.13 can be given using a slab model of the mixed layer as described by Tennekes (1973a). Here we assume no temperature jump at the top of the mixed layer. The layer above the mixed layer, the reservoir layer, has a potential temperature lapse rate, γ and a zero gradient concentration profile. The entrainment of warmer air into the mixed layer is parameterized as a fraction, a , of the surface sensible heat flux, $[\overline{w'\theta'}]_0$, here taken 0.2 (Driedonks, 1981).

The growth of the boundary layer or the entrainment velocity, w_e , can then be written as:

$$w_e = \frac{\partial \bar{h}}{\partial t} = \frac{(1+a) [\overline{w'\theta'}]_0}{\gamma \bar{h}} \quad . \quad 2.1.14$$

The entrainment flux of the component at the top of the boundary layer can be parameterized as (Stull, 1988):

$$\left[\overline{w' s_x'} \right]_{\bar{h}} = w_e (\bar{S}_x - S_x^+) \quad , \quad 2.1.15$$

where S_x^+ is the concentration of the component in the reservoir layer.

The flux of the component at the surface is parameterized as:

$$\left[\overline{w' s_x'} \right]_0 = -V_d(z_m) \bar{S}_x \quad . \quad 2.1.16$$

Using equation 2.1.15 and 2.1.16, equation 2.1.13 can be rewritten as:

$$\frac{\partial \bar{S}_x}{\partial t} + \frac{V_d \bar{S}_x}{\bar{h}} + \frac{\partial \bar{h}}{\partial t} \frac{(\bar{S}_x - S_x^+)}{\bar{h}} = 0 \quad . \quad 2.1.17$$

With equation 2.1.14, equation 2.1.17 can be rewritten and solved:

$$\bar{S}_x = \frac{S_x(0) h_0}{\bar{h}} e^{-\frac{V_d (\bar{h} - h_0)}{w_e \bar{h}}} - \frac{S_x^*}{V_d / w_e} \left[e^{-\frac{V_d (\bar{h} - h_0)}{w_e \bar{h}}} - 1 \right], \quad 2.1.18$$

where $S_1(0)$ is the concentration in the boundary layer at $t=0$ and h_0 is the initial boundary layer height at $t=0$ i.e. the time the boundary layer starts growing caused by convection.

In the early morning hours when $V_d / w_e \rightarrow 0$, equation 2.1.18 is reduced to:

$$\bar{S}_x = S_x^* + (S_x(0) - S_x^*) \frac{h_0}{\bar{h}}. \quad 2.1.19$$

In figure 2.3a an example of a diurnal course of measured oxidant and ozone and in figure 2.3b the sensible heat flux and the mixing height modelled with equation 2.1.14 are given. The sensible heat flux was taken from measurements made above a maize crop (see section 3). The initial boundary layer height and the temperature lapse rate were estimated from radiosondes released at De Bilt at 0000 and 1200 GMT. In figure 2.4 the oxidant distribution over the Netherlands for four time steps on August 14, 1988 is given. From this figure the advection of oxidant was estimated at about $0.002 \mu\text{g m}^{-3} \text{s}^{-1}$. In figure 2.3a we see a rapid increase of the oxidant concentration from 0800 till 1400 h (local time) at a more-or-less constant rate of $20 \mu\text{g m}^{-3} \text{s}^{-1}$. Part of this increase was caused by the advection but could only account for about 15% of this increase. This means that the main contribution was caused by the entrainment of oxidant from the reservoir layer (often called fumigation). Due to the almost linear increase of the sensible heat flux in this time period, the mixing height increased linearly in time as well. In the period from 0800 till 1400 h (local time) this leads to a linear increase of the oxidant concentration and is well described by equation 2.1.19. From the radiosonde it was inferred that the mixing height at 1200 GMT (1400 local time) was about 1400 m. At that level a strong temperature jump was present and no further calculations with the use of equation 2.1.14 were made. From about 1400 h (local time) the growth was much smaller and the fumigation process ceased which can be clearly seen in figure 2.3a by the relative constant oxidant concentration up to 1800 h (local time). From then on a shallow stable boundary layer formed in which the oxidant was mainly removed by dry deposition.

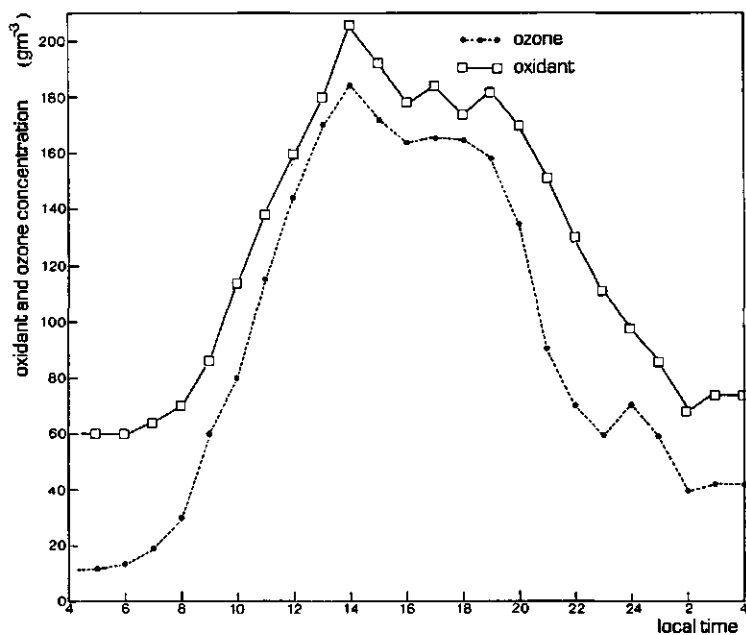


Figure 2.3a Concentration of oxidant and ozone on August 14, 1988.

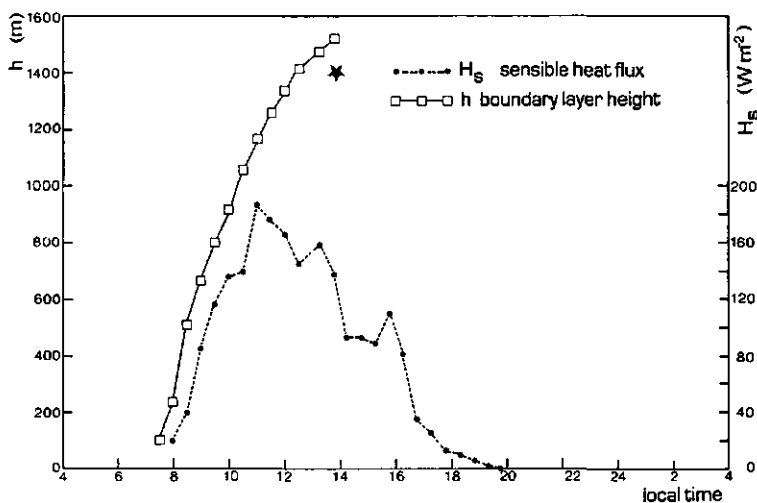


Figure 2.3b Sensible heat flux and modelled boundary layer height on August 14, 1988. A radiosonde observation of the boundary layer height is starred.

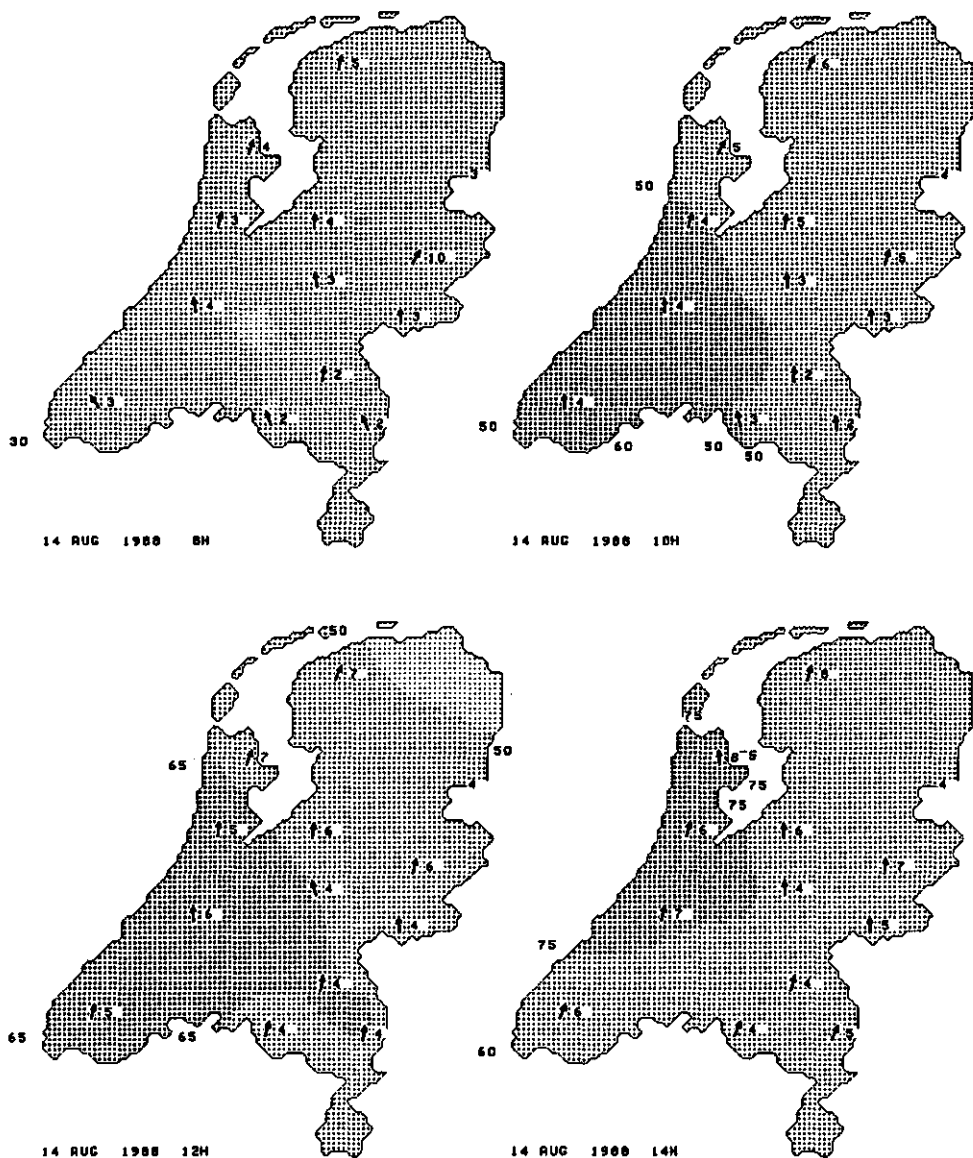


Figure 2.4 The concentration of oxidant for four points in time on August 14, 1988. The numbers outside the borders of each map indicate the values of the isopleths in ppb ($\approx 2 \mu\text{g m}^{-3}$). The arrowed numbers indicate the wind velocity. (Data from National Institute of Public Health and Environmental Protection (RIVM), Netherlands).

The influence on the measured flux of a component at the surface by the entrainment of air from the reservoir layer into the convective boundary layer was demonstrated by Wyngaard (1984). He assumed that the vertical gradient, $\partial S_x / \partial z$, will not change in time or $\partial(\partial S_x / \partial z) / \partial t = 0$. This can be written as $\partial(\partial S_x / \partial t) / \partial z = 0$. Using equation 2.1.12, this becomes:

$$\frac{\partial^2 \overline{w' s_x'}}{\partial z^2} = 0 \quad . \quad 2.1.20$$

The solution to equation 2.1.20 reads:

$$\overline{w' s_x'}(z) = \left(1 - \frac{z}{h}\right) \left[\overline{w' s_x'}\right]_0 + \frac{z}{h} \left[\overline{w' s_x'}\right]_h \quad . \quad 2.1.21$$

Though this equation is only applicable in a not rapidly growing mixed layer, the deviations in non-stationary conditions are small (Wyngaard, 1984). Next we can derive some quantitative information about the influence of the entrainment on the flux at the surface.

Consider a developing mixed layer of 400 m in the morning hours with a growing rate of 0.1 m s^{-1} and a concentration difference between the reservoir layer and the mixed layer of oxidant of $100 \mu\text{g m}^{-3}$. The influence on a typical measured flux of oxidant at 4 m of $1 \mu\text{g m}^{-2} \text{ s}^{-1}$ would be 10%.

So the surface flux of a component can be altered by entrainment, especially when the boundary layer is rapidly developing (in the morning hours) and when a large difference exists between the concentration of the component in the boundary layer and the reservoir layer, as is the case for oxidant. Van Aalst (1989) showed that the deposition velocity of oxidant at 200 m was increased up to a factor of 2 in the morning hours due to this process. The influence of the flux of ozone by entrainment can be enhanced or suppressed due to chemical reactions during the transport from the reservoir layer to the surface. But generally, the typical daily concentration patterns of oxidant are found for ozone as well (see figure 2.3a). This means that oxidant which is fumigated into the boundary layer consists mainly of ozone (Colbeck and Harrison, 1985).

2.1.3 The local time derivative of the flux of ozone applied in reference volume 1

The equation which describes the vertical flux of a scalar under horizontally homogeneous conditions is given, for example, by Businger (1982) and Busch (1973). For ozone the

following extension has to be made for the chemical reaction terms (see also Fitzgarrald and Lenschow, 1983):

$$\overline{w'Q'} = \frac{\overline{w's_2'}}{\tau_a} - \overline{w's_1'} \frac{\bar{S}_3}{\lambda} - \overline{w's_3'} \frac{\bar{S}_1}{\lambda} - \frac{\overline{w's_1's_3'}}{\lambda} . \quad 2.1.22.$$

The local derivative of the flux of ozone under horizontal homogeneous conditions can be written as:

$$\begin{array}{ccccccccc} \frac{\partial \overline{w's_1'}}{\partial t} & + & \overline{w'^2} \frac{\partial \bar{S}_1}{\partial z} & - & \frac{\partial \overline{w'^2 s_1'}}{\partial z} & = & \frac{g}{T} \overline{\theta' s_1'} & + & \frac{1}{\rho_a} \overline{p' \frac{\partial s_1'}{\partial z}} & + & \frac{\overline{w's_2'}}{\tau_a} & - & \overline{w's_1'} \frac{\bar{S}_3}{\lambda} & - & \overline{w's_3'} \frac{\bar{S}_1}{\lambda} , \\ \text{I} & & \text{II} & & \text{III} & & \text{IV} & & \text{V} & & \text{VI} & & & & & 2.1.23 \end{array}$$

where T is the mean absolute temperature; θ' denotes the fluctuations around this mean, ρ_a the density of dry air and g the acceleration due to gravity.

For simplicity we neglected the Coriolis force term and the triple order reaction term.

The same scaling as in section 2.1.1 is applied, except for the pressure fluctuation term. Pressure fluctuations were not measured in this experiment, so this term was parameterized in the often used way (e.g. Wyngaard, 1982):

$$\frac{1}{\rho_a} \overline{p' \frac{\partial s_1'}{\partial z}} \approx a \frac{\overline{w's_1'}}{\tau_w} , \quad 2.1.24$$

where a is a constant in the order of 1 and τ_w is a characteristic turbulence time scale approximated by Z/v_3 .

The same characteristic scales and typical values were used as in section 2.1.1, with the addition of a temperature fluctuation scale, T_f , with a typical value of 1 K. The following dimensionless groups of variables were derived:

I local time derivative

$$\frac{v_3 c_1}{t} = 0.0004$$

II gradient production

$$\frac{v_3^2 \Delta c_z}{Z} = 25$$

III transport of flux

$$\frac{c_1 v_3^2}{Z} = 1$$

IV buoyancy production

$$\frac{g}{T} c_1 T_f = 0.13$$

V pressure fluctuations

$$a \frac{c_1 v_3}{\tau_w} = 1$$

VI chemical reactions

$$\frac{v_3 c_2}{\tau_a} - v_3 c_1 \frac{C_3}{\lambda} - v_3 c_3 \frac{C_1}{\lambda} = 0.016 - 0.013 - 0.08 = -0.08 \quad .$$

From this scaling it can be seen that the terms II, III and V are the most important. The chemical reaction terms are very small compared to the gradient production term and the pressure fluctuation term, which means that they do not severely influence the flux measurements of ozone at one point.

A simple first estimate can be made of the importance of the chemical reactions on the measured flux by considering the pressure term compared to this chemical reaction term:

$$\frac{\tau_w c_2}{\tau_a c_1} - \tau_w \frac{C_3}{\lambda} - \tau_w \frac{c_3 C_1}{c_1 \lambda} \quad . \quad 2.1.25.$$

To show the numerical values of the ratios we substitute λ with $\eta \tau_a$ in which η is 10 with the dimensions of a concentration.

Equation 2.2.4 can be rewritten in:

$$\frac{\tau_w}{\tau_a} \left[\frac{c_2}{c_1} - \frac{C_3}{\eta} - \frac{C_1}{\eta} \frac{c_3}{c_1} \right] . \quad 2.1.26.$$

The ratio τ_w/τ_a is known as the Damköhler number and denotes the ratio between the turbulence time scale and the chemical reaction time scale. Here this number is about 0.016. Since all terms in brackets are in the order of 1, this number here indicates the influence of the chemical reactions on the measured flux at a point.

2.2 Conclusions

From the scaling exercise in section 2.1.1 it can be concluded that the term which describes the convection by turbulence or divergence of the turbulent flux of ozone was the dominant term in the mass conservation equation of ozone in these experiments. This means that the differences between the flux at the measurement height and the flux at the surface were small or:

$$\left[\overline{w' s_1'} \right]_{z_m} \approx \left[\overline{w' s_1'} \right]_0 .$$

The second important term in this scaling was the chemical reactions which produce or destroy ozone. However, an accurate estimate of this influence could not be given at first hand. From the scaling in section 2.1.3 it was found that the gradient production and the pressure fluctuation term were much larger than the chemical reaction term. Therefore it is not very likely that chemical reactions severely influenced the flux of ozone. However, more accurate estimations were made using a model of Vilà-Guerau de Arellano et al. (1991), which describes the flux divergence of the fluxes of ozone and nitrogen oxides. These model runs are given in Appendix E and are briefly commented on in chapter 4.

2.3 Measuring techniques

The measuring techniques described below were used to determine the fluxes of momentum, sensible and latent heat and ozone. For ozone this means that the first term in equation 2.1.7 was determined. Three meteorological measuring techniques were used in this study:

- Eddy correlation technique

- Profile or gradient technique
- Bowen ratio technique

The eddy correlation technique is a direct way to measure turbulent fluxes. A disadvantage of this technique is that rather fast response sensors are needed (response time typically <0.1 s). For ozone such fast response monitors have been built and used in a number of experiments (Wesely et al., 1978; Droppo, 1985, Delany et al., 1986, Zeller et al., 1989).

The equipment used in the eddy correlation technique is less robust, which makes the technique mainly operational in campaign-wise measurements.

The gradient or profile technique links the profile or gradient of a quantity to its flux with the use of semi-empirical relationships. An assumption often made here is that different scalar quantities are transported in the same way by turbulence (so-called Reynolds' analogy). The technique can be carried out with slow-response equipment (with a typical response time of 10-30 seconds) because averages of the variables of about 10 minutes are required (e.g. Wyngaard 1973, see below). This technique is applied in many experiments for the determination of the flux of ozone (Leuning et al., 1979a,b; Garland and Derwent, 1979; Droppo, 1985; Duyzer and Bosveld, 1988).

The Bowen ratio technique is also based on the principle that all scalar quantities (temperature, humidity, trace gases) are transported by the same mechanism. Along with the energy balance at the surface, the fluxes can be evaluated from averaged values of the scalar quantities. This technique is often applied in determining the energy fluxes (e.g. de Bruin, 1982). It is used in the determination of the fluxes of a scalar such as ozone (Leuning et al., 1979) and carbon dioxide (Sinclair et al., 1975).

In the profile and the Bowen ratio techniques only averages of the variables are needed, which makes them very suitable for continuous measurements.

The variables measured in the experiment show strong fluctuating signals due to the turbulent motion in the boundary layer. Especially the fluxes show a strong intermittency. Therefore they were averaged over a certain time period (denoted with the bar). This calculated mean, however, has an accuracy which is a function of these turbulent fluctuations of the variable. Wyngaard (1973) and Businger (1986) gave practical formulations to derive the accuracy of among others mean variables and fluxes. The averaging time required to determine a mean variable such as wind speed, temperature and ozone, with an accuracy of 1%, is typically 15 min. For the fluxes of these components, however, the averaging times would be a hundred

times larger in order to determine the fluxes with the same accuracy. In practice this can hardly be done because of experimental problems, furthermore the assumptions about the stationarity of the variables and fluxes in that time period will be violated. Therefore, the fluxes measured with the eddy correlation technique have to be averaged over much smaller time periods, leading to a smaller accuracy. With the averaging time used here of 30 min, the accuracy with which the fluxes are determined will be about 20%.

In the next three sections the techniques mentioned will be described in more detail.

2.3.1 Eddy correlation technique

The transport of a quantity by turbulent parcels of air or so-called eddies in the planetary boundary layer does take place on vertical length scales varying from millimetres to the height of the boundary layer.

In the eddy correlation technique the vertical air movements along with the amount or concentration of a quantity is correlated at a fixed point at the same time. If, for instance, a higher amount of a quantity is correlated with downward movements of the air and a lower amount of the quantity with upward movements, a net mass flux directed to the surface is found. A flux directed from the surface is set positive and a flux directed to the surface is set negative.

The flux, F_s , of a quantity, S , can be written as:

$$F_s = \overline{ws} \quad 2.3.1$$

and can be rewritten when decomposing the measured signal into a mean and a fluctuating part (see section 2.1) as:

$$F_s = \overline{W}\overline{S} + \overline{w's'} \quad 2.3.2$$

When $\overline{W} = 0$, the first term in equation 2.3.2 can be neglected and is reduced into the often used form:

$$F_s = \overline{w's'} \quad 2.3.3$$

Under thermally stratified atmospheric conditions or above an evaporating surface, \overline{W} is non-zero due to the density fluctuations of the air (Webb et al., 1980, see section 2.1 and 3.3.4 for practical formulations).

The fluxes of momentum, τ , sensible heat, H_s , latent heat, LE , and ozone, F_{S_1} , can be defined as (e.g. Monin and Yaglom, 1971):

$$\tau = \rho_a \overline{w'u'} \quad 2.3.4a$$

$$H_s = \rho_a c_p \overline{w'\theta'} \quad 2.3.4b$$

$$LE = L_v \overline{w'\rho'_v} \quad 2.3.4c$$

$$F_{S_1} = \overline{w'S_1'} \quad 2.3.4d$$

where c_p is the specific heat of air at constant pressure, L_v latent heat of evaporation, and where the s in equation 2.3.3 is replaced by $\rho_a u$ for momentum, $\rho_a c_p \theta$ for sensible heat, $L_v \rho_v$ for latent heat with ρ_v as the absolute humidity or the water vapour concentration (kg m^{-3}) and S_1 the concentration of ozone.

Ad 2.3.1 Some remarks on the use of the eddy correlation technique

The eddy correlation technique requires the fluctuations of the variables to be measured at the same point and at the same time. Given the physical shape of the sensors, automatically, spatial averaging of the signals over the measuring path takes place; as well, spatial separation between the sensors are introduced. Another constraint is that all fluctuations contributing to the transport of the quantity should be measured or, in other words, the (co-)variances of the variables should be measured over the entire frequency spectrum of the eddies in the boundary layer.

If the time constant (RC-time) of the sensors or measuring systems is greater than the smallest period time in the signal, the fluctuations at the high frequency part of this spectrum are attenuated.

The fluxes can be corrected for these losses by the use of given power spectra of fluxes measured with fast response sensors (Moore, 1986). The percentage loss of the flux can then be evaluated given the sensor or measuring system constants. In general, if the sensor

separation is kept smaller than 0.2 m and if the response time of the sensor (system) is less than 0.1 s the losses will be smaller than 5%.

An extra problem can occur if an obstacle, here the mast or the sensor itself, causes a distortion of the flow field. This can result in an erroneous measurement of the velocity fluctuations in all three directions. Due to this distortion a part of the vertical flux is not entirely measured but what is worse, a part of the horizontal flux is measured as a vertical flux: the so-called cross-talk. Wyngaard (1981, 1988) treats this matter extensively and provides possibilities for correcting the measured flux for idealized sensor shapes.

In chapter 3 the corrections applied in this study will be discussed in more detail.

2.3.2 Gradient or profile technique

The gradient technique describes the vertical flux, F_s , of a quantity, S , as an analogy to molecular diffusion as (e.g. Businger, 1973):

$$F_s = -K_s \frac{\partial \bar{S}}{\partial z} \quad 2.3.5$$

where K_s is the eddy diffusion coefficient for the quantity, S . The K_s is a property of the flow and depends largely on turbulence in that flow.

Characteristic turbulence scales for the different scalar quantities can be defined: a turbulence velocity scale, the so-called friction velocity:

$$u_* = (-\overline{u'w'})^{1/2} \quad 2.3.6a$$

and a turbulence scale for the quantity of interest such as temperature, absolute humidity, ozone etc., generally written as:

$$s_* = -\frac{\overline{w's'}}{u_*} \quad 2.3.6b$$

The flux, F_s , can be written as:

$$F_s = -u_* s_* \quad 2.3.7$$

The gradient in equation 2.3.5 is made dimensionless:

$$\frac{\kappa z}{u_*} \frac{\partial \bar{U}}{\partial z} = \Phi_m \quad 2.3.8a$$

$$\frac{\kappa z}{s_*} \frac{\partial \bar{\delta}}{\partial z} = \Phi_s \quad , \quad 2.3.8b$$

where κ is the von Karman's constant, here taken as 0.41. The dimensionless gradients, Φ_m and Φ_s are functions of the atmospheric stability parameter, z/L , where L is the Obukhov length scale defined by:

$$L = - \frac{T}{\kappa g} \frac{u_*^3}{w'\theta'} \quad . \quad 2.3.9$$

The Φ functions are obtained empirically by extensive experiments, and are rather well known especially for momentum and temperature (e.g. the Kansas experiment by Businger et al., 1971).

Using equations 2.3.5, 2.3.7 and 2.3.8, the eddy diffusion coefficients for scalar quantities can be written as:

$$K_s = \frac{\kappa u_* z}{\Phi_s} \quad . \quad 2.3.10$$

Here the assumption has been used that scalar quantities are transported in the same way (Monin and Yaglom, 1971; for ozone Droppo, 1985; Zeller et al., 1989), consequently the stability corrections are identical for each scalar quantity and:

$$K_\theta = K_{\rho_s} = K_{s_1} \quad . \quad 2.3.11$$

The gradient technique is often used in an integrated version, the so-called flux profile relationships (Dyer and Hicks 1970):

$$\bar{U}(z) = \frac{u_*}{\kappa} \left[\ln\left(\frac{z}{z_0}\right) - \Psi_m\left(\frac{z}{L}\right) \right] \quad 2.3.12a$$

$$\bar{S}(z) = \frac{S_*}{K} \left[\ln\left(\frac{z}{z_s}\right) - \Psi_s\left(\frac{z}{L}\right) \right] + \bar{S}(z_s) , \quad 2.3.12b$$

where $\Psi_{m,s}$ are the integrated stability functions (Appendix A). z_0 and z_s are characteristic length scales of the underlying surface for wind velocity, U , and the scalar quantity, S , respectively. They indicate the height above a virtual zero level at which is located the centre where the quantity is transmitted (as for momentum), destroyed (as for ozone) or released (as heat under daytime conditions). The z_0 , called the roughness length, is dependent on the roughness of the surface. The z_s is mainly dependent on the vertical distribution of the sources or sinks of the quantity at the surface.

When a surface has a certain obstacle height, the virtual zero level for momentum is positioned at the often called displacement height, d . Then the z in the equations should be replaced by $z-d$. The displacement height is dependent on the height of the obstacles, the mean foliage distribution and the drag coefficient of the obstacles. Jacobs and Van Boxel, (1988), found a displacement height for a maize crop when the plants were greater than 0.15 m. This 'd' cannot be obtained from the measurements explicitly, so often a parameterization of the d is used. Jacobs and Van Boxel (1988) propose for maize: $d = 0.75 H_{cr}$, where H_{cr} is the height of the crop. Because the levels of the sources and sinks of a scalar differ from that for momentum, the displacement heights differ as well. Hardly any experimental values are known for the displacement height of a scalar, and so as a first approximation, this displacement height is assumed to be similar to that for momentum.

The scaling stated above and the flux profile relationships are only applicable in the part of the surface layer where there is no direct influence of the obstacles at the surface; this is called the inertial sublayer (Tennekes, 1973b; Raupach and Legg, 1984). In the lower part of the surface layer, the so-called roughness layer, the roughness elements themselves also play a role in the scaling of the gradient of a quantity.

Garratt (1980) gives deviations of the Φ functions, as given in equation 2.3.8, dependent on a dimensionless height z/z_* , where z_* is the height of the roughness layer:

$$\Phi' = a \Phi e^{b z/z_*} , \quad 2.3.13$$

where Φ' is the a modified stability function for the roughness layer. These constants are not

universal and have to be deduced by experiments for each different site.

If the equations in 2.3.8 are integrated over height z , with these new stability functions under neutral stability (as a first approximation), we get for $z_0 < z < z_*$:

$$\bar{S}(z) = a \frac{s_*}{\kappa} \left[\ln \frac{z}{z_*} + b \frac{z-z_*}{z_*} + \frac{b^2}{4} \frac{z^2-z_*^2}{z_*^2} \right] + \frac{s_*}{\kappa} \ln \frac{z_*}{z_s} , \quad 2.3.14a$$

where z is the height above the displacement height.

The concentration difference between a measurement at point $z_2 > z_*$ (above the roughness layer) and one at point $z_1 < z_*$ (in the roughness layer) is:

$$\bar{S}(z_2) - \bar{S}(z_1) = \frac{s_*}{\kappa} \left[\ln \frac{z_2}{z_*} - a \left(\ln \frac{z_1}{z_*} + b \frac{z_1-z_*}{z_*} + \frac{b^2}{4} \frac{z_1^2-z_*^2}{z_*^2} \right) \right] . \quad 2.3.14b$$

The ratio, R_{s_*} between s_* calculated with equation 2.3.14b and equation 2.3.12b is depicted in figure 2.5 as a function of z_* for measurements at $z_2 = 5.0$, $z_1 = 1.0$ m. The constants $a=0.5$ and $b=0.7$ were taken from experiments above forests by Garratt (1980). A rule of thumb often used is that the measurement height should be larger than $10 z_0$ (Jacobs and Van Boxel, 1988). Using this as an estimate for the z_* and a z_0 for mature maize crop of 0.2 m (see section 3.4.1), it can be seen that at $z_* > 10 z_0$, the deviations from the original calculated s_* becomes larger than 10%.

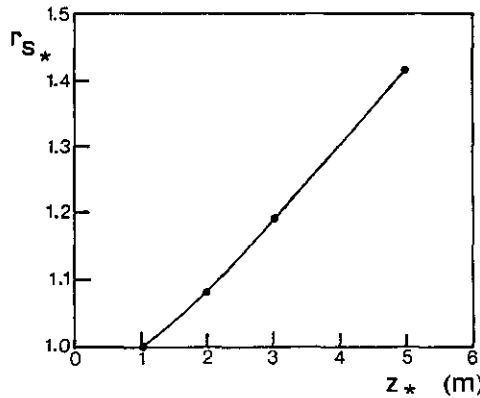


Figure 2.5 The ratio, R_{s_*} , between s_* calculated with equation 2.3.14b and equation 2.3.12b as a function of the height of the roughness layer, z_* .

An alternative derivation of the gradient technique can be given by using equation 2.1.23 under stationary conditions without chemical reactions and buoyancy effects. Using the same parameterization for the pressure fluctuation term as in equation 2.1.24, we get:

$$\overline{w'^2} \frac{\partial \bar{S}}{\partial z} - \frac{\partial \overline{s'w'^2}}{\partial z} = a \frac{\overline{w's'}}{\tau_w} . \quad 2.3.15$$

In the absence of the second term in this equation i.e. when measurements are taken well above the roughness elements, equation 2.3.15 is reduced to:

$$F_s = \overline{w's'} = \frac{\tau_w \overline{w'^2}}{a} \frac{\partial \bar{S}}{\partial z} . \quad 2.3.16$$

The absolute value of the factor in front of the gradient of S in the latter term of equation 2.3.16 can be seen as the eddy diffusion coefficient.

2.3.3 Bowen ratio technique

The Bowen ratio, β , is by definition:

$$\beta = \frac{H_s}{LE} . \quad 2.3.17$$

Using the gradient theory to describe the fluxes of sensible heat, H_s , and latent heat, LE , and by assuming similarity in the transport of heat and water vapour, i.e. using equation 2.3.11, we can write:

$$\beta = \alpha \frac{\partial \bar{\theta} / \partial z}{\partial \bar{p}_v / \partial z} , \quad 2.3.18a$$

where $\alpha = \rho_g c_p / L_v$.

If the gradients are measured as $\Delta\theta/\Delta z$ and $\Delta p_v/\Delta z$ i.e. over the same height difference, equation 2.3.18a is reduced to:

$$\beta = \alpha \frac{\Delta \bar{\theta}}{\Delta \bar{p}_v} . \quad 2.3.18b$$

The energy balance at the surface can be written as:

$$Q_n + G + S_{so} + S_b + Ph + H_s + LE = 0 \quad , \quad 2.3.19$$

where Q_n is the net radiation, G the soil heat flux, S_{so} the heat storage in the soil, S_b the heat storage in the crop and Ph the energy used in the photosynthesis. For a crop like maize the storage terms and the photosynthesis, although small, cannot always be neglected because several small terms work in the same direction. Estimations of these terms from our measurements are given in Appendix B.

The energy, A , available for the sensible and latent heat fluxes is:

$$A = Q_n + G + S_{so} + S_b + Ph \quad . \quad 2.3.20$$

Combining this available energy with equation 2.3.17, we can write:

$$H_s = A \frac{\beta}{1+\beta} \quad 2.3.21a$$

$$LE = \frac{A}{1+\beta} \quad . \quad 2.3.21b$$

In analogy with the Bowen ratio, a modified Bowen ratio can be defined between the flux, F_{S_1} , and the fluxes of sensible heat or latent heat. If again, the gradients of the quantities are measured over the same distances, the flux, F_{S_1} , can be derived from :

$$F_{S_1} = \frac{H_s}{\rho_a c_p} \frac{\Delta \bar{S}_1}{\Delta \bar{\theta}} = \frac{LE}{L_v} \frac{\Delta \bar{S}_1}{\Delta \bar{\rho}_v} \quad . \quad 2.3.22$$

Using the latter technique two estimates of the flux, F_{S_1} , are derived. If the fluxes of H and LE are derived with the Bowen ratio technique, equation 2.3.22 can be written as:

$$F_{S_1} = \frac{\Delta \bar{S}_1}{\Delta \bar{\rho}_v + \alpha \Delta \bar{\theta}} \frac{A}{L_v} \quad . \quad 2.3.23$$

The advantage of this equation above equation 2.3.22 is that F_{S_1} can be calculated even if one of the gradients of temperature or humidity is zero. That means no extra check is necessary if one of the heat fluxes is zero which can be the case during transition hours and night-time.

Chapter 3 Experimental outline

Introduction

Two types of experiments were carried out during the growing season of forage maize (*Zea mays* L. vs. *Brutus*) in 1988. In the first type of experiment the aim was to determine the fluxes of ozone, nitrogen oxides, carbon dioxide, momentum, and sensible and latent heat with the profile and Bowen ratio techniques as described in sections 2.3.2 and 2.3.3. The fluxes of nitrogen oxides were determined because of their possible influence on the flux of ozone caused by chemical reactions. The flux of carbon dioxide was determined because of its relevance to model the effects of air pollutants on crop yield.

Therefore profiles of the wind velocity, temperature, humidity and ozone, nitrogen oxides, carbon dioxide, along with the net radiation and the soil heat flux were measured. These measurements were made continuously throughout the maize growing season, i.e. from sprouting of the seeds in May up to two weeks after harvesting-time in October.

A second type of experiment was carried out in which the fluxes of ozone, sensible and latent heat and momentum were measured with the eddy correlation technique as described in section 2.3.1. These measurements were carried out incidentally during the season with conditions of no rainfall and when the fetch-to-height ratio was at least 40:1. These measurements were primarily carried out to check the fluxes obtained with the continuous measurements.

A description of the site where the experiments were carried out is given in section 3.1.

As already pointed out in section 2.3 there are different sensor requirements for the different meteorological techniques. The sensors used in the profile and (modified) Bowen ratio techniques i.e. for continuous measurements, are slow-response sensors with which a high accuracy of mean quantities is obtained. The sensors are sampled at a slow rate (0.02 Hz) to make the data flow processable. The sensors used in the eddy correlation technique, i.e. for the incidental measurements, are fast-response sensors with which the fluctuations of the

quantities are measured. These sensors are sampled at a high rate, i.e. 10 Hz. The fluxes of the quantities were calculated from these measurements using a statistical code.

The sensors used in both types of experiments are described in section 3.2. Subsequently in section 3.3 the data acquisition and processing are given as well as the corrections on the measured fluxes.

At the site more experiments were carried out including porometer measurements at the leaves of the maize crop twice every week; measurements of the chemical composition of rainfall outside the crop and throughfall of rain in the crop, and measurements of crop yield and structure every 1 or 2 weeks, dependent on the crop development. These experiments were part of a larger experimental programme in which the effect of air pollutants on agricultural crops was studied and reported elsewhere (KEMA,1989,1990).

In section 3.4 some environmental conditions and crop parameters, partly based on these measurements, are given.

3.1 Site description

The measurements were carried out at the Sinderhoeve pilot farm of the Institute for Land and Water Management Research (ICW), Renkum which is situated in the centre of the Netherlands ($51^{\circ}58'N, 5^{\circ}42'E$). The maize was planted in rows 0.75 m apart and with a separation in the rows of 0.14 m (i.e. 10 plants per m^2). The dimensions of the field were 250 x 300 m. The field was surrounded by agricultural crops, including considerable maize. In figure 3.1 a map of the site and its direct vicinity are given. The masts were positioned in the north-west part of the field to obtain the largest possible fetches under southerly and westerly winds.

In figure 3.2a the sensors and their positioning are shown. Also measurements in the crop are indicated which were part of the project but are not discussed in this thesis, except for one example in section 6.1. The measurements at the second profile mast were used as a first check on the flux measurements with the eddy correlation technique but are not discussed. The mast with continuous measurements of wind speed, dry and wet bulb temperature and trace gases can be seen in figure 3.2b.

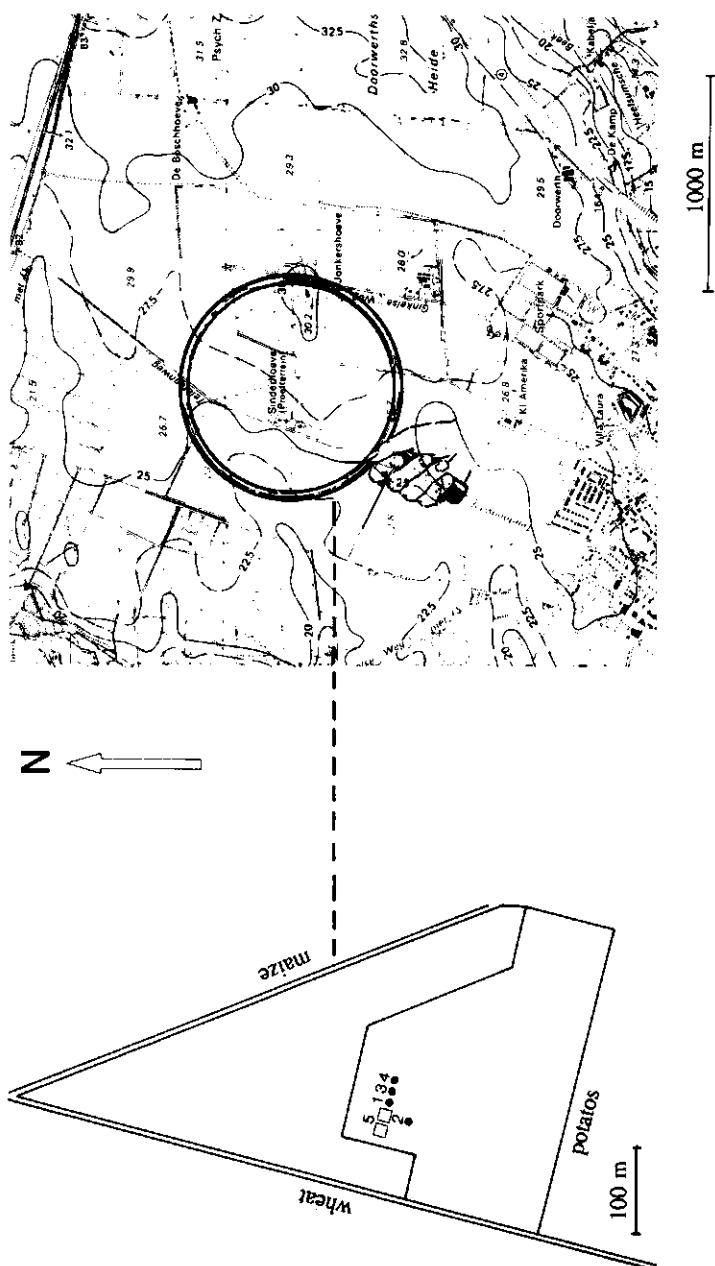


Figure 3.1 Map of the measurement site and the direct vicinity.
The positions of the masts are given in more detail in the insert.

- 1 profile mast continuous measurements
- 2 mast with radiation measurements
- 3 mast with eddy correlation measurements
- 4 extra profile mast
- 5 vans with the monitoring and data acquisition systems

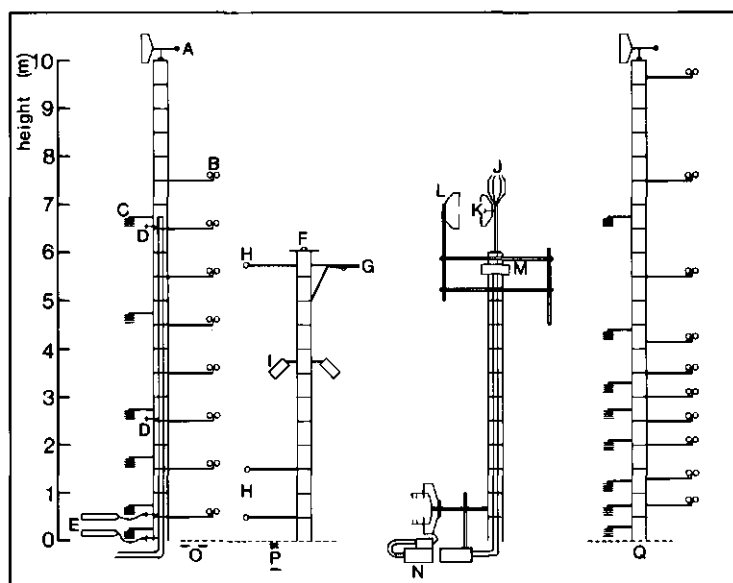


Figure 3.2a Measurement outline and sensor positions in the masts.
A-Q explained below.

A	wind direction measurements
B	wind speed "
C	dry and wet bulb "
D	air inlet
E	perforated glass tube connected to air inlet
F	global radiation measurements
G	reflected global radiation measurements
H	net radiation "
I	surface temperature "
J	fluctuation measurements of the three wind components
K	" " of temperature and ozone
L	" " of absolute humidity
M	ground station fast ozone measurements
N	eddy correlation system in the crop
O	soil heat flux measurements
P	soil temperature "
Q	additional profile measurements of wind speed and dry and wet bulb temperature

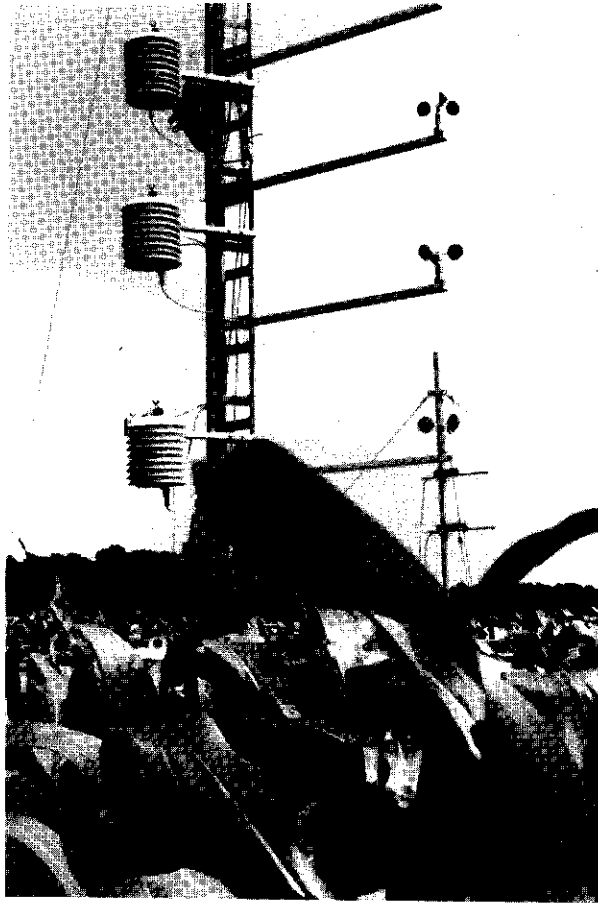


Figure 3.2b The mast with continuous measurements of wind speed (cup anemometers), dry and wet bulb temperature (psychrometer) and trace gases.

3.2 Sensors used in the experiments

3.2.1 Continuous measurements

The measurement levels of the sensors are indicated in italics.

3.2.1.1 Wind vane

(Measured at 10 m)

The wind direction was measured with a 4-bits digitized wind vane. The wind vane had 16 sectors of 22.5° . The wind direction measurements were only used for the data selection concerning the fetch.

3.2.1.2 Cup anemometers

(Measured at 0.5, 1.5, 2.5, 3.5, 4.5, 5.5, 6.5 and 7.5 m)

The mean wind speeds were measured with small sensitive cup anemometers with an accuracy of at least 3% within the measuring range of 1-15 m s⁻¹. The mean starting speed was 0.20 m s⁻¹ and the first-order response length was 0.9 m. The cup rotation speed was measured with a photo-chopper system. To avoid pulse distortion due to the long transmitting lines, current pulses were applied of 20 mA. The cup anemometers were mounted on rectangular booms, fitted to a triangular open mast with sides of 0.18 m. The booms were about 1 m long so as to avoid mast interferences (Smedman et al., 1973).

3.2.1.3 Psychrometers

(Measured at 0.1, 0.5, 1.5, 2.5, 4.5 and 6.5 m)

The mean dry bulb and wet bulb temperatures were measured with aspirated psychrometers built at the Laboratory of Physics and Meteorology. Pt-100 resistance elements were used with an accuracy of 0.02 K. The resistance elements had a diameter of about 3 mm. The aspiration speed exceeded 4 m s⁻¹ in order to avoid variations in the psychrometric constant (Harrison, 1963). The resistance elements were mounted in a construction of shields to protect the elements from direct sun radiation.

The absolute humidity, ρ_v , was calculated with the following set of equations:

$$\rho_v = \frac{e_a}{R_v T} \quad 3.1$$

$$e_a = e_w - \gamma P (T_d - T_w) \quad 3.2$$

$$\gamma = \frac{M_d}{M_w} \frac{c_p}{L_v} \quad 3.3$$

$$e_w = 6.10 + 0.44 T_w + 0.0143 T_w^2 + 0.0002689 T_w^3, \quad 3.4$$

where T_d and T_w are the dry and wet bulb temperature in °C,

e_a is the water vapour pressure of the air in mb,

e_w is the saturated water vapour pressure in mb at T_w ,

T is the absolute temperature of the air in K,

R_v is the gas constant for water vapour in $\text{J kg}^{-1} \text{K}^{-1}$,

γ is the psychrometric constant taken to be $6.73 \times 10^{-4} \text{K}^{-1}$ and

P is the atmospheric pressure in mb.

The atmospheric pressure was not measured and a constant value of 1013 mb was used. This resulted in a maximal uncertainty of $e_a - e_w$ of 4%. The accuracy in ρ_v due to error in the measurements of T_d and T_w was estimated at about 1%.

Various tests were carried out to check the performance of the psychrometers in the field by mounting them all at one level. The typical systematic difference between the psychrometers was 0.04 K for T_d and for T_w . For the humidity measurements this was about 0.04 g m^{-3} . For all three signals this was about 1% of their mean value, which is about the first estimated accuracy. Some tests without ventilation in the psychrometer housings showed no difference in the systematic differences for T_d but doubled the difference for T_w and ρ_v . It has to be noted that these tests were performed in the late season without high solar insolation.

3.2.1.4 Pyranometer

(Measured at 6 m)

To estimate the incoming short wave irradiation, a Kipp solarimeter (type CM 5) was used. This instrument has a Mol-Gorczynski cell, consisting of a 14-junction manganin-constantan thermopile. The accuracy is 3%. The sensitivity is about $12 \mu\text{V per W m}^{-2}$ and the electrical resistance is about 10Ω . The sensitive element is enclosed by a double glass dome which transmits the solar irradiation within the band width of $0.4\text{--}3.0 \mu\text{m}$. The dome was cleaned every day to avoid contamination by dust. The 98% time constant is about 30 s and the non-compensated thermopile has a temperature coefficient of about -0.2% per K.

3.2.1.5 Pyrriadiometer

(Measured at 6 m)

The net radiation was estimated with a Funk net radiometer (type Middleton). This radiometer contains a thermal transducer with 250 thermal conjunctions bonded by two blackened plates. The sensitivity of the instrument is about $42 \mu\text{V per W m}^{-2}$ and has an internal resistance of about 75Ω . The sensitive plate is enclosed with hemispherically shaped polyethylene windshields, which transmits the short and long-wave radiation within a band width of $0.4\text{--}50 \mu\text{m}$. Here, the thin domes were inflated by passing dry nitrogen very slowly through the

instrument which, meanwhile, prevented internal condensation of the domes. No precautions were taken against possible dew forming on the domes during the late afternoon and night-time. The domes were cleaned every day and replaced every month to avoid a possible reduction of the transmissivity. The accuracy of the net radiation measurements was about 3%.

3.2.1.6 Radiation thermometer

(Measured at 3.7 m)

To estimate the radiation temperature of the crop, the Heimann infra-red radiation thermometer was used (type KT 15). This instrument measures within the spectral band width of 8-14 μm . The temperature ranges between -25°C and 75°C . The accuracy is about 0.5 K. The 90% response time is about 1 s and the emissivity is programmable between 0.2 and 1.0. During the measuring period the emissivity was taken to be 0.976, as commonly used in practice (Choudhury and Idso, 1985). This thermometer has an 8° field-of-view, which means that at a measuring height of 1.5 m above the crop with an elevation angle of 45° the instrument views a surface of about 0.02 m^2 .

3.2.1.7 Soil temperature

(Measured at 2, 8 and 120 cm below the soil surface)

The soil temperatures were estimated with Pt-100 resistance thermometers. In order to avoid soil distortion as much as possible, the thermometer elements were inserted through a reference board at the desired depth. The accuracy of the resistance thermometers was 0.02 K, though the accuracy of the soil temperature measurement was largely dependent on the representativeness of the sensor site, such as soil inhomogenities and the contact of the sensor with the soil.

3.2.1.8 Soil heat flux plate

(Measured at 5 cm below the soil surface)

The soil heat fluxes were made by flux plates (TNO transducer type WS 31 Cp). Corrections were made for the flux plate dimensions and the ratio of the transducer conductivity to that of the medium, according to Philip (1961) and Overgaard Mogensen (1970). The accuracy of the sensors was 5%, but here too the representativeness of the sensor site dominated the

accuracy. For this reason the measurements were carried out in duplo. The differences between the two plates were generally smaller than 5 W m^{-2} .

3.2.1.9 Soil moisture

(Measured at 2,4,5,7,10,15,20,25,30,40,50,60 and 90 cm and carried out by ICW¹)

The soil moisture profile was made by measuring the volumetric soil moisture content with a dielectric soil moisture content meter (Halbersma and Przybyla, 1986). This technique is based on the measurement of the electrical capacitance of a soil-water-air mixture as the dielectric medium. The sensitivity of the sensors is site dependent and is calibrated against a gravimetric method to measure the water content. The accuracy of the measurements, highly dependent on the calibration and the sensor site, is estimated at 20-30%.

3.2.1.10 Trace gas measurements

(Measured at 0.1, 0.5, 2.5 and 6.5 m)

The profiles of the trace gases were measured with one monitor for each component to avoid systematic differences between the measurement levels. As well, the tube length and filters were kept similar. The measurement levels were chosen to obtain the largest gradients in the concentration profiles, i.e. close to the soil surface and close to the crop in its mature stage. This was done to increase the accuracy in the concentration profiles.

In figure 3.3 a detailed outline is given of the equipment of the continuous trace gas measurements. The air sampled at the four levels in the mast was led to the inlet over a filter with pore width of $10 \mu\text{m}$ and transported through a Teflon tube (internal diameter of 4 mm) of 25 m. The inlets at 0.1 and 0.5 m were connected to a perforated glass tube ($\varnothing = 1 \text{ cm}$) of 1 m to obtain a line averaged concentration. This glass tube was constructed in a second glass tube ($\varnothing = 3.5 \text{ cm}$) of the same length with openings ($\varnothing = 1 \text{ cm}$) facing downwards to avoid inflow of rain or dew.

The tubes were heated to avoid condensation. Each tube was connected to a valve which was driven by the computer. The tubes were subsequently connected via these valves to the inlets of the monitors. The flow rate was about 5 l per min, which means the air was transported in about 4 s to the monitors. When a tube was connected to the monitors, the other tubes

¹ Institute of Hydrology and Water Management

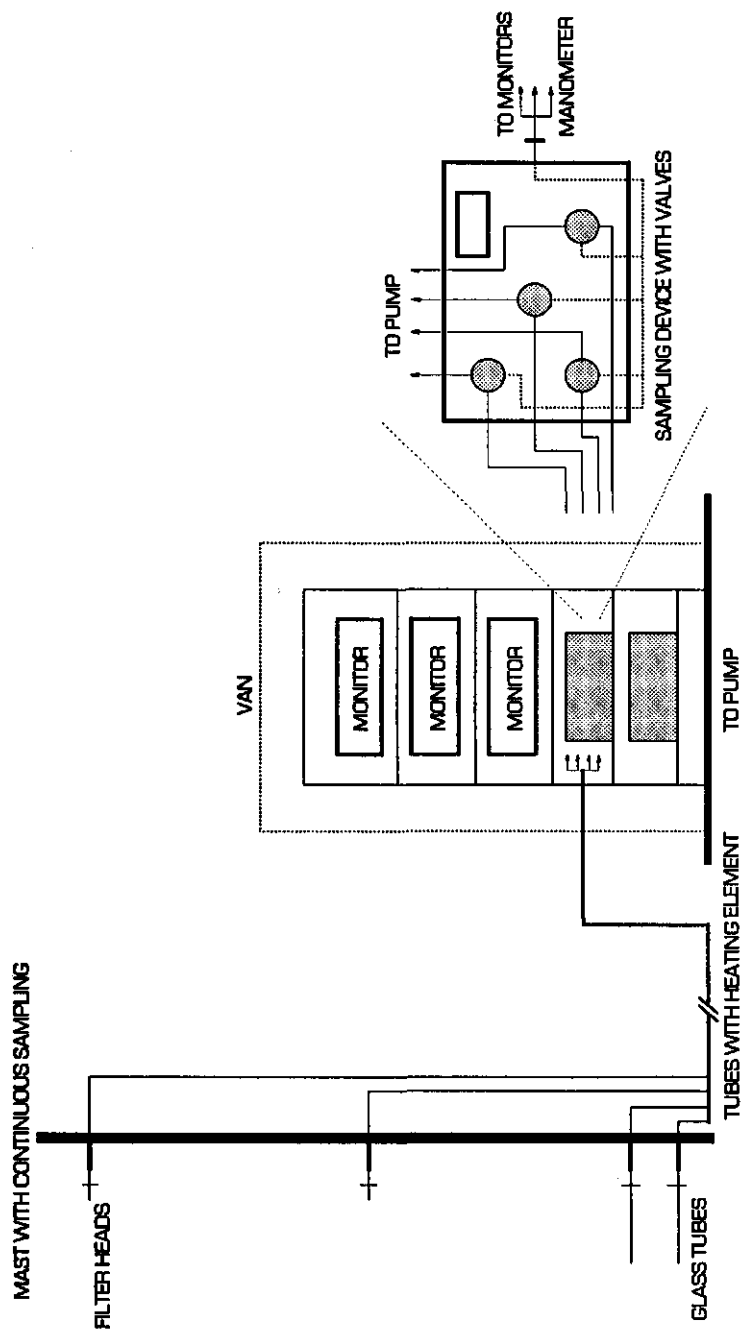


Figure 3.3 Outline of the equipment used in the continuous measurements of the concentration of ozone (and nitrogen oxides and carbon dioxide).

were flushed with about the same flow rate as the joint flow rates of the monitors. The pressure in each tube was measured just before the inlet of the monitors. The monitors were sensitive to this pressure drop in the reaction chamber and were corrected per tube for this loss.

The monitors were calibrated weekly using standard methods (KEMA, 1989).

Various tests were carried out to check the quality of the concentration measurements at the four levels. The ozone losses at the tube surface and the filter heads were examined in the laboratory by flushing the tubes with ozone rich air ($160 \mu\text{g m}^{-3}$). The losses were smaller than 0.5% and were often not detectable. In the field the four filter heads were mounted at the same level to observe the differences under field conditions. Generally, the differences between the concentrations were smaller than 0.5%. One of the main reasons for these small differences lies in the low residence times of the air in the tubes.

Due to the sequential measurement routine (see section 3.2.1), a difference between two levels was introduced. The data were screened for this effect but even at very large ozone trends (in the order of $40 \mu\text{g m}^{-3}$ per hour), no systematic differences were noticable.

The type of monitors used to detect the trace gases in these experiments are common. In the following three sections they will be described briefly. All monitors had the same sensitivity of 0-10 V over the indicated range.

Ozone (O_3) monitor

Ozone was measured with a Combustion Engineering model 8002 monitor. The monitor operates according to the chemo-luminescence method. Ozone molecules are reduced by ethylene and emit photons which are detected after passing a photo multiplier. The accuracy was 1% and the detection limit was $1 \mu\text{g m}^{-3}$. The time constant used was 10 s and the range was 0-400 $\mu\text{g m}^{-3}$.

Nitrogen oxides (NO_x) monitor

Nitrogen oxides were measured with a Monitor Labs model 8840. The monitor operates according to the chemo-luminescence method. The NO is oxidized by O_3 , leaving activated NO_2 molecules emitting photons which subsequently are detected after passing a photo

multiplier. The NO_2 is reduced to NO and subsequently detected with the ambient NO as above. So the monitor detected NO and $\text{NO} + \text{NO}_2$ denoted as NO_x . The accuracy was 5% and the detection limit $4 \mu\text{g m}^{-3}$ for NO_2 and $2.5 \mu\text{g m}^{-3}$ for NO. The time constant used was 5 s and the range $0\text{--}400 \mu\text{g m}^{-3}$ for NO_2 and $0\text{--}250 \mu\text{g m}^{-3}$ for NO.

Carbon dioxide (CO_2) monitor

Carbon dioxide was measured with a Leybold Hereaus Binos-1 monitor. The monitor operates on the infra-red absorption principle of the CO_2 in the air sample. The detection is dependent on the atmospheric pressure. The concentrations were not corrected for variations in this pressure and only concentration differences were used. The accuracy was 1% and the detection limit was 1 mg m^{-3} . The time constant used was 2 s and the range was $0\text{--}1800 \text{ mg m}^{-3}$.

3.2.2 Incidental measurements

The sensors used in the eddy correlation measurements were mounted on a 6 m mast (the third mast in figure 3.2a) in such a way that the measurement volume was as small as possible and disturbances of the air flow were prevented as much as possible.

All sensors were pointed into the mean wind direction so that no large distances in the direction of the mean flow existed ($<10 \text{ cm}$) between the sensors of the scalar fluctuation measurements and the vertical wind fluctuation measurements (hence the w-sensor). The distances perpendicular to the mean flow were kept smaller than 20 cm.

3.2.2.1 Measurements of the wind speeds

Measurements of the three dimensional wind speed were made with a sonic anemometer of Kaijo Denki, type DAT-310. The sensors operate on the principle that the travelling time of a sound wave to cross a finite sensor path is dependent on this path length, the speed of sound and on the wind speed along this path.

This sonic anemometer had sensor paths of 20 cm, a repetition rate of ca. 20 Hz and an accuracy of 1%. No errors are caused by temperature or humidity drifts.

The sonic anemometer was positioned in such a way that:

- 1) the wind was not blowing along the horizontal probes, which otherwise could generate a disturbance of the turbulent flow and

2) the vertical wind probe was pointing into the mean wind direction, so the disturbance of the turbulent flow caused by the frame of the sonic anemometer itself was kept small. For a more detailed description of the sonic anemometer see Schotanus (1982) and Van Boxel (1986).

The sonic anemometer was mounted on top of an inclinometer which measured the tilt of the sonic anemometer. The tilt was kept smaller than 0.3° .

3.2.2.2 Measurements of the temperature fluctuations

Temperature fluctuations were measured with a fast response thermocouple developed at the Laboratory of Physics and Meteorology. The thermocouple exists of copper-constantane junction, with a electronic cold junction. The sensor has a response time of at least 50 ms at a wind velocity of 2 m s^{-1} and has an accuracy of 2%. The sensitivity is about 1 K per 100 mV. The sensor was mounted on a device which could be placed close ($<10 \text{ cm}$) to the w-sensor of the sonic anemometer. The sensor is described in detail by Van Asselt et al.(1991).

3.2.2.3 Measurements of the humidity fluctuations

Measurements of the humidity fluctuations were made with a Lyman- α hygrometer. The hygrometer measures the absorption of ultra-violet radiation by water vapour over an open air sensing path. This path can be adjusted from 1-3 cm to obtain a current from 1-12 mA. The sensor sources are mounted in the measuring device in such away that the box with electronics was placed 25 cm downwind of the sonic anemometer. The sensor has a response time of 12 ms. The sensor sources are described in detail by Buck (1976).

3.2.2.4. Measurements of the ozone fluctuations

The measurements of the ozone fluctuations were made with a modified ozone monitor of the type Combustion Engineering model 8002 as described in 3.2.1.10. The monitor was modified to avoid the influence of the monitor itself on the turbulent flow field and to enable fast response measurements of the ozone concentration. The modifications are described in detail in De Bruin en Jaspers (1987).

Two modifications were made:

1) The reaction chamber with the photo multiplier and the ventilator were separated from the monitor and reconstructed into a box of $30 \times 17 \times 17 \text{ cm}^3$. A Teflon tube of 1 m with a filter

head was connected to the inlet of the reaction chamber. The delay time of the monitor plus tube was 0.8 s. The filter head was placed within 10 cm of the w-sensor of the sonic anemometer. The remaining parts of the monitor were placed in the so-called ground station in which the sample and the ethylene flow were controlled. The box with the reaction chamber was connected to the ground station with cables and tubes of 8 m and consequently could be hidden in the crop.

As a consequence of this modification the bulky part of the monitors could be moved far enough from the measurement site.

2) Some RC-filters were removed from the monitors. In this way the response time of the monitor was reduced to 0.4 s.

Due to this modification the noise of the signal was increased to 3% of the measured concentration. The noise was assumed to be uncorrelated with the vertical wind fluctuations. Lenchow and Kristensen (1985), showed that the noise of a sensor does not influence this covariance if the ratio between the variance of the noise and the variance of the atmospheric fluctuations is smaller than 1. This was always the case in our measurements.

Figure 3.4 illustrates the observed fluctuations in some time series examples of the signals of vertical wind speed, temperature, absolute humidity and ozone.

3.3 Data acquisition and data processing

3.3.1 Continuous measurements (slow-response signals)

The sensors were connected to a data logger which was controlled by a mini computer. Both were situated in a van about 30 m away from the profile mast.

The sampling routine: - the valve at a point was driven to the open position,

- the meteorological variables were scanned which took about 30 s,
- the trace gas signals were scanned sequentially four times which took about 10 s.

The routine was commenced at the top and continued towards the bottom inlet, forming one cycle, i.e. one profile of the trace gases. So, in one cycle, every signal was scanned four

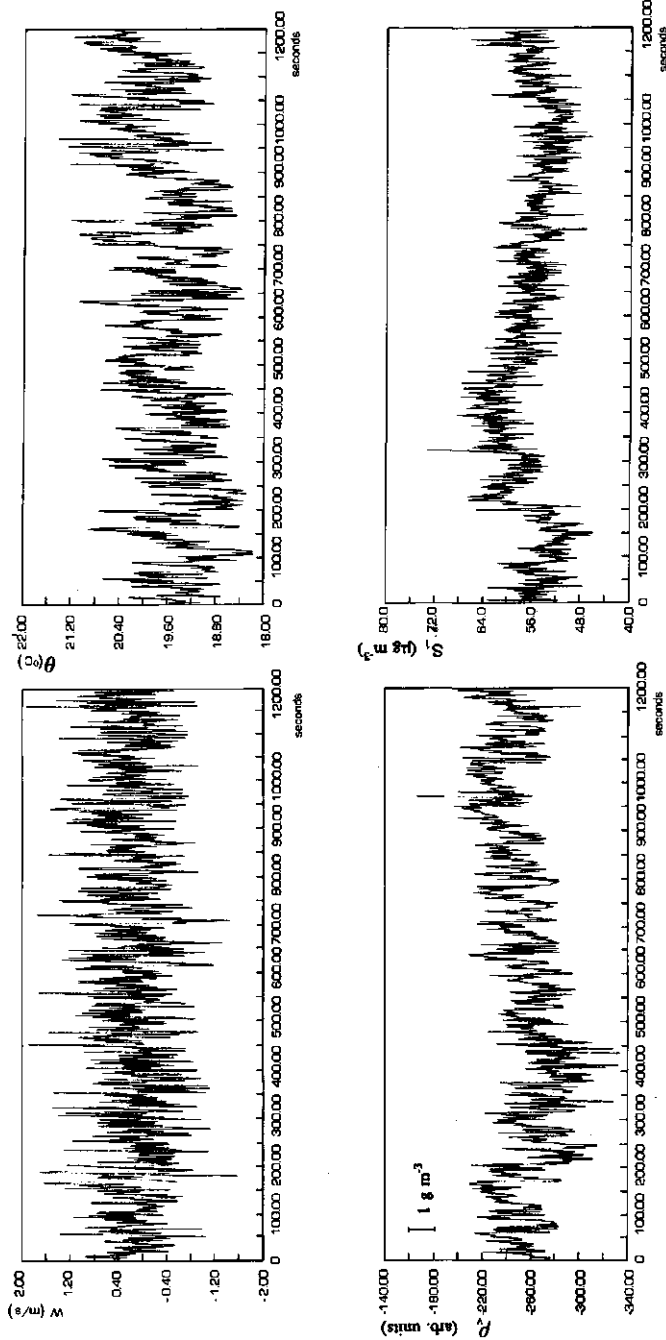


Figure 3.4 The time series of the signals of vertical wind speed, temperature, absolute humidity and ozone on July 27, 1988. The entire series is about 1200 s.

times. The duration of one cycle was restricted to 3 min. The spare time between two cycles, about 20 s, was used to adjust the monitors to the air composition sampled at the top inlet. Every five cycles all the signals were reduced to 15 min averages and stored on magnetic tape. At the laboratory the tapes were fed into a computer with which the data was transformed into its physical quantity and averaged to 30 min values.

The fluxes were calculated using the measurements of 0.5 up to 6.5 m wind speed, potential temperature, humidity, trace gases and net radiation at 6 m, and the soil heat flux. Temperature was converted to the potential temperature. The calculations were carried out with a computer code in which the measurement levels were selected with respect to the height of the crop.

The data was selected on: 1) mean wind speed at 3.5 m greater than 1 m s^{-1} and 2) fetch larger than 40:1, i.e. wind directions between 150° - 240° .

The fluxes were calculated in two ways;

1) with the Bowen ratio technique (equations 2.3.18, 2.3.21 and 2.3.23) with the sensors above the crop. The Bowen ratio was derived from the slope of the regression between the potential temperature and the humidity measurement (Sinclair et al. 1975).

2) with the profile technique (equations 2.3.9, 2.3.11 and 2.3.12) with the sensors at levels about twice the crop height, except for the lowest measurement of ozone which had to be above the crop. The equations had to be solved iteratively. The fluxes of momentum and heat were calculated via linear regression between the logarithmic height, and the wind and potential temperature measurements without stability corrections. Subsequently the fluxes were used to calculate an Obukhov length scale which in turn was used to calculate new fluxes but now with stability corrections (as given in Appendix A). Generally this took about 3-10 iterations. Only under very stable conditions these equations do not converge (Bercowitz and Prahm, 1982).

The measurements of the wet bulb temperature at 2.5 m had to be corrected during daytime in the period July 1 - August 23 due to malfunctioning of the respiration device. This was done first by calculating the evaporation from the available energy and the sensible heat

obtained from the profile technique. From this the Bowen ratio could be deduced and so the slope of the regression line between the dry and wet bulb temperature. The wet bulb temperature at 2.5 m was fitted into this regression line using the dry bulb temperature at 2.5 m and both the dry and wet bulb temperature at 4.5 and 6.5 m. The corrections were smaller than 3%.

The fluxes of sensible and latent heat derived with the profile technique, of which the sum was larger than the available energy, were eliminated from the data set. Most of the time this indicated ventilation problems in the psychrometers.

The fluxes of sensible and latent heat derived with the Bowen ratio technique were eliminated from the data set if $-0.8 < \beta < -1.2$. For these data, mostly taken during transition times, the uncertainty in the fluxes is very large because at $\beta \approx -1$ equation 2.3.21 breaks down and the errors in the measurements are strongly amplified.

3.3.2 Incidental measurements (fast response signals)

The sensors were attached to a data logger and a computer, both situated in a second van about 60 m away from the masts. The signals were sampled with 10 Hz and after passing a 4 Hz low-pass filter stored on magnetic tape. The ozone signal was not led through this filter because the tube and the filterhead themselves functioned as a low-pass filter of about 2 Hz (see Appendix C).

The magnetic tapes were processed on the computer with a statistics code developed at the Laboratory of Physics and Meteorology (Van Boxel, 1987), which calculated the mean, standard deviation, variance, skewness and kurtosis of the individual signals and covariances and correlations between two signals. A linear trend was subtracted from the signals with this code. This means that the mean vertical transport of a component was removed from the fluxes (i.e. the first term on the right-hand side of equation 2.3.2 was eliminated).

The signal of the ozone monitor was shifted 1.1 s ahead of the vertical wind fluctuation signal according to the findings in section 3.3.3c (see below).

The fluxes were calculated over 30 min periods. Runs were selected for which wind speed at 6 m was greater than 2 m s^{-1} . As a final check all runs were eliminated when the standard deviation in the calculated flux exceeded 10% of the flux, then a statistically reliable covariance was calculated. This led to an elimination of 10% of the measurements of the flux of ozone.

3.3.3 Practical implications of using the eddy correlation technique

It was pointed out in section 2.3.1 that some corrections in the eddy correlation measurements had to be made due to some shortcomings of the sensors and their possible interference on the flow field. We will give a brief description of these corrections here.

a) Corrections due to flow distortion

Due to the presence of the sensors and the mast a distortion of the flow field can be induced. Especially the disturbance on the vertical velocity fluctuations are of interest. Wyngaard (1988) gives a description for the disturbed vertical velocity w and for the flux, F_s , of a scalar. The measured flux, F_{sm} , can be written as:

$$F_{sm} = \overline{w_m' s_m'} = (1 + d_{33}) \overline{w' s'} + d_{31} \overline{(u'^2 + v'^2)^{1/2} s'} , \quad 3.5$$

where d_{33} is the attribute to the vertical wind component due to the created vertical velocity, d_{31} is the attribute to the vertical wind component due to the horizontal wind component. An approximation of d_{31} is given by:

$$d_{31} = \frac{\bar{W}}{(\bar{U}^2 + \bar{V}^2)^{1/2}} . \quad 3.6$$

An estimation of d_{33} has to be derived from measurements or from calculations for simple geometrical bodies. Both ways were not possible here to investigate but though this influence is small compared to the second term in equation 3.5, here we neglected this term.

The second term, or the so-called cross-talk term, indicates that part (namely d_{31}) of the horizontal turbulent fluxes which is measured as a vertical turbulent flux.

The covariances between the fluctuations of the lateral wind and the concentration of ozone were calculated and used in the second term of equation 3.5. Practically by neglecting the first term in equation 3.5 this correction becomes identical to the tilt correction. For our data this correction was on average less than 5%. Generally, the vertical wind speed was positive, which is typical for a bottom-heavy construction.

b) Corrections due to sensor line averaging and sensor separation

For the corrections on sensor line averaging and sensor separation, equations proposed by

Moore (1986) were used but are not given here. As already pointed out the measurements were performed in such a way that only a lateral separation existed which was at a maximum 20 cm. Therefore these corrections were very small (a few per cent).

c) Corrections due to limited frequency response of the ozone monitor

The ozone monitor can be treated as a first-order linear system with a time constant RC. This time constant causes an attenuation and a phase shift of the incoming signal dependent on its frequency. The attenuation of the signal is given by:

$$attn = \frac{1}{(1 + 2\pi nRC)^{1/2}} \tag{3.7}$$

where n is the natural frequency of the eddies.

The time shift between the signal of the ozone monitor and that of the sonic anemometer was found by optimizing the correlation between the two signals, dependent on the time shift between them. This is illustrated in figure 3.5 for three 30 min runs. The maximum absolute correlation occurred at 1.1 s. In this time shift, the delay time due to the residence time of the air in the filterhead, tube and reaction chamber is included. The time shift agrees well with the sum of this delay time (0.8 s) and the time constant of the ozone monitor (0.4 s).

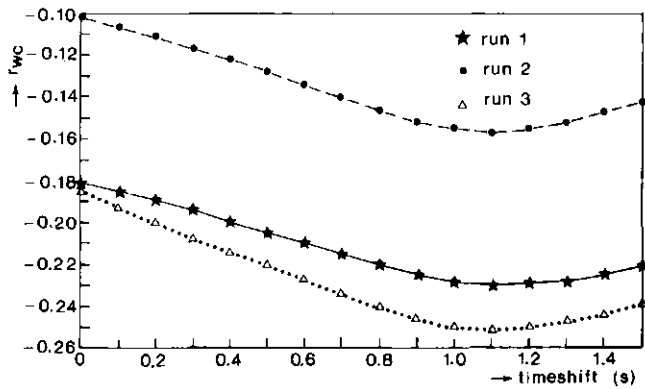


Figure 3.5 The correlation of the fluctuations of the vertical wind and concentration of ozone, r_{wc} , as a function of the time shift between both signals. The positive shift means a shift of the ozone signal ahead of the wind velocity signal. This is indicated for three runs.

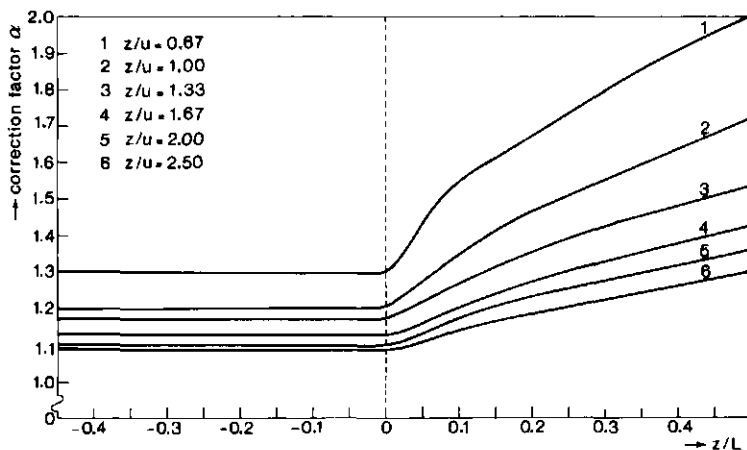


Figure 3.6 The correction factor, α , applied to the flux of ozone dependent on atmospheric stability, z/L , and z/u .

The damping of the fluctuations of the concentration of ozone caused by the tube and the filterhead seemed to be unimportant compared to the attenuation by the monitor itself. The tube and filterhead function like a low-pass filter of about 2 Hz (see Appendix C).

The corrections in b and c are frequency-dependent and should be treated simultaneously on a given spectrum or cospectrum of the flux. Here we used idealized variance and covariance spectra for momentum and sensible heat, taken from Kaimal et al. (1972). The total corrections due to these errors are about 5% for momentum, sensible and latent heat fluxes. For the flux of ozone they are entirely dominated by the limited frequency response of the ozone monitor.

Figure 3.6 shows the correction factor, α , applied to the flux of ozone, dependent on atmospheric stability, z/L , windspeed U and measurement height, z_m . It can be inferred that a loss of about 10-20% of the flux occurred during unstable conditions at moderate wind speeds, i.e. $\bar{U} < 4 \text{ m s}^{-1}$, which was generally the case under our conditions. Under stable conditions this loss was about 30-40 % of the flux.

d) Corrections due to limited averaging time

Because the covariances are averaged over a certain time interval, large-scale eddies with a time scale larger than the averaging time are only partly detected. The loss of this turbulent transport was estimated at 5%, taken from McBean (1972). All fluxes were corrected with this fixed value.

3.3.4 Corrections due to density fluctuations

Webb et al. (1980) showed that a mean vertical velocity due to density fluctuations exists and can be estimated with:

$$\bar{w} = 1.61 \frac{\overline{w'\rho_v'}}{\bar{\rho}_a} + (1 + 1.61\bar{q}) \frac{\overline{w'\theta'}}{\bar{\theta}} \quad 3.8$$

where q denotes the specific humidity.

The fluxes of latent heat and the trace gases were corrected for this effect. For the trace gases all being analyzed at the same temperature only the first term in equation 3.8 was used.

The corrections were smaller than 5%.

3.4 Some environmental conditions and plant parameters

Introduction

In this section some environmental conditions and plant parameters are given which influence the development of maize during the growing season and consequently are important in the interpretation of the measurements.

3.4.1 Plant parameters

Maize was seeded on April 25 and harvested on October 12, 1988. The majority of the seeds sprouted after 2 to 3 weeks. The development of the Leaf Area Index, LAI and the crop height, H_{cr} , are graphically presented in figure 3.7. The LAI is defined as the one-sided leaf area per unit ground surface ($m^2 m^{-2}$). We see that in the beginning of the growing season, the plants grew slowly in length as well as in the LAI. From the second half of June till the second half of July, the crop height and the LAI increased very rapidly to the maximum value for the season, i.e. 2.25 m and 4.6, respectively. In the second half of August the LAI

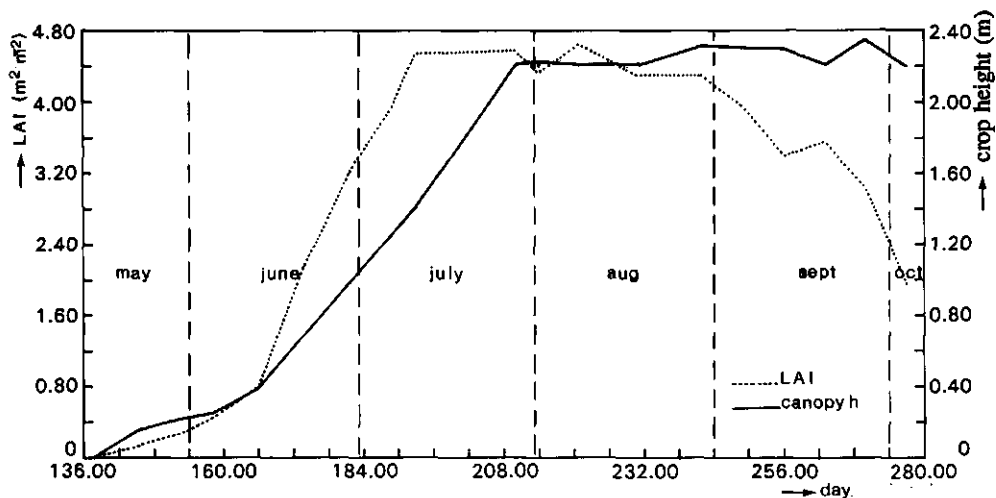


Figure 3.7 The development of the leaf area index, LAI, and the crop height during the growing season of 1988.

decreased slowly till harvesting time while the crop height remained constant. To get a better understanding of the crop structure during the season, the Leaf Area Density, LAD, of the crop for five days is given in figure 3.8. The LAD is defined as the leaf area expressed per unit canopy volume ($\text{m}^2 \text{m}^{-3}$). From this figure it can be inferred that in the beginning of the season the leaves were concentrated in the top layers (see profiles of June 6, June 30, July 11). Progressing into the season the leaves were more equally distributed with height (see profile August 28). When the crop was senescing the bottom half of the leaves were dead (see profile October 3).

The development of the roughness length, z_0 , over the season is given in figure 3.9. The z_0 was calculated from the linear regression between wind measurements and logarithmic height as described in section 3.3.1. The z_0 in the beginning of May was taken from earlier measurements made at the same site above bare soil (Beck, 1988). The z_0 developed from 0.5 cm up to a maximal value in September of 20 cm.

In figure 3.10 the biomass yield differentiated into several plant parts is given. The determination of the root mass was incomplete because only the main root system was sampled. The biomass which was stored in the leaves remains rather constant after the

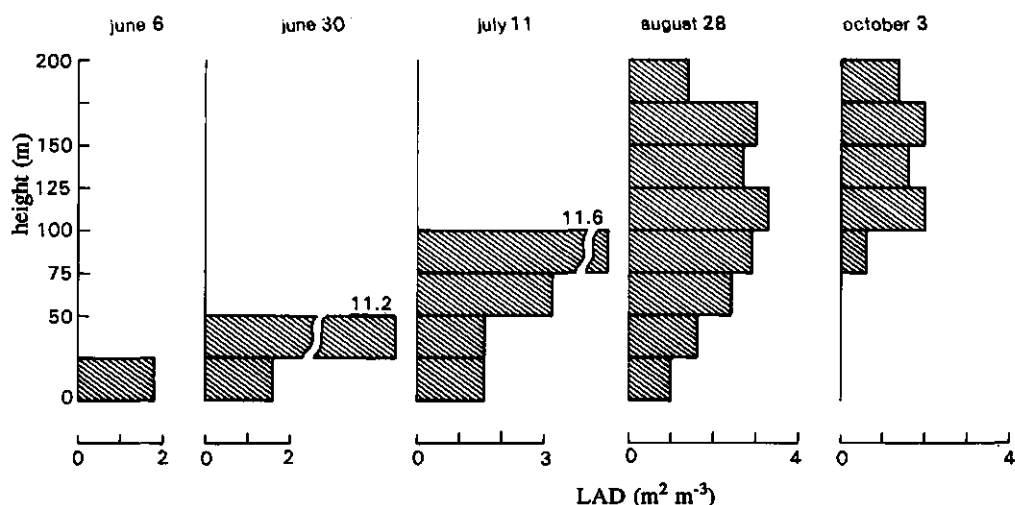


Figure 3.8 The leaf area density, LAD, of the maize crop for five days during the growing season of 1988.

maximum LAI is achieved. The decay of the LAI, starting in August, was caused by the senescing of the leaves, i.e. drying and curling of the leaves, resulting in a smaller LAI with an equal dry-matter content. By the end of July the cobs started to gain in weight. From September on the dry matter of the stems decreased. The crop was still gaining dry matter when it was harvested in October.

3.4.2 Description of the soil

The soil consisted of sand, in which a humic top soil had been developed by the addition of farmyard manure (Halbersma and Przybyla, 1986). The soil consisted of 1.3% C (carbon from the organic compound) and had a P_H of 5.0. The soil particle fraction smaller than $2\text{ }\mu\text{m}$ was 4% and the fraction larger than $50\text{ }\mu\text{m}$ was 78%.

3.4.3 Water balance

There was no direct measurement on the water balance of the crop. However, water soil content and precipitation measurements were done to obtain an insight into the water resources of the plants.

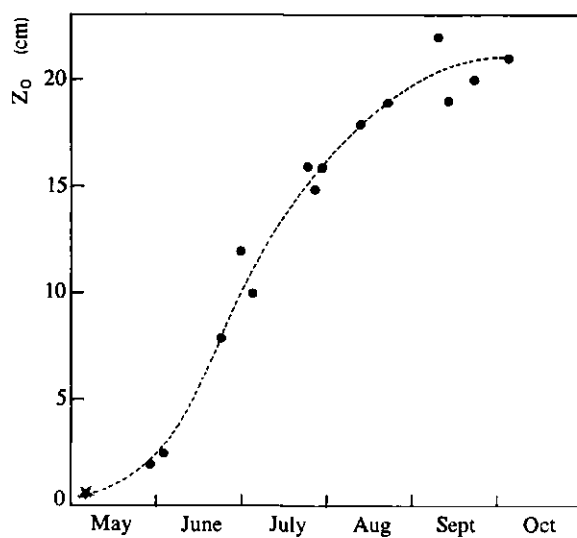


Figure 3.9 The development of the roughness length, z_0 , of the surface, i.e. the soil and the maize crop during the growing season of 1988.

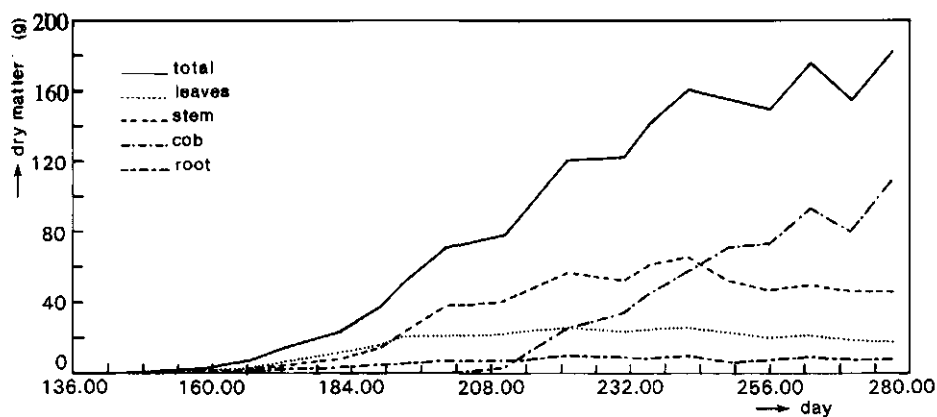


Figure 3.10 The biomass yield of the maize crop during the growing season of 1988, differentiated into several plant parts.

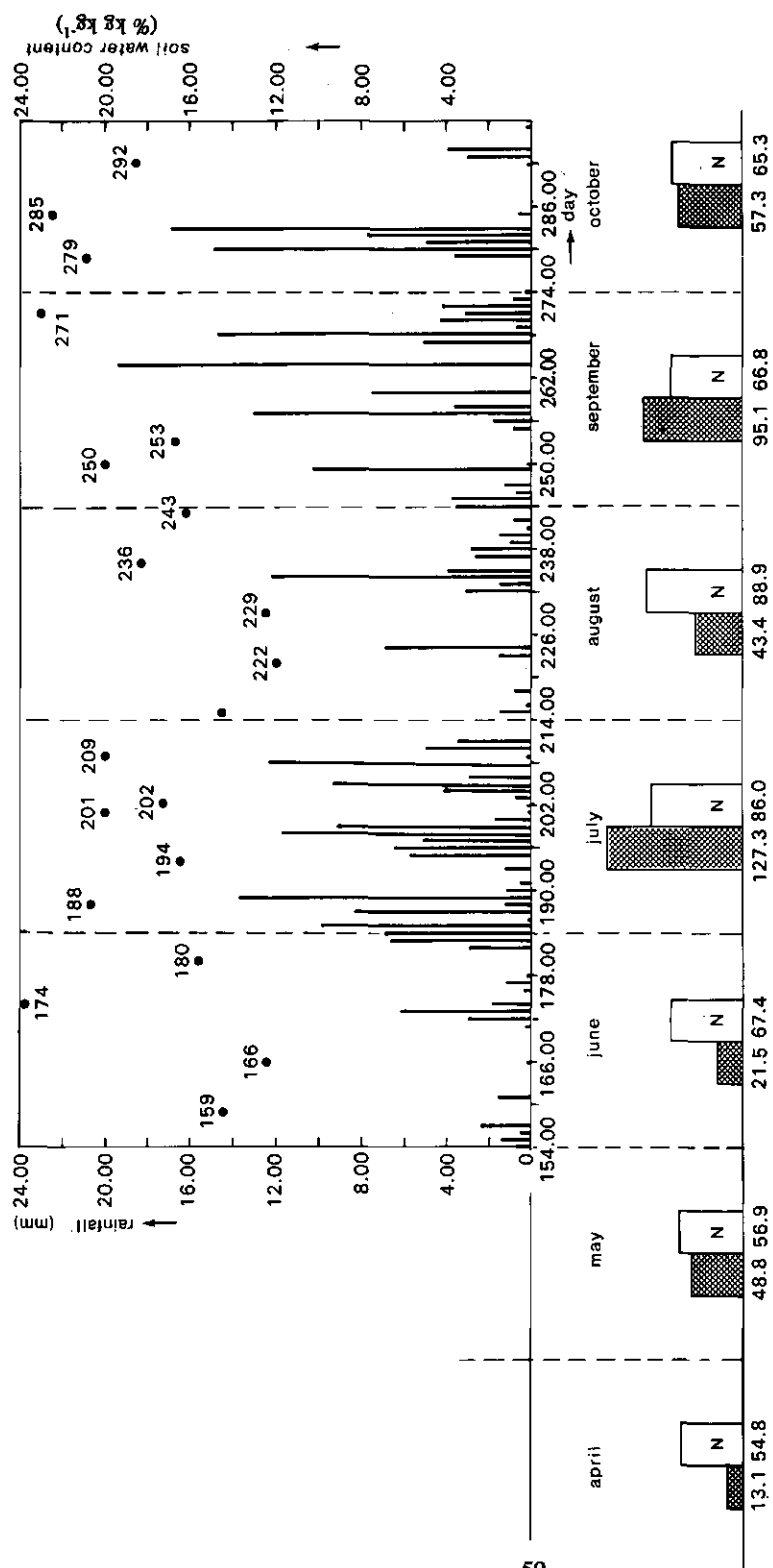


Figure 3.11 The rainfall measurements from June through October 1988 (thin bars). The cumulative monthly rainfall and the average monthly rainfall over the last 30 years are indicated in bar graphs. Data for April and May are taken from the meteorological observation site at Wageningen, about 10 km from the maize field. In the upper part of the figure, the soil water content measurements are indicated with dots.

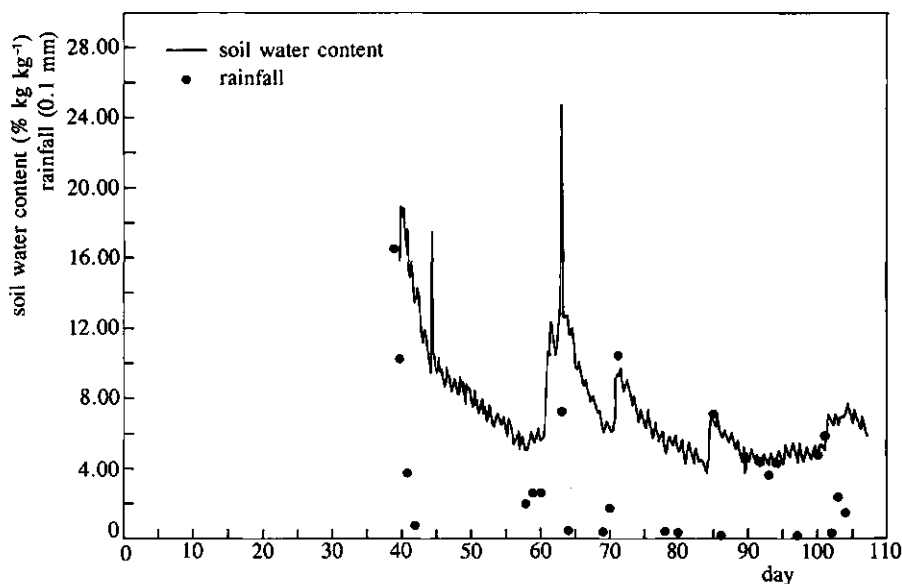


Figure 3.12 Example of continuous soil water content measurements in 1989. Also indicated are the rain events (dots). The time axis indicates the days after seeding.

3.4.3.1 Precipitation

The daily rainfall is depicted in figure 3.11. The growing season of 1988 was not particularly wet but some remarks on the rain distribution throughout the season should be made:

- 1) the months prior to sprouting and the first growing stage till the beginning of June were relatively dry,
- 2) in July the amount of rainfall was 50% higher than normal and rainfall occurred on 28 days,
- 3) in August the amount of rainfall was 50% lower than normal and there was a dry spell of seven days (12-18 August),
- 4) in September and October the rainfall was about normal.

3.4.3.2 Soil water measurements

The soil water content and soil water potential measurements are also depicted in figure 3.11.

We see that the soil water content varied from 12-24% kg kg^{-1} . The water content of the upper 2 cm of the soil varied rapidly during the day due to the soil evaporation on one hand and the percolation and water usage by the roots on the other. The ability of the soil to bind water is illustrated in figure 3.12, with continuous measurements of soil water content in the same soil in 1989. It can be seen that the soil water content dropped sharply after a rainfall. For instance, on day 63 the soil water content decreased from 27 to 13% kg kg^{-1} in a few hours after a rain event of 0.7 mm. During the growing season of 1988, the soil water content never dropped below a value at which the plants were not able to take up soil water.

Chapter 4 Accuracy of the fluxes and comparison of the techniques

In this chapter the accuracy of the fluxes derived with the meteorological techniques will be given. The emphasis lies on the accuracy of the flux of ozone. First the most important sources of error and uncertainty for the three techniques are given in section 4.1. In section 4.2 the uncertainty caused by chemical reactions is discussed. A comparison of the three techniques is made in section 4.3. Finally, in section 4.4 conclusions are drawn.

4.1 Accuracy of the fluxes derived with the meteorological techniques

4.1.1 Profile and modified Bowen ratio technique

The accuracy in the fluxes derived with the profile and modified Bowen ratio techniques are partly caused by the errors in the measured differences of the quantities. For the fluxes derived with the profile technique the accuracy is decreased by:

- the uncertainty in the displacement height, d , and the von Karman's constant, κ ;
- errors in the stability functions, Ψ , due to an error in the calculated Obukhov length scale.

The accuracy in the fluxes derived with the modified Bowen ratio technique is decreased by the errors in the measurements of the energy balance.

The errors can be random or systematic.

4.1.1.1 Errors in the measured differences of the variables

Systematic errors in the measured differences or profiles were kept small by checking the data as soon as they were processed, and if necessary sensors were adjusted or replaced. Also recalibrations were carried out during and after the growing season.

The systematic errors in the measured concentration differences were kept small by using the same monitors and tube lengths and filters etc. So calibration errors or drifts of the monitors were excluded from these differences.

All the sensors measuring the meteorological variables and the trace gas concentrations have an accuracy of about 1 %. This accuracy will generally lead to a much lower accuracy of the

measured differences of the quantities of tens of % and depends strongly on the magnitude of this difference. In table 4.1 the accuracies of the differences along with typical measured differences are shown. These typical differences should be seen as a rough indication of the differences occurring during daytime hours. The accuracy of the differences can be much larger during transition hours, especially for temperature or humidity during night-time. In such cases the inaccuracies can easily exceed 100%.

An example of the course of the concentration of ozone at 2.5 and 6.5 m is given in figure 4.1. It can be seen that the differences between the concentration at these two heights are about $1-4 \mu\text{g m}^{-3}$, i.e. 1-4% of the concentration.

Table 4.1 Typical values for differences, the ratio of the difference with the mean and the accuracy of the differences

Variable	Typical difference and ratio difference/mean in %		accuracy
Wind speed	0.5-1 m s^{-1}	20-40%	10-20%
Temperature	0.1 - 0.5 K	NA	10-40%
Absolute humidity	0.3 - 1.0 g m^{-3}	3-10%	10-40%
Ozone concentration	1 - 4 $\mu\text{g m}^{-3}$	1-5%	10-50%

NA = not applicable

For the fluxes derived from profiles of more than two measurement levels the accuracies are increased by a factor $(n-1)^{-1/2}$ where n is the number of measurement levels.

4.1.1.2 The total accuracy of the fluxes

The uncertainties in the displacement height, d, and von Karman's constant, κ , can lead to errors in the fluxes which might be systematic. The error in the displacement height, d, is estimated assuming an error of 20% in the parameterization of d; for the present measurements this was: $d = 1.50 \pm 0.25$ (m). This leads to an error of about 10% in u_* and s_* under neutral conditions. For the flux of ozone determined from the 2.5 and 6.5 m levels, the error in s_* is 15%. If an uncertainty of 5% in the κ is assumed, i.e. $\kappa = 0.41 \pm 0.02$,

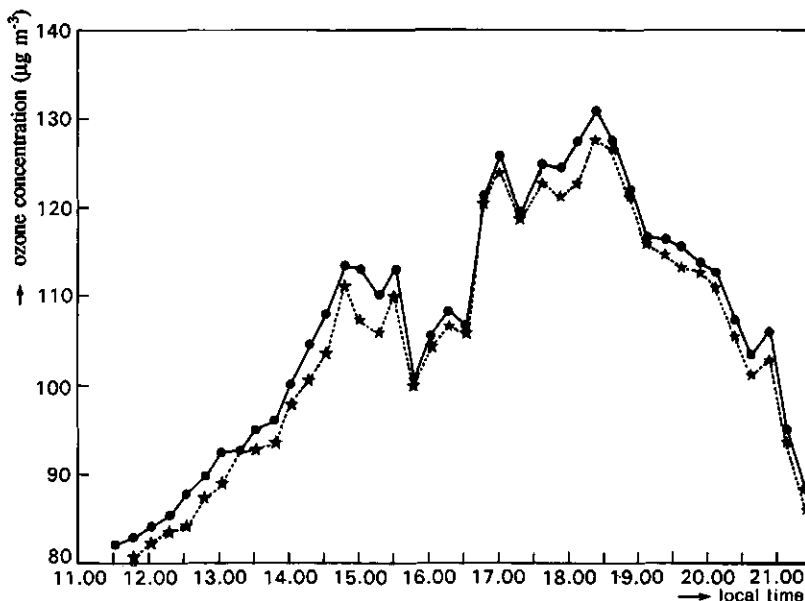


Figure 4.1 The course of the concentration of ozone at 2.5 (stars) and 6.5 m (dots) on July 25, 1988.

this will lead to an uncertainty in u_* and s_* of 5%. Together this could lead to a systematic error of about 20% in the flux of ozone.

The total accuracy of the fluxes was calculated according to the probable error method (described in Fritschen and Gay, 1979; Sinclair et al., 1975 and Appendix F) in which it is assumed that the errors are normally distributed and will compensate each other to a limited degree. The accuracies are depicted in table 4.2 at the end of this chapter. In these calculations the values from table 4.1 were used. Here the systematic errors caused by the uncertainties in the d and κ were neglected.

The error in u_* and s_* , due to the stability functions caused by an error in the Obukhov length scale, L , are estimated to be smaller than 5%. This is due to the fact that the stability functions were relatively small because the measurements were taken close to the surface. This will lead to a decrease of the total accuracy of the fluxes derived with the profile technique of about 10%. The total accuracy of the flux of ozone derived with the profile technique was 20-53%.

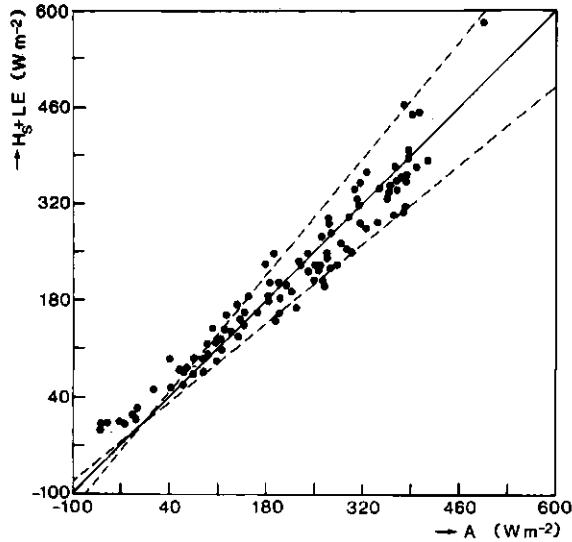


Figure 4.2 The sum of the sensible and latent heat fluxes, $H_s + LE$, derived with the eddy correlation technique against the available energy, A . The dashed lines indicate the 20% deviation of the 1:1 line.

Best regression line $y = 0.90x + 21$ ($cc. = 0.97$) and regression line without intercept $y = 1.00x$ ($cc. = 0.96$).

The error in the fluxes derived with the modified Bowen ratio technique is increased by an error in the energy balance measurements. This error is estimated to be smaller than 5%. The error made in the energy balance during night-time can be larger, caused by dew formation on the pyrrometers. The total accuracy of the measurement of the flux of ozone with this technique was 13-58%.

As can be inferred from table 4.2, the total accuracy of the fluxes is dominated by the error in the differential measurements; those values can be kept as a realistic first estimate of the total accuracy.

4.1.2 Eddy correlation technique

The accuracy of the fluctuation measurements are in the order of 1%. However, the covariances of the fluctuations or the fluxes show a lesser accuracy because the intermittency of the fluxes is much larger than that of the individual signals. This was pointed out in section 2.3. With an averaging time of 30 min the derived accuracy of the flux of ozone is estimated

to be about 20%. So the accuracy of the fluxes derived with the eddy correlation technique is dominated by the variations of the flux itself during a 30 min run.

To give a quality check on the used eddy correlation measurements the sum of the fluxes of sensible and latent heat are plotted against the available energy, A (as defined in section 2.3.20), in figure 4.2. As can be seen the correlation is high and nearly all data lie between the 20% scatter lines, which agrees well with the above estimate. Systematic differences were not detected.

4.2 Uncertainty in the flux of ozone due to chemical reactions

To determine the importance of chemical reactions on the flux of ozone (as discussed in section 2.1), the model of Vilà-Guerau de Arellano et al. (1991) was used in which the set of equations describing the concentrations of ozone and nitrogen oxides are solved. Model runs were made for two days and are discussed in Appendix E. From these model runs it was found that the ratio between the flux at 6 m and at the surface during the day was about 0.9 and ranged between 0.63 and 1.23. The scatter in this ratio is caused, among others by the uncertainties in the reaction constants and the measurements of the concentration of nitrogen oxides. It was also found that the triad of ozone and nitrogen oxides was far out of equilibrium caused mainly by the influence of other chemical reactions with nitrogen oxide. Corrections to the flux of ozone were not applied. This means that on a daily basis the chemical reactions could have caused an uncertainty in the flux of ozone of 5-10%. In other experiments as well it is generally found that the corrections to the flux of ozone due to these reactions are smaller than 10% (Fitzjarrald and Lenschow, 1983; Duyzer and Bosveld, 1988).

4.3 Comparison of the meteorological techniques used

The data used in this section consists of measurement runs for which all three meteorological techniques were available, i.e. 9 days or 94 runs of 30 min. All data were taken during day-time with neutral or unstable atmospheric conditions, except on August 18 when the measurements with the eddy correlation technique were continued till midnight.

A comparison is given between the turbulence parameter, u_* , (friction velocity) and the sensible heat flux, H_s , derived both with the eddy correlation and the profile techniques, see figures 4.3a and b. We see that there is a certain scatter but systematic differences between

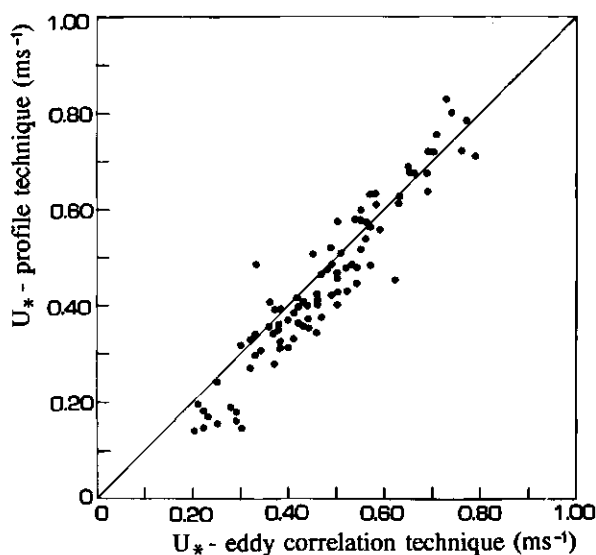


Figure 4.3 a The friction velocity, u_* , derived with the profile technique and the eddy correlation technique.

Best regression line $y = 0.90x + 0.07$ (cc. = 0.95) and regression line without intercept $y = 1.04x$ (cc. = 0.94).

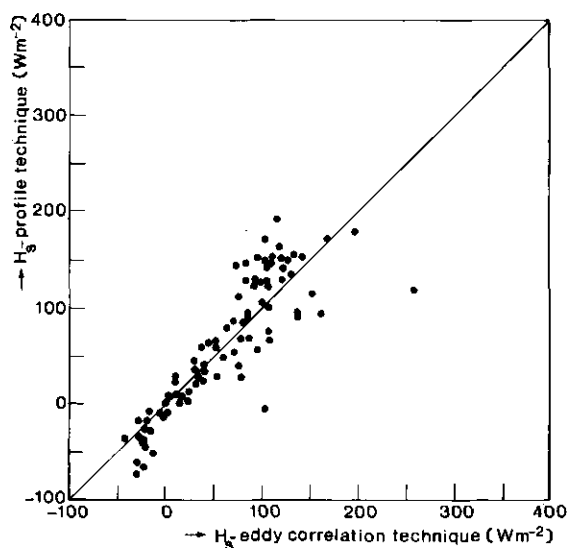


Figure 4.3 b as in a) but for the sensible heat flux, H_s .

Best regression line $y = 1.01x - 1.5$ (cc. = 0.87) and regression line without intercept $y = 1.00x$ (cc. = 0.87).

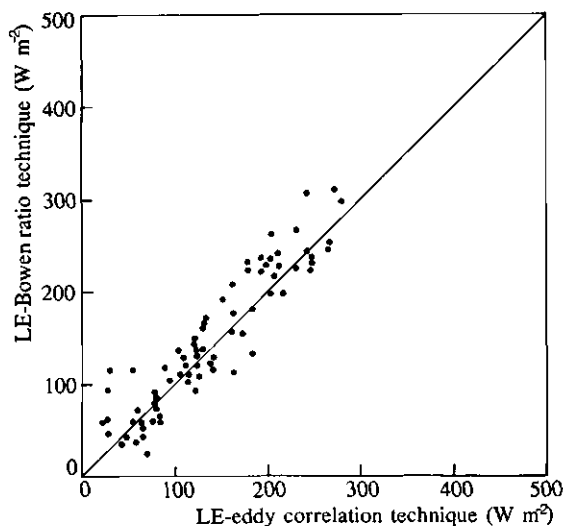


Figure 4.3 c The latent heat flux, LE, derived with the Bowen ratio technique and the eddy correlation technique.
 Best regression line $y = 0.99x + 10.8$ (cc. = 0.93) and regression line without intercept $y = 1.00x$ (cc. = 0.92).

the two techniques were not present. At $u_* < 0.5 \text{ m s}^{-1}$ the profile technique slightly underestimates the u_* by less than 10%. When the sensible heat flux exceeded 100 W m^{-2} the profile technique tended to overestimate this flux by 20%. This can be due to small radiation effects on the psychrometer's energy balance. Nevertheless, it was concluded that the deviations caused by systematic errors like the uncertainties in the displacement height or von Karman's constant were relatively small.

In figure 4.3c the latent heat flux derived with the Bowen ratio technique versus the eddy correlation technique has been depicted. The agreement between the two techniques is good. A small systematic overestimation of 10 W m^{-2} by the Bowen ratio technique was detected. At small fluxes, i.e. $LE < 30 \text{ W m}^{-2}$, the Bowen ratio technique largely overestimated the flux derived with the eddy correlation technique. In these cases the humidity gradients are small, leading to large systematic errors.

A comparison between the fluxes of ozone derived with the eddy correlation, profile and the modified Bowen ratio technique is shown in figures 4.4a,b,c (for convenience sake the sign of the fluxes of ozone was altered). The scatter in figures 4.4a and b is large and mainly due

to random errors in all three techniques. The profile technique evidently showed absolute smaller values than the eddy correlation and modified Bowen ratio techniques. This is possibly due to the fact that the lowest level at which the concentration of ozone was measured was close to the surface, in this case about $6 z_0$. For this data set a reduction of about 40% in the flux of ozone was found. As was discussed in the previous section part of this deviation can be caused by uncertainties in the displacement height. Varying the d for momentum with $\pm 25\text{cm}$, this could only account for about 15% of the observed deviation. Only at $d < 0.75\text{m}$ can this explain deviations larger than 40%. This means that the displacement height for ozone would be considerably lower than for momentum, say about 1 m or half the crop height.

Another explanation can be found in the breakdown of the flux profile relationships close to the roughness elements. It was demonstrated in figure 2.5 that such deviations occur when the height of the roughness layer, $z_* > 25 z_0$ under neutral conditions. With a $z_0 = 0.2\text{ m}$ this $z_* = 5\text{ m}$ (above d). However, with such a thick roughness layer, the fluxes of momentum and sensible heat would also have shown deviations from the eddy correlation measurements (figures 4.3a and b). Therefore it is very likely that both effects were present and did account for the observed reduction in the flux of ozone.

From figure 4.4b it can be inferred that the modified Bowen ratio technique showed no large systematic deviation from the eddy correlation technique. The modified Bowen ratio technique slightly underestimated the flux of ozone by 10%. From this comparison it was concluded that a) the modified Bowen ratio technique is applicable close to the surface (i.e. roughness elements),

b) sensible heat and latent heat (water vapour) and ozone are transported in roughly the same way and

c) chemical reactions did not cause a large divergence of the flux. With the eddy correlation technique the flux was measured at 6 m, whereas the gradient of ozone was determined at the geometrical height, in this case 3.9 m.

The comparison between the profile and the modified Bowen ratio technique showed a much higher correlation, with the latter technique clearly giving larger absolute values. The less scatter indicates that the major error in these fluxes was caused by the error in the differential

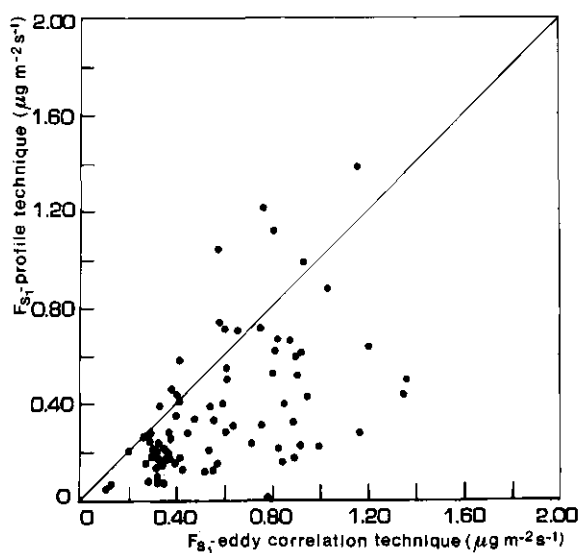


Figure 4.4 a The flux of ozone, F_{S_1} , derived with the profile and the eddy correlation techniques.

Best regression line $y = 0.52x - 0.036$ ($cc. = 0.53$) and regression line without intercept $y = 0.62x$ ($cc. = 0.52$).

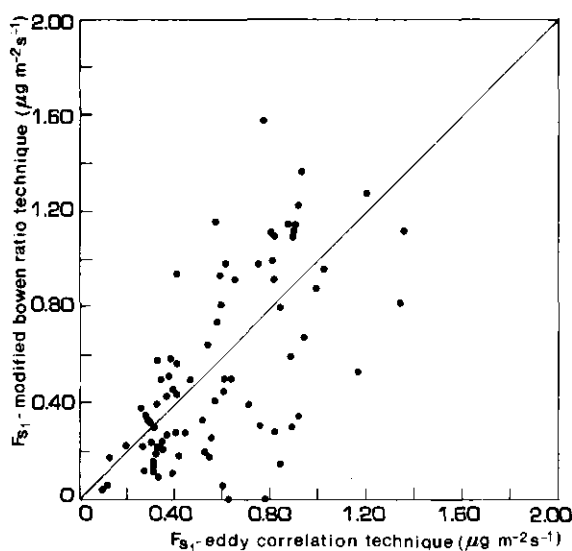


Figure 4.4 b as in a) but for the modified Bowen ratio technique and the eddy correlation technique.

Best regression line $y = 0.85x - 0.020$ ($cc. = 0.63$) and regression line without intercept $y = 0.91x$ ($cc. = 0.63$).

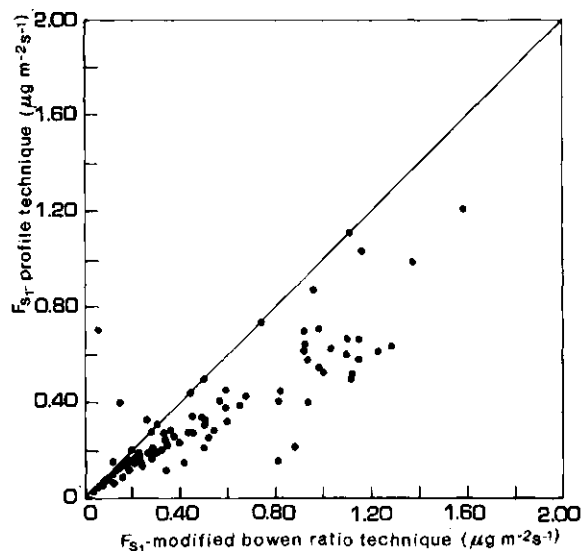


Figure 4.4 c as in a) but for the profile technique and the modified Bowen ratio technique. Best regression line $y = 0.57 x - 0.026$ (cc. = 0.85) and regression line without intercept $y = 0.64 x$ (cc. = 0.84).

measurements of the ozone concentration between 6.5 and 2.5 m. Illustrations of the course of the flux of ozone throughout the day measured with the three meteorological techniques on four days, are given in figure 4.5a-d (for convenience sake the sign of the flux was altered). On June 30, when the measurements were taken well above the surface, the three techniques produced about the same flux of ozone. On the other days it can be seen that the profile technique showed lower absolute values than the other two techniques. The eddy correlation and modified Bowen ratio technique did scatter around the same mean. This indicated that most of the uncertainties in the fluxes are caused by random errors.

The time integrals of the fluxes of ozone in daytime for these nine days are depicted for the eddy correlation and modified Bowen ratio technique in figure 4.6. The differences between the two techniques were small ($\pm 10\%$). This means that a reliable estimate of the daytime deposition of ozone can be obtained by the eddy correlation and the modified Bowen ratio technique with an accuracy of about 10%, though the accuracy of the half-hour values used is much smaller (20-50%).

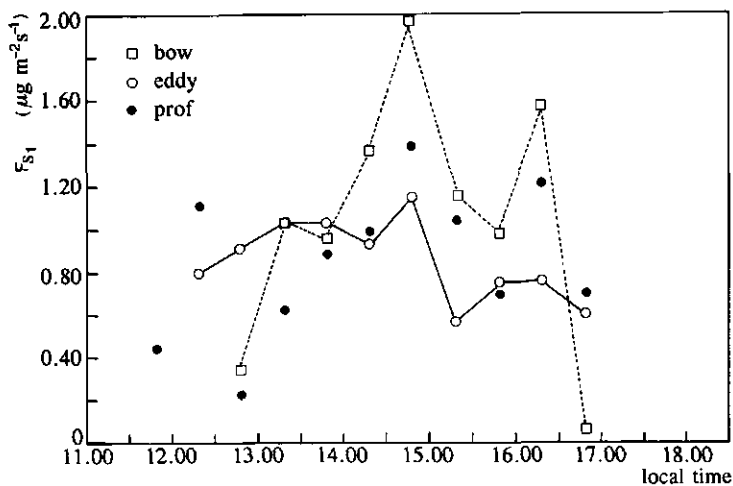


Figure 4.5 a The course of the flux of ozone derived with the eddy correlation, profile and modified Bowen ratio techniques on June 30, 1988.

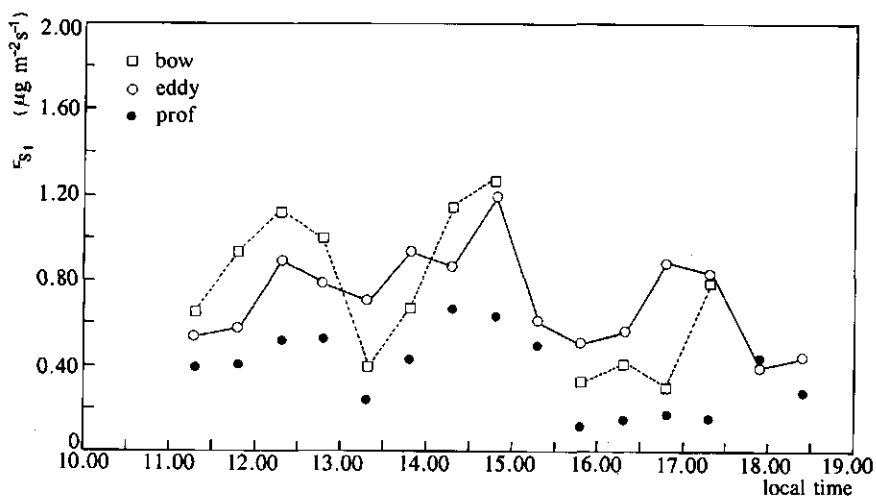


Figure 4.5 b as in a) but for July 25, 1988.

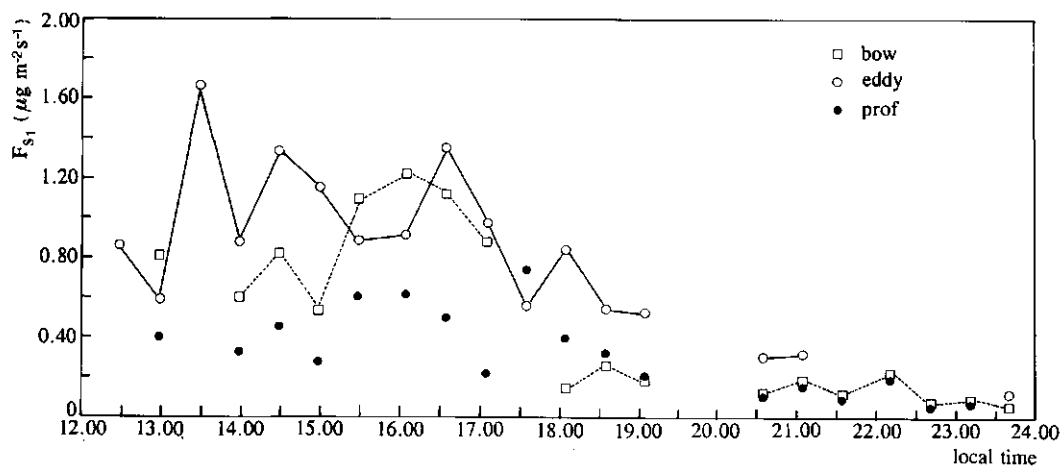


Figure 4.5 c as in a) but for August 18, 1988.

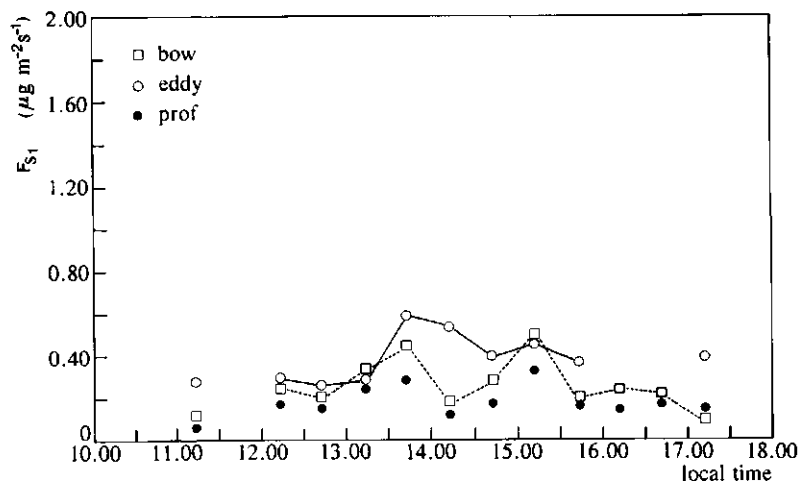


Figure 4.5 d as in a) but for September 22, 1988.

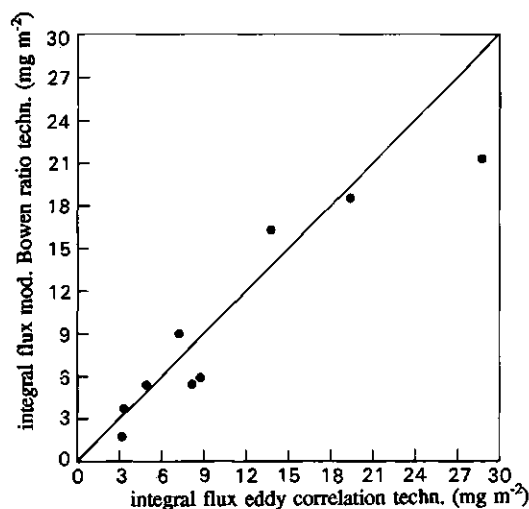


Figure 4.6 The daytime integrals of the flux of ozone derived with the eddy correlation technique and the modified Bowen ratio techniques given for nine days in 1988. Best regression line $y = 0.80x - 549$ (cc. = 0.94) and regression line without intercept $y = 0.87x$ (cc. = 0.94).

4.4 Conclusions

The accuracies of the fluxes were strongly determined by the errors in the measurements of the difference or in the profiles of the variables.

An overview of the inaccuracies of the fluxes of ozone determined with the three different meteorological techniques along with the major error sources and corrections are given in table 4.2.

The profile technique gave systematically lower values for the flux of ozone (determined with the ozone concentration measurements at $6z_{om} + d$ and $30z_{om} + d$) than the eddy correlation and modified Bowen ratio techniques. A reduction of about 40% of the flux of ozone was found during near-neutral and unstable atmospheric conditions. This was caused a) by an inadequate use of the profile technique close to the roughness elements and b) the uncertainty in the displacement height for ozone. The latter indicates that the displacement height for ozone would be much smaller (about 1m or about half the crop height).

The flux of ozone determined with the modified Bowen ratio technique was moderately consistent with that determined with the eddy correlation technique; systematic deviations

were not found. From this comparison it was concluded that a) the modified Bowen ratio technique is applicable close to the surface (i.e. roughness elements), b) sensible heat, latent heat (water vapour) and ozone are transported in roughly the same way and c) chemical reactions did not cause a large divergence of the flux. With the eddy correlation technique the flux was measured at 6 m whereas the gradient of ozone was determined at the geometrical height, in this case 3.9 m.

In order to obtain an accurate estimate on the influence of chemical reactions on the flux of ozone, model runs with a set of equations which describe the concentrations of ozone and nitrogen oxides were made. On a daily basis the systematic deviations between the flux at 6.5 m and 2.5 m were 5-10%.

A reliable estimate of the daytime deposition of ozone (accuracy about 10%) was obtained by the modified Bowen ratio and the eddy correlation techniques though the inaccuracy of the half-hour values is much greater (20-50%).

Table 4.2 Overview of the accuracies of the fluxes of ozone derived with three meteorological techniques. Also the main sources of error and corrections applied are indicated. ΔX is the difference between the measurement levels at 2.5 and 6.5 m.

Technique	Accuracy	Main error source	Corrections applied
Profile	20-53%	Measurements of ΔC	Density fluctuations <5%
Mod. Bowen ratio	13-58%	Measurements of $\Delta C, \Delta T, \Delta p_v$	Density fluctuations <5%
Eddy correlation	20%	Intermittency of the flux in measurement time interval	Density fluctuations <5% flow distortion/tilt correction <7% bad frequency response $L < 0$ <20% $L > 0$ <40% loss of large-scale eddies to flux 5% (fixed value)

Chapter 5 The resistance and conductance of a maize crop and bare soil to ozone

Introduction

In this chapter the resistance and conductance¹ of a maize crop and bare soil to ozone are evaluated from the data obtained in the experiments as described in chapter 3. In section 5.1 a theoretical background of a resistance model will be given which is used in the evaluation of the resistances and conductances from the measurements. The resistance of the bare soil to ozone is given in section 5.2. Section 5.3 discusses the resistances and conductances of a maize crop on several days in the growing season of 1988. A comparison is made between the surface conductance to ozone and the crop conductance to ozone deduced from the crop conductance to water vapour. From this comparison estimates on the partitioning of the flux of ozone to the crop and the soil are made.

5.1 Theoretical background of the resistance model used

In describing the transport of a quantity between a reference height, z_{ref} , and the surface where the quantity is transmitted, destroyed or generated, a resistance model is often used (e.g. Thom, 1975).

In general, the resistance of this layer for the transport of the quantity is calculated as in an electrical analogy. The resistance is the ratio of the driving force, i.e. the difference of the quantity over this height (i.e. such as a potential) and the flux density (i.e. the current) of the quantity. A possible resistance model for the transport of momentum from z_{ref} to a crop and the underlying soil is shown in figure 5.1a. In this model r_{aa} is the resistance to the transport of momentum from z_{ref} to the top of the crop. This resistance is often written as the integral of the eddy diffusion coefficient, K_m , for momentum (defined in equation 2.3.5), over height. At each level in the crop momentum is transmitted by form drag, skin friction and

¹ Both the terms resistance and its reciprocal, conductance, will be used, and do not indicate different variables.

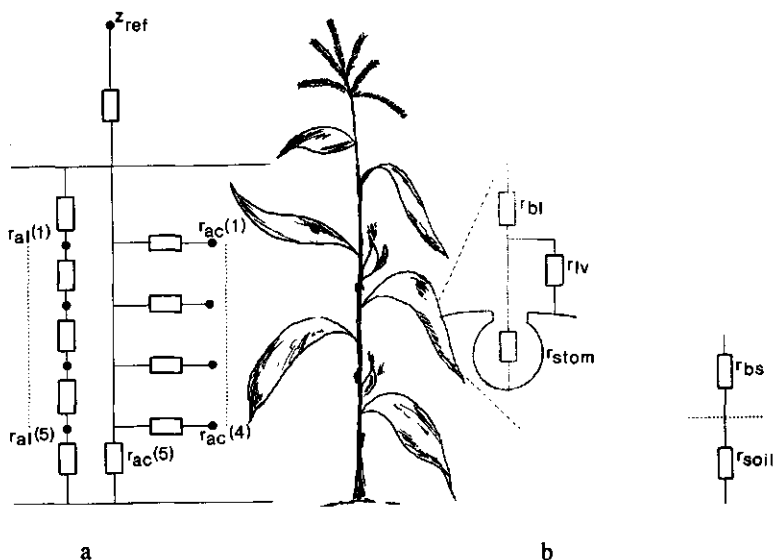


Figure 5.1a Resistance model for the transport of momentum from a reference height z_{ref} to the crop and soil. In b, an extension of a), i.e. for a scalar.

pressure forces to the leaves and stems. At each level therefore a resistance to the transport of momentum is implemented, denoted by r_{al} 's. These values are related to the local eddy diffusion coefficient in each layer. The r_{ac} 's are resistances to the transport of momentum directly from the top of the crop to the different levels in the crop and the soil. The exchange

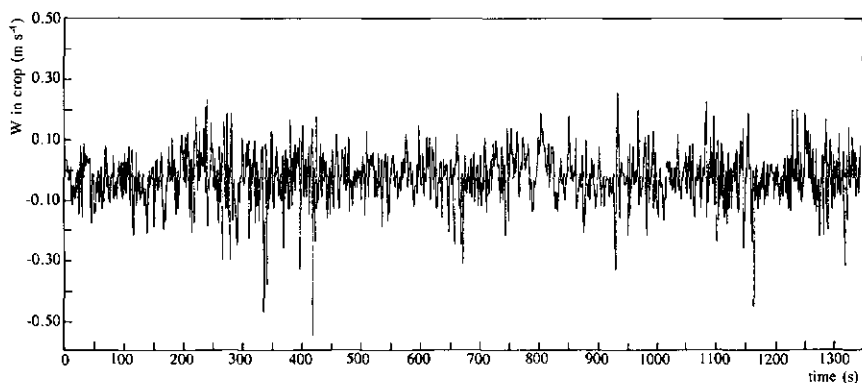


Figure 5.2 Time series of the vertical wind velocity measured in the crop 0.5 m above the surface.

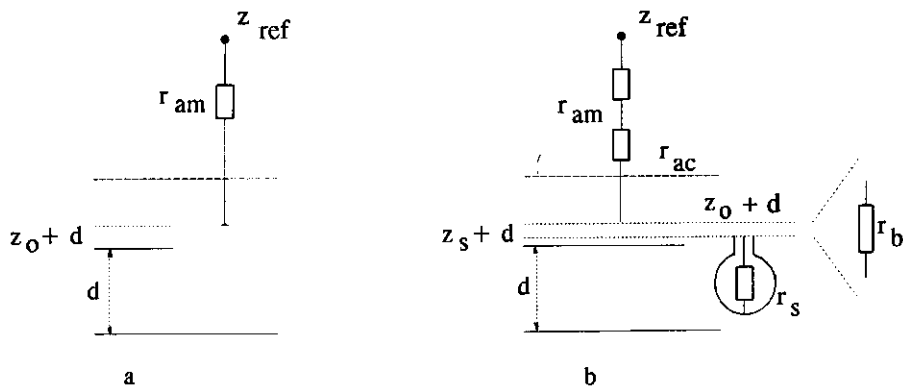


Figure 5.3a Simplified resistance model or Big leaf model for a crop for the transport of momentum. Figure b the same model but for a scalar.

process between the air above the crop and the air in the crop has a strongly intermittent and non-local character (Raupach and Thom, 1981; Finnigan, 1985; Shaw, 1985). Therefore at every level in the crop and at the soil a resistance is needed to describe this non-local exchange with the air above the crop. This intermittency is illustrated in figure 5.2 with a time-series of the vertical wind speed taken in the crop at about 0.5 m. Large downward directed drafts of up to 0.5 m s^{-1} were observed. These so-called gusts of air occurred at about every 100-200 s and lasted for about 5-10 s.

For a scalar the transport process can be described roughly by the same resistance scheme as far as the positioning of the resistances is concerned. To describe the transport to and in the leaves and the soil the scheme in figure 5.1a has to be extended with two resistances as illustrated in figure 5.1b. The r_{bl} and r_{bs} indicate the resistance to the transport in a layer by molecular diffusion close to the leaf and soil surface. A stomatal resistance, r_{stom} , and a soil resistance, r_{soil} , are needed to account for the transport of the scalar in the stomatal cavities and in the pores of the soil by molecular diffusion, and as well for the rate at which the scalar is released or destroyed at the surface. The r_{lv} denotes the resistance to the uptake or release of a scalar at the plant surfaces, i.e. stems, leaves, etc.

We see that a large variety of resistances is needed to describe the exchange process of a

scalar with a crop and the underlying soil. It is not an easy task to determine all the numerical values of these resistances. For that reason often an even more simplified resistance model is used, especially in the description of the transport of water vapour and air pollution (e.g. Fowler, 1978; Baldocchi et al., 1987; Hicks et al., 1989). The major simplification exists in the neglect of the physical shape of the vegetation; so no vertical distribution of sources and sinks of quantities are modelled. This model is often referred to as the so-called 'Big leaf' model (this type of model was introduced earlier by Penman in 1948). This simplified resistance model for momentum and scalars is given in figure 5.3a and b.

From figure 5.3a we see that for momentum the resistance r_{am} is used to describe the total resistance of the transport between z_{ref} and $z_0 + d$. The r_{am} consists of the original r_{aa} in figure 5.1a and a resistance which is the sum of all the resistances in the crop, which are coupled in series or parallel, accounting for the transport and transmittance of momentum in the crop. In figure 5.3b the total resistance, r_{as} , for the transport of a scalar from z_{ref} to the surface, consists of at least four resistances which are coupled in series. So this r_{as} can be written as:

$$r_{as} = r_{am} + r_{ac} + r_b + r_s \quad . \quad 5.1$$

For the transport of the scalar to the surface, which contains several sinks or sources for every particular scalar, the resistance, r_s , is incorporated. When considering the transpiration this surface resistance is always considered as the resistance of one big stomate from which all the water vapour is released.

The flux profile relationships (see section 2.3.2) can be used as a framework to reveal the significance and values of the resistances in this model.

The resistance, r_{am} , to the transport of momentum between z_{ref} and z_0 is by definition, for example Thom (1975):

$$r_{am} = \frac{\bar{U}(z_{ref}) - \bar{U}(z_0)}{u_*^2} = \frac{\bar{U}(z_{ref})}{u_*^2} \quad . \quad 5.2$$

With the use of the flux profile relationships (see section 2.3.2) we get:

$$r_{am} = \frac{1}{u_* \kappa} \left[\ln\left(\frac{z-d}{z_0}\right) - \psi_m\left(\frac{z-d}{L}\right) \right] . \quad 5.3$$

The resistance, r_{as} , to the transport of the scalar from z_{ref} to the leaf surface, stomata or the soil surface is :

$$r_{as} = \frac{\bar{S}(z_{ref}) - \bar{S}(0)}{F_s} , \quad 5.4$$

where $\bar{S}(0)$ is the concentration of the scalar at $z=0$.

This resistance is better known in its reciprocal value, the deposition velocity, V_d , as defined by Chamberlain (1953), (see section 2.1.1).

A resistance, r_{sc} , to the transport of a scalar from z_{ref} to $z_s + d_s$ can be written as:

$$r_{sc} = \frac{\bar{S}(z_{ref}) - \bar{S}(z_s + d_s)}{F_s} , \quad 5.5$$

where d_s is the displacement height for the quantity S .

As already stated in section 2.3.3, this displacement height as a first approximation for a scalar, d_s , was assumed to be similar to that for momentum. Differences between these two length scales and the roughness length scales (see section 2.3.2) indicate the different levels of the sources and sinks between momentum and the scalar.

Again, with the use of the flux profile relationships, this difference of a scalar quantity between the height, z_{ref} , and the vegetated surface or stomata, can be written as:

$$\Delta \bar{S} = \bar{S}(z_{ref}) - \bar{S}(z_s + d_s) = \frac{s_*}{\kappa} \left[\ln\left(\frac{z-d_s}{z_s}\right) - \psi_s\left(\frac{z-d_s}{L}\right) \right] , \quad 5.6$$

where z_s is the ' z_0 ' for the quantity S (see section 2.3.2).

Dividing both sides of equation 5.6 with the flux, F_s , defined as $u_* s_*$ (as in equation 2.3.7), equation 5.5 can be rewritten as:

$$r_{sc} = \frac{1}{u_* \kappa} \left[\ln\left(\frac{z-d}{z_0}\right) + \ln\left(\frac{z_0}{z_s}\right) - \psi_m\left(\frac{z-d}{L}\right) + \psi_m\left(\frac{z-d}{L}\right) - \psi_s\left(\frac{z-d}{L}\right) \right] , \quad 5.7a$$

or:

$$r_{sc} = \frac{1}{u_* \kappa} \left[\ln\left(\frac{z-d}{z_0}\right) - \psi_m\left(\frac{z-d}{L}\right) \right] + \frac{1}{u_* \kappa} \left[\psi_m\left(\frac{z-d}{L}\right) - \psi_s\left(\frac{z-d}{L}\right) \right] + \frac{1}{u_* \kappa} \ln\left(\frac{z_0}{z_s}\right) . \quad 5.7b$$

Now we can split r_{as} or V_d^{-1} into three different resistances.

The aerodynamic resistance, r_{am} , as was defined in equation 5.2. Note that if a r_{am} is calculated in the roughness layer with the use of equation 5.3, it can possibly be in error due to the modification of the flux profile relationships in that layer (see section 2.3.2).

An excess aerodynamic resistance, r_{ac} , which accounts for the difference in the atmospheric stability functions between momentum and a scalar quantity.

The resistance, r_b , is the correction in the profile relationships for different z_0 between momentum and scalars. For heat the value of $\ln(z_0/z_s)$ is about 2 for rough surfaces (Wesely, 1983). For ozone this value has to be corrected for the difference in molecular diffusion between heat and ozone, i.e. by multiplying this ratio by $Le^{2/3} = (K/D(O_3))^{2/3} = 1.2$ (Monteith, 1973). The r_b is often expressed as:

$$r_b = \frac{1}{u_* B} , \quad \text{where} \quad B = \kappa \left[\ln \frac{z_0}{z_s} \right]^{-1} . \quad 5.8$$

This B is called the resistance ratio (Chamberlain, 1966). With the value used here $B=0.167$.

The difference between the resistances to turbulent transport of momentum and a scalar from a reference height to the z_0 of the quantity can be given with the ratio:

$$\frac{r_{am}}{r_{sc}} = \frac{r_{am}}{r_{am} + r_{ac} + r_b} . \quad 5.9$$

So in this simple resistance model all the resistances to the transport of momentum to the

crop and the soil are incorporated in r_{am} . For a scalar these resistances are incorporated in r_{ac} and r_b as well.

The concentration difference in the last pathway in the resistance model can be written as:

$$\bar{S}(z_s + d_s) - \bar{S}(0) = F_s r_s = u_* s_* r_s \quad . \quad 5.10$$

Equation 5.10 can be used along with equations 5.4, 5.5 and 5.7, and r_s will end up as the last link in the chain of the resistances:

$$r_{as} = V_d^{-1} = r_{am} + r_{ac} + r_b + r_s \quad , \quad 5.11a$$

or

$$r_s = V_d^{-1} - (r_a + r_{ac} + r_b) \quad . \quad 5.11b$$

In most cases the density or concentration of the quantity at the surface cannot be measured. Assumptions or estimates on this surface value have to be made. For instance, the water vapour pressure in the stomata of plants is saturated at the leaf temperature (Monteith, 1963). For ozone, a very reactive chemical component, the concentration at the surface, i.e. at the stomatal tissues (Thomson et al., 1966, Heath, 1975) or soil pores, is assumed to be zero (Turner et al., 1973).

The resistance model depicted in figure 5.3 is often used in two different ways. One is to estimate the flux of a quantity. With estimates or measured values of the resistances the deposition velocity, V_d , is calculated with equation 5.11a. Using this value, along with a measured or modelled concentration of the quantity, the flux is found. This is often applied in air pollution models (Wesely, 1989, Hicks et al. 1991).

Another way in which the resistance model is used, is to reveal the value of r_s for a scalar. Using measurements of the fluxes of momentum, sensible heat and a scalar, along with the measurements of the wind speed, temperature and concentration of the scalar, all the resistances, except r_s , in equation 5.11b can be calculated. Now the resistance, r_s , can be found as a residual resistance. This residual resistance is often regarded as the surface resistance of the 'Big leaf' suggesting that it depends solely on the properties of the surface and the component. However, by calculating the surface resistance as a residual resistance all the shortcomings of the resistance model are incorporated. For instance, the transport of a

quantity in a crop is not modelled and will add another variation in this resistance. As well, the uncertainty in the assumption on the concentration at the surface leads to an erroneous surface resistance.

5.2 The resistance of bare soil to ozone

5.2.1 Method of calculation

The resistance model as depicted in figure 5.3 was used to show the resistances of bare soil to ozone from the measurements of the fluxes. A selection from the data set of the continuous measurements in 1988 was made where the LAI of the crop was smaller than 0.5. This coincided with a coverage of the soil by the crop of less than 10%. So the measured flux of ozone was mainly caused by the destruction of ozone by the soil.

The resistance, r_{soil} , of the bare soil were calculated with:

$$r_{soil} = \frac{\bar{S}_1(z_{ref})}{F_{S_1}} - (r_{am} + r_{ac} + r_b) \quad , \quad 5.12$$

where F_{S_1} is the flux of ozone in $\mu\text{g m}^{-2} \text{s}^{-1}$ and $S_1(z_{ref})$ the concentration of ozone at z_{ref} (here the concentration at 6.5 m).

The resistances r_a , r_{ac} and r_b were calculated with the terms given in equation 5.7b. The r_{ac} was generally smaller than 10% of r_a . The fluxes of ozone and sensible heat were derived with the modified Bowen ratio technique; the flux of momentum was calculated with the profile technique.

The uncertainty in the calculated resistances is dominated by the uncertainty in the flux of ozone and so is estimated at 20-50%. The uncertainties in r_a , r_b and r_{ac} are estimated at about 20% each. Generally, the sum of these three resistances is much smaller than the surface resistance (< 20%) leading to a small influence on the uncertainty of the surface resistance.

5.2.2 Results and discussion

The harmonic mean of the soil resistances to ozone during daytime between 1200 and 1600 h (local time) for this data set are given in table 5.1.

An example of the course of the resistance to ozone is demonstrated in figure 5.4 from May

Table 5.1 The harmonic mean of the soil resistances to ozone between 1200 and 1600 h for four days in 1988

Date	r_{soil} (s m ⁻¹)
May 26	145
May 30	212
May 31	244
June 3	244

30-31. From 1700-1900 h on May 30 there was a spell of rain of 3.5 mm. The resistances on those days ranged from about 120-600 s m⁻¹.

The resistances given in table 5.1 are higher compared to those found for other types of soils but are only slightly higher than resistances found for sandy soils (Turner et al., 1973, Galbally and Roy, 1980). Apparently ozone is destroyed relatively slowly at sandy surfaces. The diurnal variations in the resistance of the soil to ozone can be due to variations in the state of the soil, like the soil temperature and soil wetness. The soil temperature did not vary much on these days. The soil water content varied because of rainfall and dew rise. The resistance on May 30 increased after this rain from 150 to 300 s m⁻¹. Clearly on both days

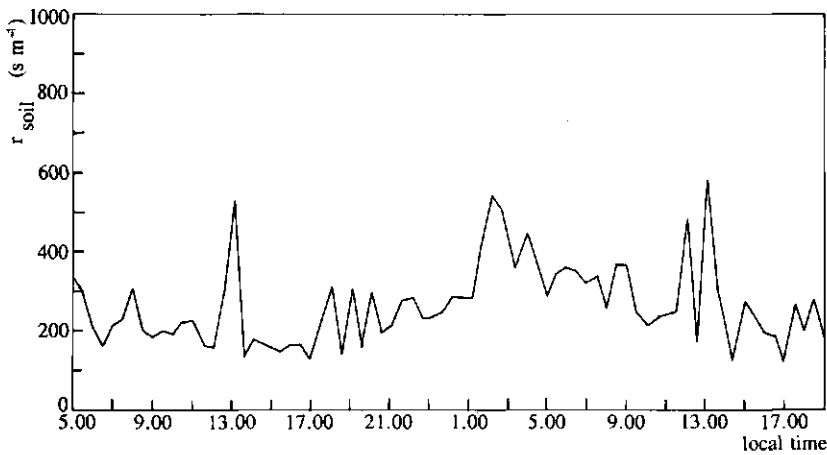


Figure 5.4 The pattern of the soil resistance to ozone, r_{soil} , May 30-31, 1988.

a gradual decrease in the soil resistance to ozone from 400 s m^{-1} in early morning to about 120 s m^{-1} at 1700 h took place. This can be due to the drying of the top soil.

In many experiments a strong dependency of the resistance on the soil water content is found for various soils (Turner et al., 1973; Leuning et al. 1979; Galbally and Roy, 1980). Two main reasons are given for this observed dependency. One is that ozone is destroyed much slower at a wetted surface or free water. The surface resistance to ozone found in measurements above water and snow are about $1000\text{-}2000 \text{ s m}^{-1}$ (Wesely et al., 1981). The second reason is that a wet soil surface has a smaller effective surface at which the ozone can be destroyed due to the water film around the soil particles and in which the pores are filled with water. This dependency was also found in an experiment carried out in gas exchange chambers with the soil of the measuring site at different soil water content levels (see Appendix D). It was found that the resistance of the soil decreased from 120 to 70 s m^{-1} as the soil water content decreased from 14 to 0% (kg kg^{-1}). Turner et al. (1973) found a surface resistance for sand to ozone of 68 s m^{-1} .

5.3 The resistance and conductance of a maize crop and the underlying soil to ozone

5.3.1 Method of calculation

The surface resistance, r_s , and conductance, V_s , to ozone was calculated with:

$$r_s = V_s^{-1} = \frac{\bar{S}_1(z_{ref})}{F_{S_1}} - (r_{am} + r_{ac} + r_b) \quad . \quad 5.13$$

As was pointed out in section 5.1 this r_s is the resistance of the surface, i.e. the crop and the underlying soil, to ozone.

An estimate on the uptake of ozone by the crop via the stomata was made in the following way. The assumption was used that if water vapour is released by the stomata meanwhile ozone is transported into the stomata by molecular diffusion and destroyed at the stomatal tissues (mesophyll tissues). This analogy between ozone uptake and water vapour release is found in many experiments using various vegetations (Rich et al., 1970; Mukhammal, 1965; Turner et al., 1974). An estimation of this uptake was made using the crop conductance to water vapour, V_w , calculated as:

$$V_w^{-1} = \frac{\bar{\rho}_v(T_{leaf}) - \bar{\rho}_v(z_{ref})}{E} - (r_{am} + r_{ac} + r_b) , \quad 5.14$$

where: E is the absolute humidity flux in $\text{kg m}^{-2} \text{s}^{-1}$,

$\rho_v(z_{ref})$ is the absolute humidity at z_{ref} in kg m^{-3} ,

$\rho_v(T_{leaf})$ is the absolute humidity in the stomata at leaf temperature T_{leaf} .

The $\rho_v(T_{leaf})$ is estimated as:

$$\rho_v(T_{leaf}) = \frac{e_s(T_{leaf})}{R_v (T_{leaf} + 273.15)} ,$$

where R_v is the gas constant for moist air. The saturated water vapour pressure was estimated with equation 3.3.

The T_{leaf} is estimated as:

$$T_{leaf} = \frac{H}{\rho_a c_p} (r_{am} + r_{ac} + r_b) + T(z_{ref}) ,$$

where $T(z_{ref})$ is the air temperature at z_{ref} .

To obtain the crop conductance to ozone, V_c , the V_w was corrected for the difference between the molecular diffusion coefficient of water vapour and ozone:

$$V_c = D(\text{O}_3)/D(\text{H}_2\text{O}) V_w = 0.61 V_w . \quad 5.15$$

Important in this estimate is the assumption that the measured evapotranspiration from which V_w is calculated, originates mainly from the transpiration by the crop through the stomata. Generally the transpiration of a healthy plant is entirely through its stomata (e.g. Jarvis, 1981; Monteith, 1973).

The evaporation of the soil underneath a maize crop is relatively small, studied by Al-Kaisi et al. (1989) and Jacobs et al. (1987). They found that the soil evaporation contributed less than 5% to the total evapotranspiration when the LAI of the crop was greater than 2. This was even the case in well watered conditions. Tanner and Jury (1976), and Choudhury and Monteith (1988) showed that the soil evaporation was severely diminished, i.e. less than 5% of the total evaporation as the vegetation above the soil had an LAI greater than 1.

The difference between the surface conductance to ozone, V_s , and the crop conductance to ozone, V_c , can be used to observe additional pathways for the destruction of ozone. This

excess conductance, V_{exc} , and excess resistance, r_{exc} , reads:

$$V_{exc} = r_{exc}^{-1} = V_s - V_c \quad . \quad 5.16$$

In this excess resistance all possible sinks for ozone other than the stomata are incorporated, such as the resistance to the transport of ozone to the lower plant parts and the soil.

An estimate on an in-crop aerodynamic resistance, r_{inc} or $r_{ac}(5)$ in figure 5.1a, the resistance to non-local transport from above the crop to the soil, can be made by subtracting a soil resistance to ozone from this r_{exc} .

The uncertainties in the surface conductance, V_s , is dominated by the uncertainty in the flux of ozone and is about 20%. The uncertainty in the crop conductance, V_c , is somewhat greater because of the uncertainty in the difference between the absolute humidity in the stomata and at the reference height, which was about 20%. The total uncertainty in V_c is estimated at about 30%.

5.3.2 Data used and results

A selection of 10 days was made in which the crop development ranged from the exponential growing stage to senescing. The data from the incidental measurements was used, i.e. the fluxes of momentum, sensible and latent heat, and ozone were measured with the eddy correlation technique. The soil was covered entirely by the crop (with a LAI>3). All data before 1200 h local time was discarded to avoid a large contribution of the evaporation of the remaining free water present as dew or interception water after rainfall during the night or early morning (not after 0900 h local time). The amount of dew was generally smaller than a few tenths of a mm as measured on several days throughout the season (Jacobs et al., 1990). On these selected days there was enough energy available to evaporate the dew in a few hours. The same holds for the interception water after a rain shower. It has never been observed that the crop contained free water on the leaves. On July 6, 19 and 28 and September 12 the top of the soil surface was still wet due to rainfall a few hours prior to the measurements. The crop has never been subjected to water stress as was already pointed out in section 3.4.

The surface conductances to ozone, V_s , and the crop conductance to ozone, V_c , were averaged

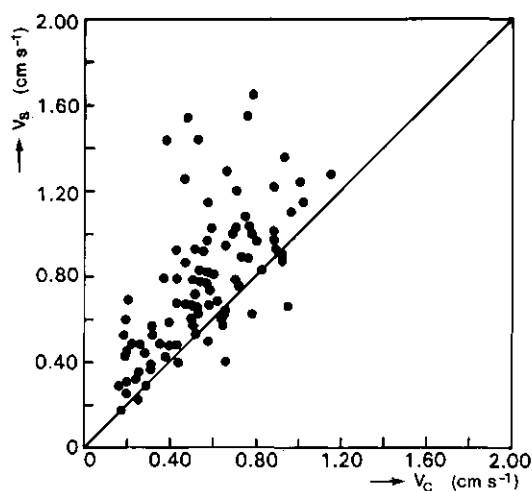


Figure 5.5 The surface conductance to ozone, V_s , versus the crop conductance to ozone, V_c , for 10 days in 1988.

from 1200-1600 h local time (i.e. 1000-1400 GMT, on October 4 this was 1100-1500 GMT) and are presented graphically in figure 5.5. In this period the conductances show the smallest variations in time and so a more representative value of the conductances could be obtained.

In Table 5.2a the global radiation, R_g , the Bowen ratio, β , the friction velocity, u_* , the ozone concentration and flux, S_1 and F_{S_1} , as well as in Table 5.2b the resistances and conductances are given as means or ranges of the half-hour runs from 1200-1600 h local time. Also the flux of ozone to the crop and soil are given as a percentage of the total flux of ozone.

In figures 5.6 a-f six examples of the daily course of V_c and V_s are given. In figure 5.7 a-f, the fluxes of sensible and latent heat, H_s and LE ; the available energy, A , and the flux and the concentration of ozone, F_{S_1} , and S_1 , on these six days are given. For a convenient presentation the sign of the flux F_{S_1} has been changed. The figures 5.6 and 5.7a-f can be found at the end of this chapter.

The r_{inc} was calculated for measuring days where the soil was relatively dry and a fixed tentative value of 150 s m^{-1} for the soil resistance was used according to the results in section 5.2.

Table 5.2a Global radiation, Bowen ratio, friction velocity, concentration and flux of ozone for 10 days in 1988.

Date in 1988	Global radiation (W m ⁻²) range	Bowen ratio mean	Friction velocity (m s ⁻¹) mean	Concentration of ozone (µg m ⁻³) range	flux of ozone (µg m ⁻² s ⁻¹) range
June 30	242-813	0.56	0.35	100-184	0.57 - 1.15
July 6*	314-856	0.30	0.56	82-102	0.61 - 0.82
19*	138-592	0.70	0.39	40-104	0.31 - 0.90
25	288-802	0.40	0.71	74-98	0.40 - 1.20
28*	315-745	0.48	0.39	76-98	0.27 - 0.60
Aug. 12	131-602	0.25	0.54	84-114	0.50 - 0.85
18	554-656	0.46	0.43	64-214	0.10 - 1.36
Sept. 12*	67-435	0.00	0.68	42-54	0.34 - 0.42
22	126-479	0.73	0.39	32-82	0.28 - 0.54
Oct. 4	262-422	2.00	0.33	72-84	0.30 - 0.39

The asterik indicates days on which rainfall occurred a few hours prior to the measurements.

5.3.3 Discussion

General

The surface resistance to ozone, r_s , ranged from 79 to 175 s m⁻¹ (table 5.2b). This is lower than the resistances found for the soil in section 5.2. For this data this means that the destruction of ozone by the crop and the underlying soil was twice that of bare soil. Figure 5.5 shows the correlation between the surface conductance to ozone, V_s , and the crop conductance to ozone, V_c . It can be seen that the V_s was generally larger than the V_c . The best linear regression being a 1:1 line with a positive offset; $V_s = V_c + 0.2$ (cc. = 0.64). This means that besides the uptake by the stomata there was clearly another important sink of ozone. On average for these 10 days the excess conductance, V_{exc} , was 30% of the total conductance of the surface to ozone or, in other words, 30% of the flux of ozone was to the

Table 5.2b The aerodynamic resistances, r_a , the resistance, r_b , the surface conductance, V_s , the crop conductance, V_c , the surface resistance, r_s and r_e , the excess conductance and resistance, V_{exc} and r_{exc} , r_{inc} , and percentage of the total flux of ozone to the crop and the soil for 10 days in 1988.

Date in 1988	r_a, r_b ($s\ m^{-1}$) mean	V_s, V_c ($m\ s^{-1}$) mean	r_s, r_e ($s\ m^{-1}$) harmonic mean	V_{res}, r_{res} ($m\ s^{-1}$, $s\ m^{-1}$) mean	r_{inc} ($s\ m^{-1}$)	% of F_{S1} to crop and soil resp.
June 30	31, 20	0.85, 0.40	118, 250	0.45 222	72	47, 53
July 6	21, 12	0.91, 0.74	110, 135	0.16 602		81, 19
19	27, 17	0.87, 0.88	115, 114	<0 >1000		100, 0
25	14, 9	1.26, 0.74	79, 135	0.52 192	42	59, 41
28	25, 16	0.66, 0.69	151, 145	<0 >1000		100, 0
Aug. 12	18, 13	0.82, 0.57	122, 175	0.25 400	250	70, 30
18	21, 16	0.73, 0.48	137, 208	0.25 400	250	66, 34
Sept.12	11, 9	1.00, 0.86	100, 116	0.14 714	120	86, 14
22	19, 16	0.91, 0.54	110, 185	0.37 270	120	59, 41
Oct. 4	20, 19	0.57, 0.20	175, 500	0.37 270		35, 65

soil and the remaining plant parts. In table 5.2b it can be seen that this value ranged between 0 and 65%. Leuning et al. (1979a) and Wesely et al. (1978) found in their experiments above a mature maize crop that the flux of ozone to the soil varied from 20-50% of the total flux of ozone.

As can be inferred from figures 5.6 a-f the surface conductance of ozone, V_s , showed a large variation throughout the day, i.e. a large midday value around $1\ cm\ s^{-1}$ and decreased to a much lower night-time value of $0.2\ cm\ s^{-1}$, as on August 18. This is observed in many studies above all kind of vegetation (maize: Wesely et al., 1978; Leuning et al., 1979a; grass: Delany, 1986; soybean: Hicks et al., 1989). In these studies the variation is attributed to the daily variation in the stomatal aperture. The crop conductance, V_c , showed a smaller variation, which indicated that also during night-time ozone is taken up by the crop. However, the measured evapotranspiration is small, which led to a large uncertainty in the calculated crop

conductance. Besides, it is uncertain whether the contribution of the soil transpiration to the evapotranspiration was as small as it was during daytime.

From table 5.2b it can be seen as well that the differences between the average conductances, V_s and V_c , varied considerably from day to day. Some aspects on these differences will be described below and are illustrated with examples.

Influence of soil wetness

On July 19 and 28 the differences between V_s and V_c were very small. The correlation between the half-hour values of V_s and V_c during those days was relatively high, as is illustrated on July 19, figure 5.6b. For these days this would mean that nearly all the ozone was taken up via the stomata and no other large sink was present. On these days the soil was still wet due to rainfall a few hours prior to these measurements. The good correlation between V_s and V_c , on a half-hourly basis, thus indicated as well that ozone is slowly destroyed at the wet soil surface and also at the remaining plant parts such as the cuticle. The resistance of the cuticle to ozone is found larger than 1000 s m^{-1} in experiments (Baldocchi et al., 1987; Meyers and Hicks, 1988).

On June 30, July 25, August 18, September 22 and October 4, V_s and V_c differ significantly, as can be inferred from the diurnal patterns of the conductances in figure 5.6 a,c,d,e,f. No rainfall occurred prior to the measurements so the soil surface was relatively dry. Generally, during these days the correlation between the two conductances was low, with a systematically larger V_s than V_c , about a factor of 2. These measurements clearly showed that an extra sink of ozone was present. About 50% of the flux of ozone was directed towards the soil and the remaining plant parts.

Influence of u_a and LAI

Besides the influence of the soil wetness, the variations in the exchange of the air above the crop with the soil and the lower plant parts also played an important role in the observed differences between V_s and V_c . This exchange process is dependent, among others on turbulence and the leaf density of the crop. The influence of turbulent mixing on the exchange process was illustrated, using u_a as an indicator of this mixing, with the measurements on July 6, 19, 28 and September 12. As can be inferred from table 5.2a rainfall occurred a few hours prior to the measurements. The u_a on July 6 and September 12 were higher, about 0.5-0.6 m

s^{-1} than on July 19 and 28, when it was about $0.3\text{--}0.4 \text{ m s}^{-1}$. The difference between the V_s and V_c was very small on the days with the lower u_* but on days with a higher u_* there was a small difference, indicating that there was some destruction of ozone at the soil and remaining plant parts (of about 16%). The same influence of u_* on the exchange process was observed on July 25 and August 18 as well. On these two days the soil was dry while the u_* was higher on July 25 than on August 18 (0.71 and 0.43 m s^{-1} respectively) resulting in a higher difference between V_s and V_c .

The influence of the leaf area density on the exchange process can be demonstrated by the measurements on June 30, August 18, September 22 and October 4. On these days there was a large difference between V_s and V_c . The u_* ranged from $0.3\text{--}0.4 \text{ m s}^{-1}$ and it was expected that the turbulent mixing on these days was not very different from each other. The leaf area density on these days differed largely, as can be inferred from figure 3.6 (section 3.4). On June 30 the crop was still growing, with a majority of the leaves in the t.p layers. On September 22 and October 4 the crop was senescing, resulting in a less dense crop. It was in particular on October 4 that the leaves were yellow and vertically inclined. It can be seen from table 5.2b that in the less dense crops especially on June 30 and October 4, the difference between the V_s and V_c was relatively great which indicated a greater exchange with the soil and lower plant parts.

The in-crop aerodynamic resistance, r_{inc} , ranged from $42\text{--}250 \text{ s m}^{-1}$ (see Table 5.2b) and should be seen as an indicative value. This resistance has about the same value as the soil resistance to ozone of about 150 s m^{-1} . The dependence of u_* and LAI on r_{inc} was similar, as described above for the exchange process, i.e. lower values of r_{inc} are found for days with a relatively high u_* or relatively low LAI.

This means that if the extra pathway in the destruction of ozone is modelled by means of a simple resistance model, the in-crop resistance should be taken into account.

Influence of atmospheric stability

In the afternoon of June 30, July 25, August 18 and September 22 (figures 5.6 a,c,d,e) the V_s decayed and approached the value of V_c . This indicated that the strength of the sinks other than the stomata diminished. This coincided with an increase of the atmospheric stability, i.e. the sensible heat flux decreased or became negative (figures 5.7 d,e). Which may be caused by the decrease of the exchange of the air above the crop with the soil and remaining plant

parts. A very significant reduction in the penetration of gusts into a forest canopy was observed by Shaw et al. (1988) when the stability of the air above the forest turned from unstable to stable. At this point the top layer of the crop is the most important sink of ozone resulting in similar conductances of the surface and the crop to ozone. This means that the observed daily variation in the surface conductance above a crop is caused by the transpiration of the crop, as well as by the diminished exchange of air above the crop with the soil due to atmospheric stability effects.

5.3.4 Conclusions

The conductance of ozone to a maize crop is determined by the uptake of ozone by the stomata, the destruction of ozone at the soil surface and the transport of ozone to the soil. When the soil surface was wet (i.e. rainfall occurred a few hours before the measurements), the surface conductance and the crop conductance to ozone coincided. The conductance of the remaining plant parts to ozone was small compared to the stomatal or soil conductance to ozone.

The exchange of ozone with the soil was dependent on the turbulent mixing (expressed with u_*), the stability of the air flow above the crop and the leaf area density.

The typical daily pattern in the surface conductance to ozone was caused by the state of the aperture of the stomata as well as by the variations in the exchange process between the air above the crop and the soil due to stability effects.

Under dry soil conditions, the flux of ozone to the soil was 25-50% of the total flux of ozone. If the flux of ozone under such conditions, is described with a simple resistance model, the extra destruction at the soil should be modelled using an in-crop aerodynamic resistance.

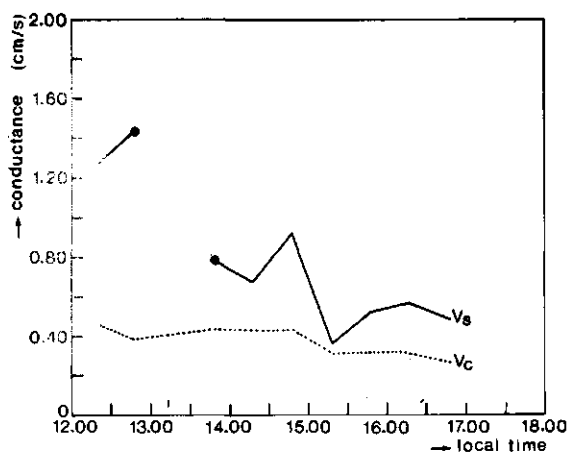


Figure 5.6 a Daily course of the surface conductance to ozone, V_s , and the crop conductance to ozone, V_c , on June 30, 1988.

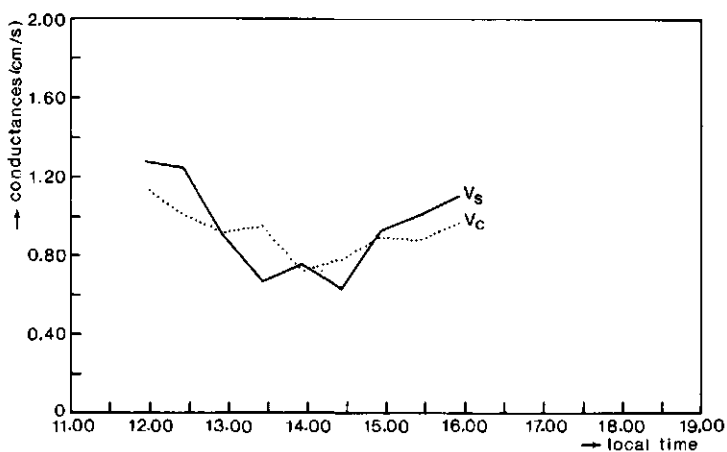


Figure 5.6 b as in a) but for July 19, 1988.

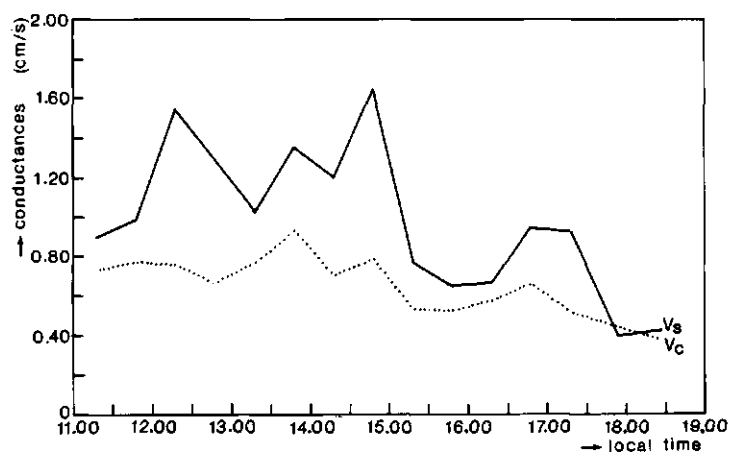


Figure 5.6 c as in a) but for July 25, 1988.

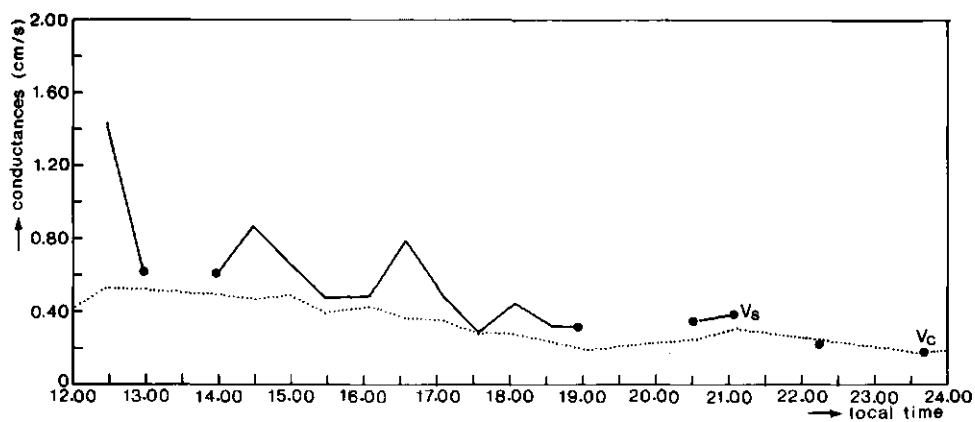


Figure 5.6 d as in a) but for August 18, 1988.

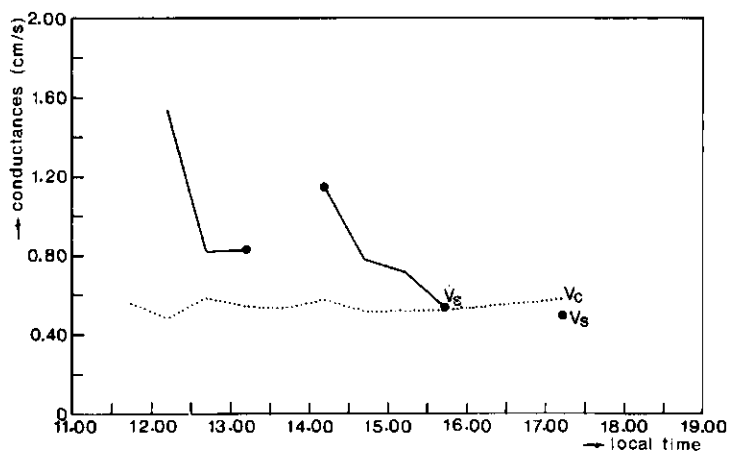


Figure 5.6 e as in a) but for September 22, 1988.

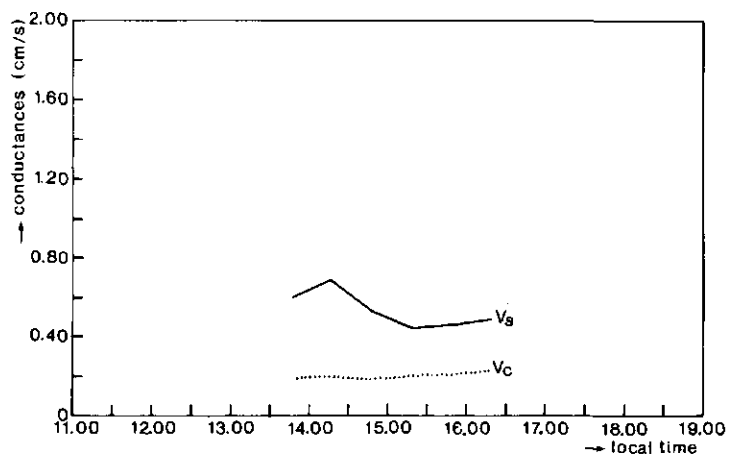


Figure 5.6 f as in a) but for October 4, 1988.

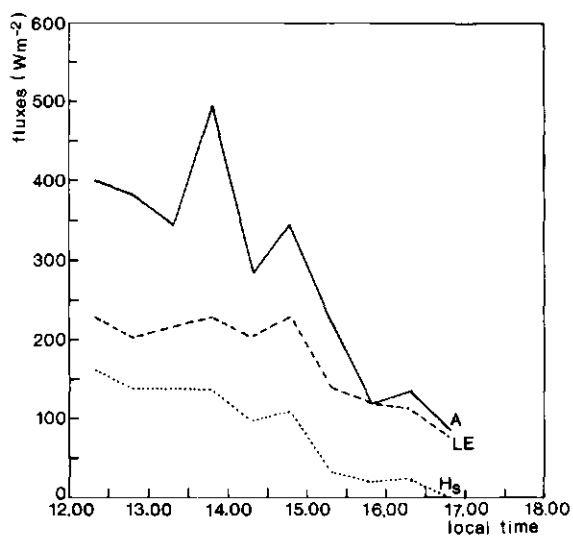
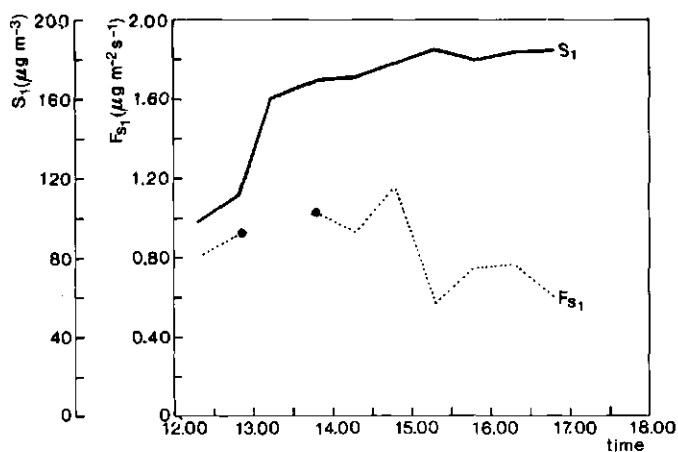


Figure 5.7 a The flux and the concentration of ozone (F_{S1} and S_1) in upper figure and the fluxes of sensible and latent heat (H_s and LE) and the available energy (A) in lower figure on June 30, 1988.

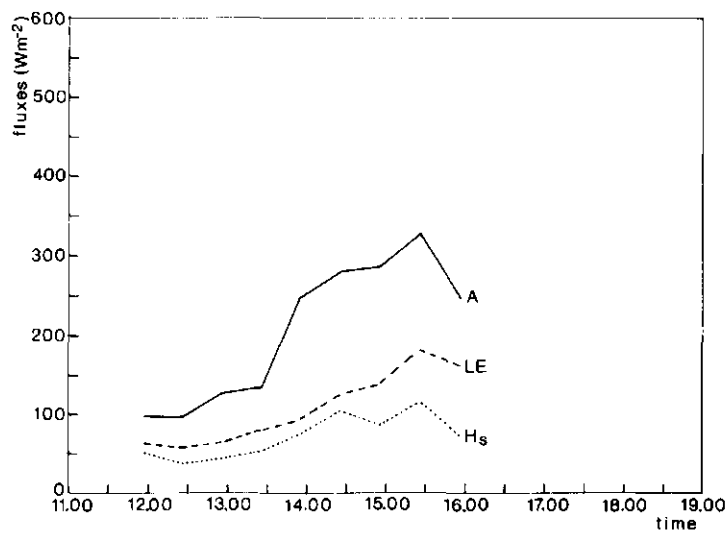
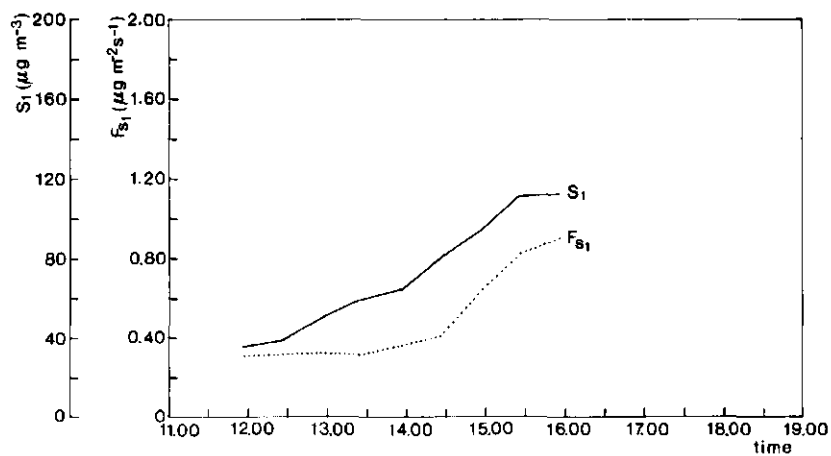


Figure 5.7 b as in a) but for July 19, 1988.

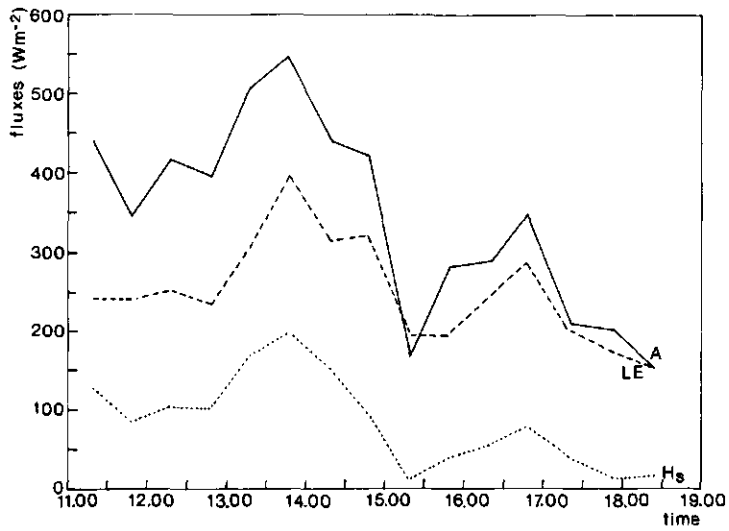
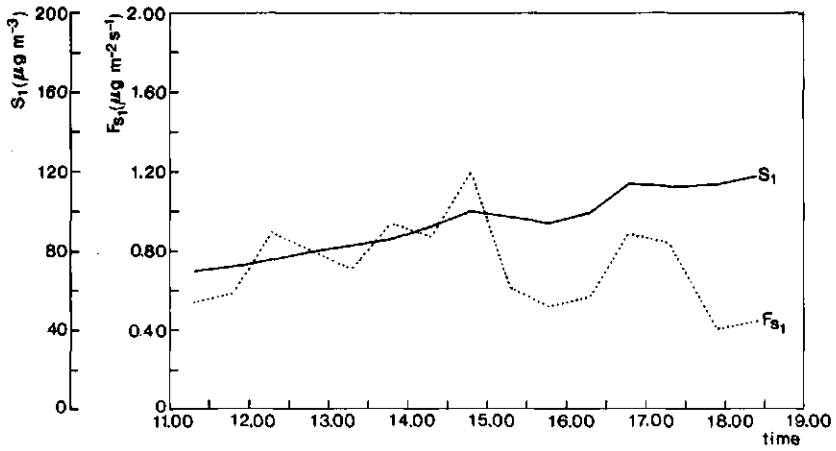


Figure 5.7 c as in a) but for July 25, 1988.

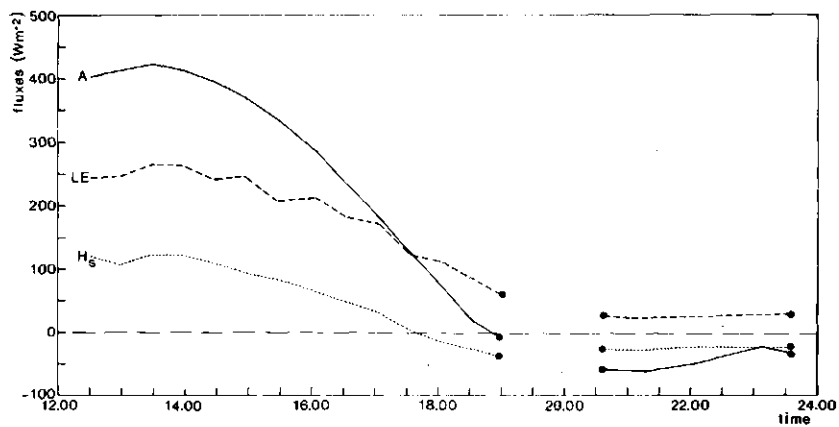
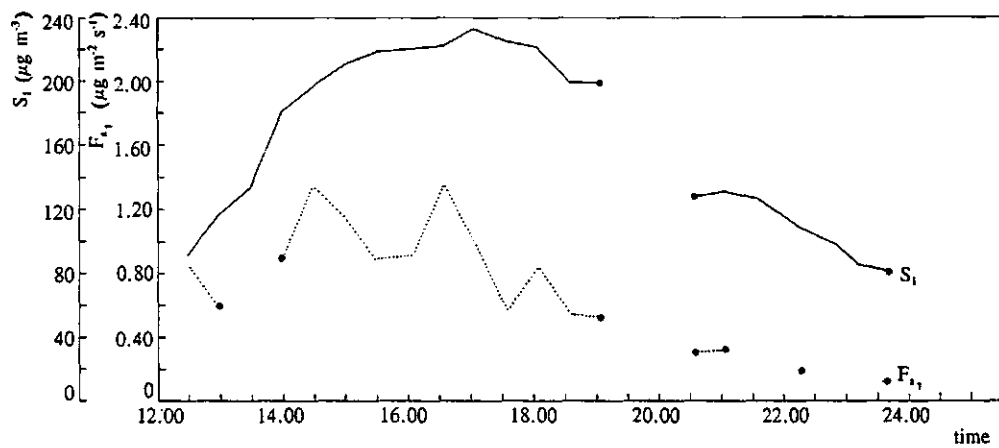


Figure 5.7 d as in a) but for August 18, 1988.

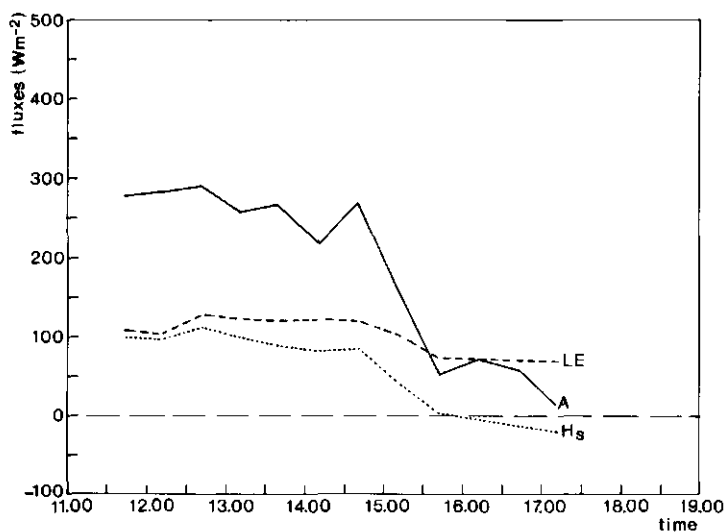
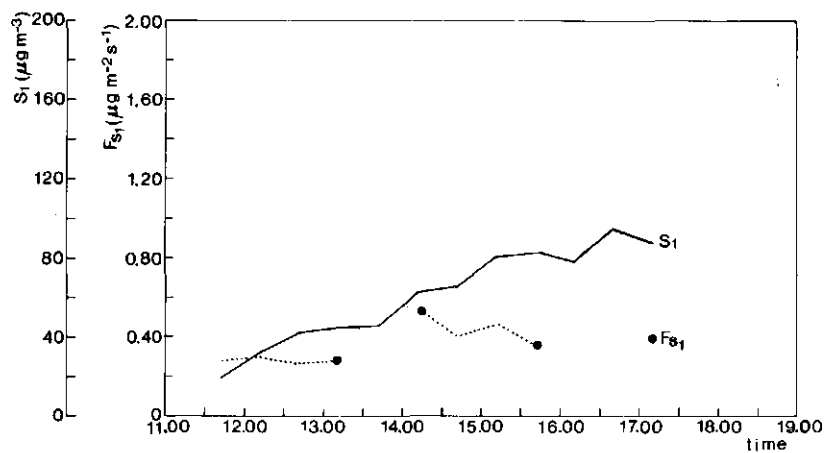


Figure 5.7 e as in a) but for September 22, 1988.

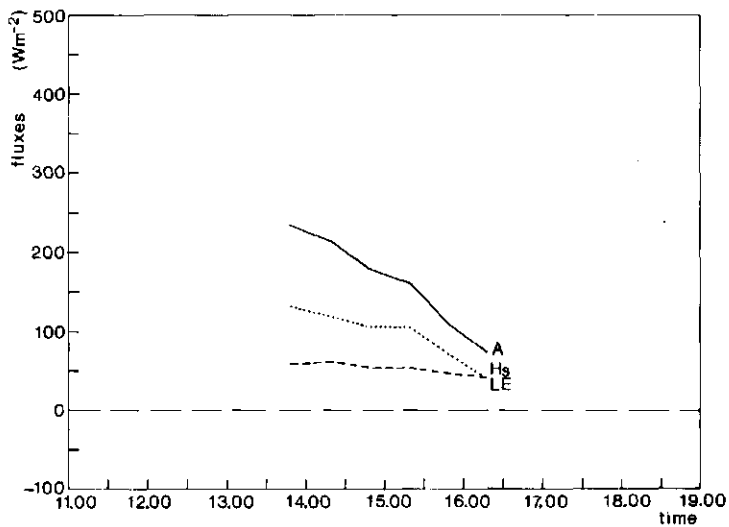
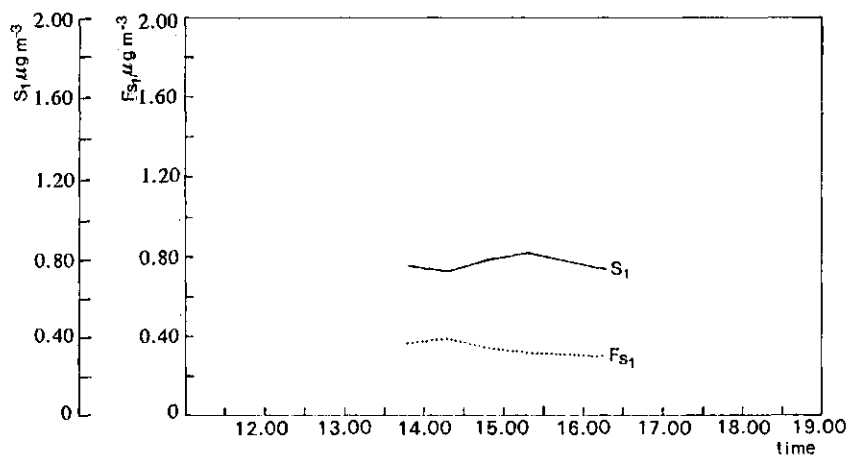


Figure 5.7 f as in a) but for October 4, 1988.

Chapter 6 Overview of the deposition of ozone and its governing factors during the growing season of maize in 1988

Introduction

In this chapter an overview of the deposition of ozone, as well as its governing factors such as the concentration of ozone and the surface resistance (and conductance) to ozone, are presented for the growing season of maize in 1988. All data were derived from the continuous measurements. The emphasis lies on the time integrals of the fluxes or the deposition of ozone. This deposition is partitioned into an uptake of ozone by the crop and the destruction of ozone at the soil, according to the findings in section 5.3. Also some assessments on the daytime deposition (deposition during daylight) and crop uptake of ozone, using mean measured variables, are presented. In section 6.1 the method of calculation is given. In section 6.2 the results are presented and discussed. Conclusions are given in section 6.3.

6.1 Method of calculation

From the continuous measurement data set of 1988, 23 days were selected on a fetch-to-height ratio of 40:1 and no large gaps in the time series of the measurements were present i.e. not larger than 1 h. For this data set, time integrals were calculated of the flux of ozone derived with the modified Bowen ratio technique as explained in section 2.3.3 and 3.3.1. Omissions were filled in with data assuming that the previous value would serve as the best estimate. This was not repeated more than twice per gap. During night-time the fluxes were assumed to be zero if the equations used in the profile technique did not converge or if $\bar{U} < 1 \text{ m s}^{-1}$. A check was done on the value of the fluxes so that they were not larger than 1.6 times the value derived with the profile technique during unstable and neutral atmospheric conditions (the profile technique generally underestimated the fluxes by 40% under such circumstances, see chapter 4). If the fluxes could not be calculated due to malfunctioning of sensors used in the modified Bowen ratio technique, again 1.6 times the flux derived with the

profile method was taken.

The integrals were calculated for a certain period (between t_1 and t_2) as follows:

$$I_x = \int_{t_1}^{t_2} F_{S_1} dt , \quad 6.1$$

where F_{S_1} is the flux of ozone.

The integrals or deposition were calculated over three periods:

total deposition I_t : with t_1 at early morning between 0000-0600 h (local time) and t_2 the same but for the next day,

daytime deposition, I_d (deposition during daylight): with t_1 the time when the global radiation, R_g , becomes greater than 0 and t_2 the time when R_g becomes smaller than 0 and

midday deposition I_m : with t_1 is 1200 h and t_2 is 1600 hours (local time), i.e. for all days measured before September 25, 1000-1400 GMT otherwise 1100-1500 GMT.

The following averages were calculated over the same period of time as the daytime flux, I_d :

- the deposition velocity, V_d , of ozone with equation 2.1.9,
- the surface and crop conductance, V_s and V_c , to ozone with equations 5.13 - 5.15 and the surface resistance, r_s ,
- the mean concentration of ozone during daytime $[O_3(d)]$ and day and night $[O_3(dn)]$,
- the dose as: dose = $[O_3(d)] (t_2 - t_1)$.

The daytime uptake of ozone by the crop, I_c , was estimated with:

$$I_c = \frac{V_c(4)}{V_s(4)} I_d , \quad 6.2$$

wherein the 4 indicates an average between 1200-1600 h (local time). The destruction of ozone by the soil and the lower plant parts, I_{so} , was estimated with:

$$I_{so} = I_d - I_c . \quad 6.3$$

The mean V_c was calculated from 1200-1600 h to avoid the influence of the evaporation of dew and rain on the transpiration measurements. In the case of measurement problems the V_c

derived with the eddy correlation technique was used. So, in this approach it was assumed that the ratio between the two conductances was representative for the entire day.

An estimation of the daytime deposition of ozone, $I_d(\text{est})$, was made by:

$$I_d(\text{est}) = \bar{V}_d [\bar{O}_3] (t_2 - t_1) \quad . \quad 6.4.$$

For a convenient presentation of the results the sign of the fluxes was changed. So a positive value of a deposition means a net loss of mass per m^2 per time period $t_2 - t_1$. All flux integrals or depositions are in mg m^{-2} ; the dose is expressed in $\text{mg m}^{-3} \text{ h}$.

The accuracy of 10% of the flux integrals presented in chapter 4 was typically valid under daylight conditions so, for the daytime and midday deposition. During night-time, as pointed out in the same chapter, the quality of the fluxes was uncertain due to much larger errors in the differential and radiation measurements. Also omissions (which mostly occurred during night-time) increase the uncertainty. However, the contribution of these fluxes to the total deposition was small (about 20%, see section 6.2). Therefore the accuracy of the total deposition was estimated to be smaller than 20%.

6.2 Results and discussion

The integrals and averages calculated according to section 6.1 are given in table 6.1 at the end of this chapter. In figure 6.1 the mean concentration of ozone during daytime and day and night are given. In figure 6.2 the deposition of ozone over the three time periods is shown. The deposition of ozone decreased after August, as can be inferred from figure 6.2. This is partly due to the decrease of the ozone concentration (figure 6.1). The total deposition of ozone on a day varied from 5-50 mg m^{-2} , with an average of 19.0 mg m^{-2} . The daytime deposition formed on average 83% of the total integral. This means that nightly ozone fluxes did occur but accounted for a minor part, about 17%, of the total deposition of ozone. The midday deposition accounted for 45% of the daytime deposition.

In figure 6.3 the deposition velocity, V_d , and the surface conductance of ozone, V_s , are depicted. It can be seen that the deposition velocity of ozone is mainly determined by the surface conductance of ozone. The best regression line through the origin is $V_d = 0.79 V_s$ ($\text{cc} = 0.95$). In other words the aerodynamic resistance, r_a and the resistance of the quasilaminar

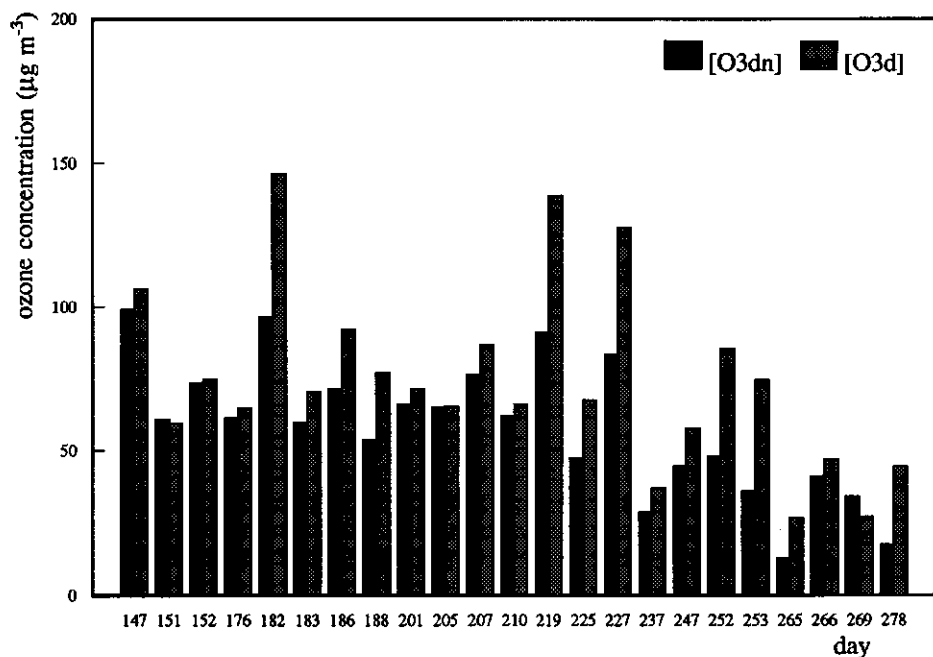


Figure 6.1 The concentration of ozone (at 6.5 m) given as a mean over day and night, dn, and daytime mean, d, for 23 days in 1988.

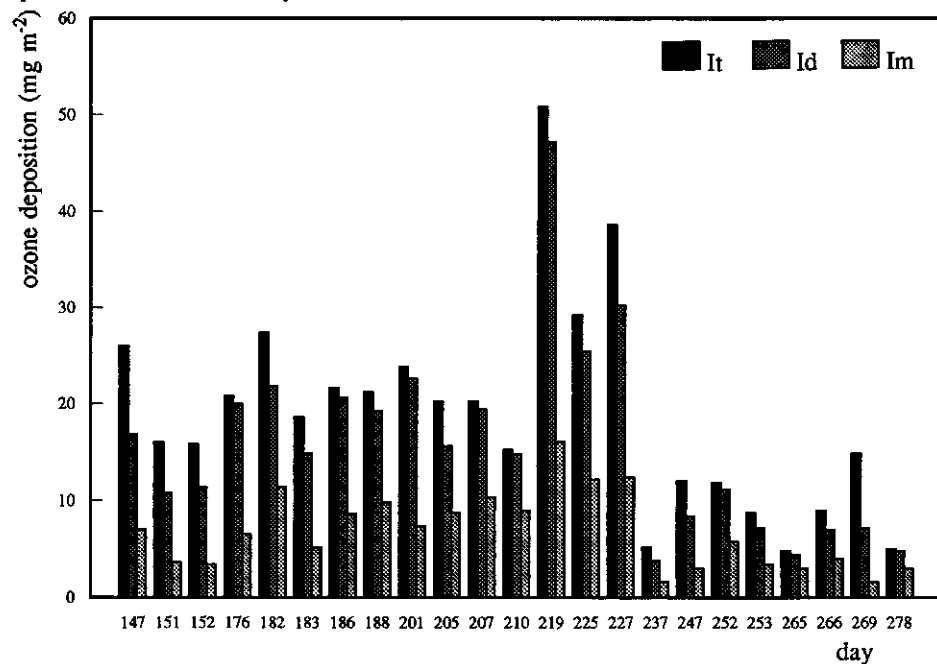


Figure 6.2 The deposition of ozone per day calculated over three periods, total, I_t , daytime, I_d and midday deposition, I_m .

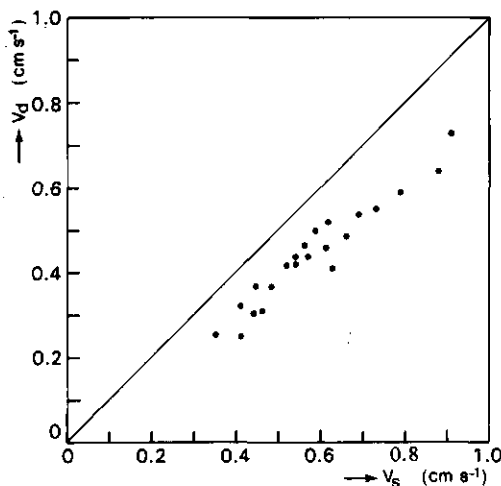


Figure 6.3 The deposition velocity of ozone, V_d , against the surface conductance to ozone, V_g .

sublayer close to the surface, r_b , are small compared to the surface resistance to ozone. They both account for about 20% of the total resistance to the transport of ozone from about 4 m above the crop to the surface during daytime conditions.

In table 6.2 the results of the linear regression between the measured daytime deposition, I_d and three assessments of the deposition are presented for days where LAI > 3 (days 182-269). Also in table 6.2 the linear regression is given between the uptake by the crop, I_c , and two assessments. In the table these assessments, denoted by the variable X, are the concentration of ozone, $[O_3(d)]$, the dose and the product of the concentration, deposition velocity, V_d , and the time period, $I_d(\text{est})$. In the regression analysis with I_c only the first two assessments were used.

It can be seen that with the mean daytime concentration a reasonable estimate on the deposition of ozone can be made. A better estimate is made if the time period is included or the dose is used. Only empirical relationships are obtained in these two cases which can describe the scatter in the deposition. An empirical constant should be used to convert the concentration and dose to an actual deposition. In the latter case this is similar to a constant seasonal surface conductance to ozone of 0.52 cm s^{-1} . The reason why these relationships serve rather well, is because of the small day-to-day variability of the surface conductance to ozone (see table 6.1).

In figure 6.4 the daytime deposition of ozone, I_d , versus $I_d(\text{est})$ is shown. From this figure, as well as from table 6.2, it can be inferred that the $I_d(\text{est})$ gives the best estimate of I_d . This means that with a mean deposition velocity, a mean concentration and the time period, the integral of the flux of ozone can be described very accurately. This value slightly underestimates the deposition of ozone by about 10%. This underestimation is due to loss in correlation between the deposition velocity and the concentration of ozone on a daily basis. In Appendix G is shown that this underestimation is maximal 20% if the daily patterns of ozone and its deposition velocity are similarly represented with two sine shape functions.

Table 6.2 Linear regression analysis of three assessments of the daytime deposition of ozone, I_d and the uptake by the crop, I_c . In the first column the assessments are given (denoted with variable X). In the second column the regression lines with and without intercept are given. In the next two columns the standard error and the correlation coefficient are given per regression line.

Assessment variable X	Regression lines between X and Y $Y = I_d$	Standard error in estimated Y	Corr. coeff.
$[O_3(d)]$	$Y = 0.25 X - 3.06$ $Y = 0.23 X$	6.76 6.62	0.79 0.79
$[O_3(d)] (t_2 - t_1)$	$Y = 23.8 X - 4.8$ $Y = 19.4 X$	4.80 5.06	0.90 0.88
$V_d [O_3(d)] (t_2 - t_1)$	$Y = 1.25 X - 3.22$ $Y = 1.1 X$	2.76 3.04	0.97 0.96
	$Y = I_c$		
$[O_3(d)]$	$Y = 0.12 X + 3.46$ $Y = 0.16 X$	5.34 5.34	0.62 0.58
$[O_3(d)] (t_2 - t_1)$ Dose	$Y = 13.3 X + 0.68$ $Y = 14.0 X$	4.12 3.98	0.80 0.79

In figure 6.5 the integrals of the flux to the crop, I_c , and the soil, I_{so} , are given. The distribution of the integrals was very irregular and no clear seasonal trend was observed. This pattern is caused by the concentration of ozone (see below) and the destruction of ozone at the soil. The latter is influenced among others by the soil wetness and the exchange process with the soil.

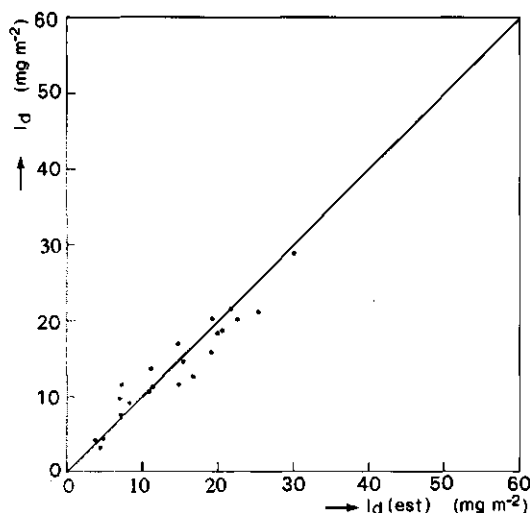


Figure 6.4 The daytime deposition of ozone, I_d , versus the estimated daytime deposition, $I_d(\text{est})$.

These factors did not show a clear seasonal pattern. It should be noted that the daytime uptake was based on the assumption that the ratio between the crop and surface conductances, averaged between 12-16 hours, served as a good estimate. However, as could be inferred from the findings in chapter 5, this will lead to an overestimation of the uptake because this ratio often approaches unity in the afternoon.

From table 6.2 it can be inferred that the dose served as a reasonable estimate for the daytime uptake of ozone by the crop. The concentration alone is not such a good indicator for this uptake. The daytime uptake by the crop ranged from $2.8 - 25.2 \text{ mg m}^{-2}$, with an average of 12.8 mg m^{-2} for, on average, a 12 hour period (or about 4 mg m^{-2} leaf area). This uptake formed 50-100% of the daytime deposition. For the entire season, this was on average 86%. This is larger than the 50-80% found in other experiments (Leuning et al. 1979a; Wesely et al., 1978). One of the reasons for this is the rainfall pattern of the 1988 growing season which often led to a relatively wet soil and consequently to a reduced destruction of ozone at the soil. Besides, the sandy soil at the experimental site had a somewhat higher surface resistance to ozone than was found for other soils (Turner et al., 1973). Leuning et al. (1979) found a daytime uptake by a maize crop of 14 mg m^{-2} leaf area. One of the reasons for this difference

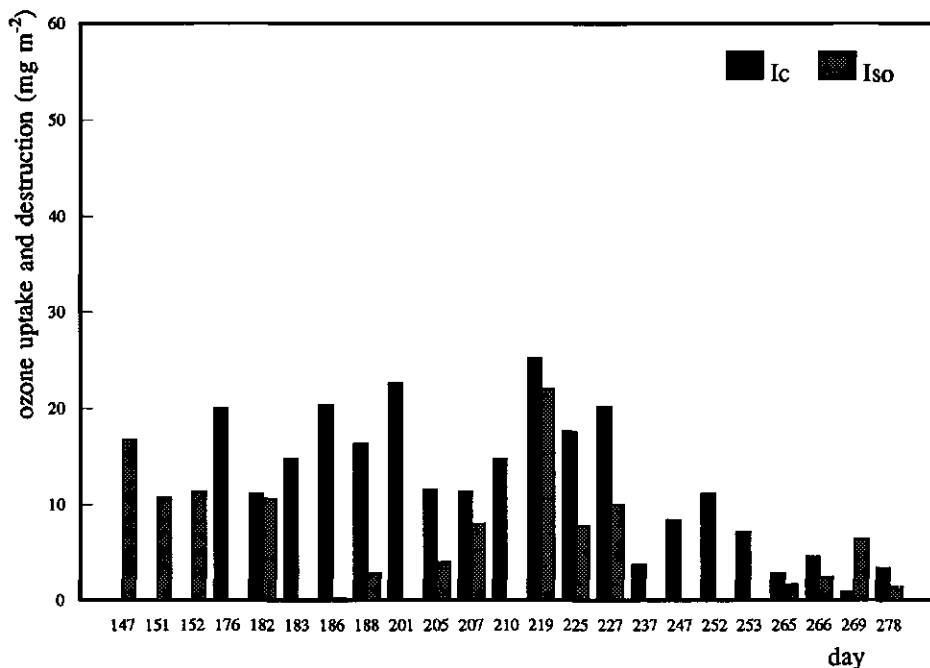


Figure 6.5 The daytime uptake of ozone by the crop, I_c and destruction at the soil, I_{so} .

with the results obtained here, was the much higher ozone concentration during their measurements made in the USA and Canada.

The surface resistance over the entire season varied from $102\text{--}286\text{ s m}^{-1}$ with an average of 167 s m^{-1} . These values are similar to those found in other experiments done above maize (Wesely et al., 1978; Leuning et al., 1979a). These surface resistances to ozone are somewhat higher than found for some other agricultural crops such as soybean and grass (Wesely et al., 1978; Hicks et al., 1989; Garland and Derwent, 1979). The surface resistance showed a weak seasonal pattern. Above bare soil, the resistance in the beginning of the season was larger than 200 s m^{-1} . In July and August, when the crop was healthy and mature, the lowest values were found (around 150 s m^{-1}). In September and October, when the crop was senescing, the scatter in the values was larger ($102\text{--}227\text{ s m}^{-1}$). The variations in the surface resistance are dominated by the stomatal resistance, the soil resistance and an in-crop aerodynamic resistance to ozone, as was pointed out in chapter 5. Since the latter two resistances did not

show a distinct seasonal pattern, the pattern in the surface resistance to ozone is irregular. Especially when the crop is senescing and becomes less dense, did the surface resistance vary more due to the variations in soil wetness and the exchange process with the soil.

6.3 Conclusions

The total deposition of ozone (during day and night) varied from 5-50 mg m^{-2} , with an average of 19.0 mg m^{-2} . The daytime deposition formed on average 83% of the total deposition. This means that the deposition during night-time accounted for a minor part (about 17%) of this total deposition. The total deposition showed a seasonal pattern, largely caused by the seasonal pattern of the concentration of ozone. This is illustrated by the findings that the daytime deposition of ozone can be well estimated by the average daytime concentration of ozone. A more accurate estimate is obtained if the time period over which the flux is calculated is included. The best estimate of the daytime deposition of ozone is obtained by using the average values of the concentration, the deposition velocity and the time period. This value gives a small underestimate (of 10%) of the daytime deposition due to some loss in correlation between the deposition velocity and the concentration.

The uptake by the crop varied from 2.8 - 25.2 mg m^{-2} , with an average of 12.8 mg m^{-2} . This uptake was 50-100% of the daytime deposition of ozone, with an average of 86%. This uptake can be reasonably estimated with the dose of ozone.

Table 6.1 Overview of the deposition of ozone, I_t (entire day), I_d (daytime), I_m (midday), and I_d (est) estimated deposition (mg m^{-2}); dose (mg m^{-3} h); the deposition velocity; V_d , the surface conductances, V_e and V_c during daylight (cm s^{-1}); surface resistance to ozone during daylight (s m^{-1}), r_s ; the surface conductances from 1200-1600 h (indicated with (4)); the concentration of ozone during the entire day, $[O_3(\text{dn})]$ and daylight hours, $[O_3(\text{d})]$ ($\mu\text{g m}^{-3}$), in the growing season of maize in 1988

Day#	Date	t_2-t_1	I_t	I_d	I_m	I_c	I_{s0}	I_d (est)	Dose	V_d	V_e	r_s	$V_e(4)$	$V_c(4)$	$[O_3(\text{dn})]$	$[O_3(\text{d})]$
147	526	13.5	26.0	16.8	7.0	0.0	16.8	12.6	1.43	0.25	0.41	244	0.69	-	99.2	106.2
151	530	13.5	16.0	10.8	3.6	0.0	10.8	10.6	0.81	0.37	0.48	208	0.47	-	60.8	59.6
152	531	13	15.8	11.4	3.4	0.0	11.4	11.2	0.97	0.32	0.41	244	0.41	-	73.6	74.6
176	624	14.5	20.8	20.0	6.6	20.0	0.0	18.4	0.94	0.64	0.88	114	0.64	0.84	61.4	64.6
182	630	8.5*	27.4	21.8	11.4	11.2	10.6	21.6	1.24	0.49	0.66	152	0.76	0.39	96.4	146.2
183	701	14.5	18.6	14.8	5.2	14.8	0.0	17.0	1.02	0.46	0.56	179	0.59	0.69	59.6	70.4
186	704	13	21.6	20.6	8.6	20.4	0.2	18.8	1.20	0.44	0.54	185	0.77	0.76	71.4	92.2
188	706	13.5	21.2	19.2	9.8	16.4	2.8	15.8	1.04	0.42	0.52	192	0.83	0.71	53.6	77.2
201	719	13.5	23.8	22.6	7.4	22.6	0.0	20.2	0.96	0.59	0.79	127	0.87	0.88	66.2	71.4
205	723	14	20.2	15.6	8.8	11.6	4.0	14.6	0.91	0.44	0.57	175	0.95	0.71	65.0	65.2
207	725	13	20.2	19.4	10.4	11.4	8.0	20.2	1.13	0.50	0.59	169	1.26	0.74	76.4	86.8
210	728	10.5*	15.2	14.8	9.0	14.8	0.0	11.6	0.70	0.46	0.61	164	0.66	0.69	62.0	66.2
219	806	13.5	50.8	47.2	16.0	25.2	22.0	36.4	1.87	0.54	0.69	145	0.92	0.49	91.2	138.6
225	812	12	29.2	25.4	12.2	17.6	7.8	21.2	0.81	0.73	0.91	110	0.82	0.57	47.4	67.6
227	814	12	38.6	30.2	12.4	20.2	10.0	28.8	1.53	0.52	0.62	161	0.66	0.44	83.6	127.6
237	824	12.5	5.2	3.8	1.6	3.8	0.0	4.2	0.46	0.25	0.35	286	0.23	0.83	28.6	37.0
247	903	11.5	12.0	8.4	3.0	8.4	0.0	9.0	0.66	0.37	0.45	222	0.49	0.92	44.6	57.6
252	908	10.5	11.8	11.2	5.8	11.2	0.0	13.6	0.90	0.42	0.54	185	0.45	0.48	48.0	85.4
253	909	10.5	8.8	7.2	3.4	7.2	0.0	11.6	0.78	0.41	0.63	159	0.32	0.45	36.0	74.6
265	921	10.5	4.8	4.4	3.0	2.8	1.6	3.2	0.28	0.31	0.46	217	0.90	0.59	12.8	26.8
266	922	10.5	9.0	7.0	4.0	4.6	2.4	9.8	0.49	0.55	0.73	137	0.75	0.50	41.0	46.8
269	925	11.5	14.8	7.2	1.6	-	-	7.6	0.31	0.69	0.98	102	0.72	-	34.0	27.0
278	1004	9	5.0	4.8	3.0	3.4	1.4	4.4	0.40	0.30	0.44	227	0.37	0.26	17.6	44.6
mean of all data			19.0	15.9	6.8	10.8	4.7		0.46	0.60	0.60	167	0.67	-	57.8	70.2
from day 182-269			19.6	16.7	7.4	12.5	3.8		0.48	0.62	0.62	161	0.71	0.64	56.5	70.3

* less than an entire day used

Chapter 7 Summary and recommendations

To observe the flux or deposition of ozone above a maize crop, experiments were carried out during the growing season of maize in 1988. The flux of ozone was determined using meteorological techniques. The measurements used in the present study were carried out under atmospheric conditions in which the vertical divergence of the flux of ozone was the dominant term in the mass conservation equation of ozone. That is, under such conditions, the flux measured at a certain height served as a good estimate of the flux at the surface. This was demonstrated in chapter 2 by a scaling exercise of the mass conservation equation and the time dependency of the flux of ozone in order to reveal the importance of the various terms in the equations. The second important term in this scaling is the chemical reactions which produce and destroy ozone (section 2.1.1). However, an accurate estimate of this influence could not be given at first hand. More accurate estimates were made with a model which describes the vertical divergence of the flux of ozone and nitrogen oxides. By scaling the equation of the local time derivative of the flux of ozone (section 2.1.3) it was found that the gradient production and pressure fluctuation term were much larger than the chemical reaction term. From this scaling and the model calculations it was concluded that the chemical reactions did not severely influence the flux of ozone.

Three meteorological techniques were used to assess the flux of ozone: the eddy correlation technique, the profile technique and the modified Bowen ratio technique. The theoretical background to these techniques was given in chapter 2. Chapter 3 and 4 presented the experimental outline and the accuracy of the measurements, respectively.

It was found that the accuracies of the fluxes were strongly determined by the errors in the differential measurements or the profiles of the variables. The accuracy of the flux of ozone measured with the profile technique was 20-53%. For the modified Bowen ratio technique this was 13-58%. The accuracy of the eddy correlation fluxes was about 20%. This was mainly caused by the intermittency of the flux in the 30 min time interval over which they were averaged.

A comparison between the three techniques was made for nine days. The profile technique gave systematically lower values for the flux of ozone than the eddy correlation and modified Bowen ratio techniques. A reduction of about 40% of the flux of ozone was found, calculated from the ozone concentration at $6 z_{om} + d$ and $30 z_{om} + d$, during near-neutral and unstable atmospheric conditions. This was caused by a) an inadequate use of the profile technique close to the roughness elements and b) an uncertainty in the displacement height for ozone. The flux of ozone determined with the modified Bowen ratio technique was moderately consistent with that determined with the eddy correlation technique and no systematic deviations were found. This indicates that: a) the modified Bowen ratio technique is applicable close to the surface, b) sensible and latent heat (water vapour) are transported in roughly the same way and c) chemical reactions did not cause large systematic deviations, i.e. no large flux divergence between the two techniques existed though the fluxes were measured at different heights.

The time integrals over the day of the fluxes of ozone derived with the modified Bowen ratio and the eddy correlation techniques agreed very well. This means that a reliable estimate of the daytime deposition of ozone (accuracy $\pm 10\%$) was obtained using these techniques. The accuracy of the 30 min values, however, is much smaller (20-50%).

In chapter 5 a resistance model was used to deduce the ability of the surface to destroy ozone, expressed in the surface resistance, from the flux measurements. This was done for bare soil as well as the crop - soil system as a whole when the soil was entirely covered by the crop. The resistance of the soil to ozone was dependent on the soil water content, i.e. the soil surface resistance increased with increasing soil water content.

In the evaluation of the magnitude of the different parallel sinks of ozone such as the stomata and the soil surface, the conductances of the surface and the crop to ozone were used. An estimate on the crop conductance to ozone i.e. the stomatal uptake of ozone, was made using the analogy to the transpiration of the crop.

The surface conductance to ozone was mainly determined by the uptake of ozone by the stomata, the destruction at the soil surface and the transport towards the soil. When the soil surface is wet (i.e. rainfall occurred a few hours prior to the measurements) the surface conductance and the crop conductance to ozone coincided.

The conductance of the remaining plant parts (mainly the cuticle) to ozone was small

compared to the stomatal or soil conductance to ozone.

The exchange of ozone with the soil was mainly determined by the turbulent mixing (expressed by the friction velocity), the stability of the air above the crop and the leaf area density.

When the soil surface is not wet (i.e. no rainfall a day before the measurements), the flux of ozone towards the soil can be 25-50% of the total flux of ozone. In such circumstances the flux of ozone should be modelled using a surface resistance in which the soil resistance to ozone, as well as an in-crop aerodynamic resistance are incorporated. This in-crop aerodynamic resistance depends among others on the turbulent mixing above the crop and the leaf area density.

A more quantitative analysis of the exchange of ozone with the crop and the underlying soil can be made by using more complex canopy flow models such as those by Meyers and Hicks (1988), Li et al., (1985). In such models the non-local transport of momentum and scalars are described. With these models a more detailed sink distribution of ozone in the crop can also be made using, for instance, measured profiles of ozone in the crop (Raupach, 1989). Another outcome of these models can be a parameterization of the in-crop aerodynamic resistance for use in air pollution dispersion models.

In chapter 6 an overview of the deposition of ozone and the governing factors during the growing season of maize were presented. The total deposition of ozone calculated as the time integral of the flux over the entire day, varied from 5-50 mg m⁻², with an average of 19.0 mg m⁻². The daytime deposition accounted for on average 83% of the total deposition. The deposition during night-time was small compared to the total deposition (17%). The total deposition showed a seasonal pattern. This pattern is largely caused by the seasonal pattern of the concentration of ozone. This is illustrated by the findings that the daytime deposition of ozone can be well estimated by the average concentration of ozone. A better estimate is obtained if the time period is included over which the flux is calculated i.e. the dose of ozone. The main reason for this good estimate is the relatively small fluctuations in the mean daytime surface conductance to ozone. The best estimate of the daytime deposition of ozone is obtained by using the average values of the concentration, the deposition velocity and the time period. This value gives a small underestimate (10%) of the daytime deposition due to some loss in correlation between the deposition velocity and the concentration.

The uptake by the crop varied from 2.8 - 25.2 mg m⁻², with an average of 12.8 mg m⁻². This uptake was 50-100% of the daytime deposition of ozone, with an average of 86%. This uptake can be reasonably estimated with the dose of ozone.

To reveal a seasonal trend in the uptake of ozone by the crop, a data series of at least several growing seasons is necessary to obtain full coverage on all wind directions and environmental situations in which the crop was grown. It is especially the coupling of these data to the effects on plants such as a reduction in crop yield that requires very long data series, since the climatic 'noise' on these data is very large. Therefore a more appropriate approach would be to evaluate all available measurements in this field by means of coupled flow - crop growth models. This data set can be used, for example, to verify such models in which the exchange of air pollutants with the crop and the soil is described.

Samenvatting

Ozon (O_3) is een chemische component, die voorkomt in de troposfeer en stratosfeer. De aanwezige ozon in de atmosferische grenslaag (het laagste deel van de troposfeer) is hoofdzakelijk het gevolg van de volgende processen.

In de troposfeer wordt ozon geproduceerd via de fotolyse van stikstofdioxide (NO_2) onder invloed van zonlicht bij 300-410 nm en wordt afgebroken via de reactie met stikstofoxide (NO). Omdat deze reacties vrij snel zijn, vormen deze een evenwicht: het zogenaamde fotostationaire evenwicht. Deze reacties leiden niet tot een netto produktie van ozon. Een produktie van ozon treedt op als stikstofoxide geoxideerd wordt tot stikstofdioxide zonder de consumptie van ozon. Deze reacties zijn aanwezig in de atmosferische oxidatiecyclus van vluchtige organische stoffen (VOS), die aanwezig zijn in verontreinigde gebieden. Zo kunnen bijvoorbeeld onder zonnige omstandigheden en een stagnerend weertype (bv. een hoge drukgebied), de zogenaamde zomersmogepisodes ontstaan met hoge ozonconcentraties.

Ozon wordt getransporteerd tussen de atmosferische grenslaag en de lagen daarboven. De dagelijkse gang van de grenslaag zorgt ervoor, dat ozon uitgewisseld wordt met de daarboven gelegen reservoirlaag. Andere meteorologische fenomenen zoals fronten en convectieve cellen (bv. Cumulonimbi) kunnen ervoor zorgen dat ozon uit hogere luchtlagen getransporteerd wordt.

Ozon is een sterke oxidant en wordt daardoor snel aan oppervlakken afgebroken zoals planten en allerlei materialen. Dit wordt de droge depositie van ozon genoemd en neemt naar schatting 30% van het totale troposferisch ozonbudget in beslag.

Ten gevolge van antropogene emissies van stikstofoxiden en VOS is de ozonconcentratie in de afgelopen 20 jaar op het noordelijk halfrond met 1% per jaar gestegen.

Ozon kan schade veroorzaken aan planten. Ozon dringt hoofdzakelijk binnen via de huidmondjes van de planten en richt zo de grootste schade aan. Bij hoge ozonconcentraties kunnen effecten als necrose (vlekken op de bladeren) en chlorose ontstaan. Op de lange

termijn bij buitenluchtconcentraties kan ozon een gewasderving teweegbrengen bij landbouwgewassen. Eerder gemaakte schattingen lieten zien dat in Nederland de gewasderving ten gevolge van luchtverontreiniging 5% bedroeg, waarvan 70% door ozon veroorzaakt.

Om de effecten van ozon op planten te kunnen bestuderen, worden allerlei proefopstellingen gebruikt waarbij de planten gedurende een zekere tijd met een bepaalde hoeveelheid ozon begast worden. Meestal gebeurt dit gedurende kortere perioden, variërend van uren tot weken, bij relatief hoge ozonconcentraties. De proefopstellingen verschillen hoofdzakelijk in de wijze waarop omgevingsinvloeden kunnen worden gecontroleerd (bv. hoeveelheid licht, water). In deze onderzoeken worden de gevonden effecten gekoppeld aan de dosis die de planten ontvangen, en zogenaamde dosis-effectrelaties worden opgesteld. De dosis wordt gedefinieerd als het produkt van de concentratie en de begassingstijd. Omdat de planten onder gecontroleerde omstandigheden gehouden worden, is deze dosis gekoppeld aan de opname van ozon door deze planten.

Het is moeilijk om de resultaten uit deze experimenten direct toe te passen op gewassen onder veldomstandigheden. Landbouwgewassen worden in het algemeen geteeld onder veel langere perioden, waarin de groeiomstandigheden en de ozonconcentratie sterk variëren. Onder veldomstandigheden is het niet in eerste instantie mogelijk om de opname en de effecten van ozon te koppelen aan de concentratie van of de dosis aan ozon. Om schattingen van deze opname te maken moeten of metingen of modelmatige berekeningen uitgevoerd worden. In dit onderzoek zijn metingen verricht om de opname van ozon door een landbouwgewas onder veldomstandigheden te bepalen. De metingen zijn uitgevoerd aan maïs gedurende het groeiseizoen van 1988.

De opname van ozon door het gewas is bepaald met behulp van meteorologische technieken. Met deze technieken wordt de flux van een komponent boven het gewas bepaald. Het voordeel van deze technieken is, dat een waarde van de flux bepaald wordt die representatief is voor een groot oppervlak (orde van grootte hectares). Een nadeel is, dat ze slechts onder strikte omstandigheden te gebruiken zijn. In hoofdstuk 2 worden de gebruikte technieken uitgelegd. In hetzelfde hoofdstuk worden de atmosferische omstandigheden, die typisch aanwezig waren tijdens de experimenten gebruikt om de termen in de vergelijkingen die het behoud van ozon en de flux van ozon beschrijven te schatten. Uit deze zogenaamde schaling kwam naar voren dat in de meeste gevallen de term, die de fluxdivergentie van ozon

beschrijft, dominant was. Dat betekent, dat de flux van ozon die boven het gewas bepaald is, niet noemenswaardig afwijkt van de flux van ozon aanwezig juist boven het oppervlak. De tweede belangrijke term was de chemische reacties van ozon met stikstofoxides. Een nauwkeurige schatting van de invloed van chemische reacties op de flux van ozon konden niet met deze schaling bepaald worden. Er zijn berekeningen uitgevoerd met een model dat de vergelijkingen, die de divergentie van de flux van ozon en stikstofoxides ten gevolge van chemische reacties beschrijven, oplost. Het bleek dat systematische verschillen van 10% konden optreden. In de schaling van de vergelijking, die de flux van ozon beschrijft, bleek dat de chemische reactie term klein was ten opzichte van de produktieterm van de flux (kleiner dan 10%). De uiteindelijke conclusie was, dat de chemische reacties geen grote afwijkingen (kleiner dan 10%) gegeven kunnen hebben tussen de flux van ozon op de meethoogte en de flux van ozon vlak boven het gewas.

Drie meteorologische technieken zijn gebruikt om de flux van ozon naar het oppervlak te bepalen: de eddy-correlatie-techniek, de profieltechniek en de gemodificeerde Bowen-verhoudingstechniek. De sensoren die gebruikt zijn in de experimentele opstelling en enkele omgevingsomstandigheden (zoals regenval, bodemvocht) en gewasparameters (zoals gewashoogte en -opbrengst) zijn vermeld in hoofdstuk 3.

In hoofdstuk 4 is de nauwkeurigheid van de fluxen gegeven en zijn bovenstaande technieken onderling vergeleken. De nauwkeurigheid van de fluxen bepaald via verschildmetingen (profiel- en gemodificeerde Bowen verhoudingstechniek) werden voornamelijk bepaald door de fouten in de gemeten verschillen. De nauwkeurigheid van de flux van ozon bepaald met de profieltechniek was 20 - 53%; die met de gemodificeerde Bowen verhoudingstechniek 13 - 58%. De nauwkeurigheid van de flux van ozon bepaald met de eddy-correlatie-techniek bedroeg 20%, en werd voornamelijk bepaald door de fluctuaties van de flux gedurende het tijdsinterval waarover de flux werd gemiddeld (namelijk 30 minuten).

In hetzelfde hoofdstuk is een vergelijking uitgevoerd tussen de drie technieken gebaseerd op 9 meetdagen (ongeveer 94 half uur-waarnemingen). De profieltechniek leverde systematisch een 40% lagere flux op ten opzichte van de eddy-correlatie- en gemodificeerde Bowen verhoudingstechniek. De oorzaak hiervan ligt enerzijds aan een incorrecte toepassing van de profieltechniek, namelijk te dicht op het oppervlak, en anderzijds door een niet toepasselijke verplaatsingshoogte voor ozon. De flux van ozon, gemeten met de gemodificeerde Bowen

verhoudings techniek kwam redelijk goed overeen met die gemeten met de eddy-correlatie-techniek. Dit geeft aan, dat:

- a) de gemodificeerde Bowen verhoudingstechniek dicht bij het oppervlak gebruikt kan worden,
- b) ozon en vocht (en voelbare warmte) min of meer op dezelfde manier door turbulentie getransporteerd worden, en
- c) chemische reacties een verwaarloosbare invloed hadden op de divergentie van de flux van ozon (de technieken zijn toegepast op verschillende hoogten).

Met beide technieken konden schattingen van de dagelijkse depositie van ozon met een nauwkeurigheid van ongeveer 10% gegeven worden.

In hoofdstuk 5 is uit metingen, waarbij gebruik werd gemaakt van een zogenaamd weerstandsmodel, het vermogen afgeleid waarmee het oppervlak ozon afbrak, uitgedrukt in de oppervlakte weerstand. De oppervlakteweerstand is een eigenschap van het oppervlak voor bijvoorbeeld de afbraak van ozon of de afgifte van waterdamp door het oppervlak. Hier is gebruik gemaakt van een zeer eenvoudige modelbenadering door het gewas op te vatten als een blad zonder verticale dimensie. In feite is dit blad dus opgebouwd uit het gewas zelf, onderliggende bodem en de tussenliggende luchtstroming.

De oppervlakteweerstand van de bodem voor ozon wordt grotendeels bepaald door het vochtgehalte van de bodem. Dat wil zeggen, dat als de bodem nat is de weerstand relatief hoog is en vice versa.

In de evaluatie van de putten van ozon, zoals de huidmondjes en de bodem, werden de geleidingen gebruikt (de geleiding is de reciproke van de weerstand). Een schatting van de gewasgeleiding van ozon, ofwel de opname door de huidmondjes, werd gemaakt met behulp van de transpiratie van het gewas. Uit de metingen zijn zowel de oppervlaktegeleiding van ozon (d.w.z. de geleiding van het gewas en de bodem), als de gewasgeleiding bepaald. Het bleek, dat onder omstandigheden van een natte bodem (d.w.z. dat een regenbui enkele uren voor de metingen plaatsvond) de geleidingen goed overeenkwamen. Dat betekent dat praktisch alle ozon via de huidmondjes opgenomen werd. Tegelijkertijd betekende dit dat de rest van de plant (o.a. cuticula) moeilijk ozon afbreekt. Bij droge bodemomstandigheden bleek de oppervlaktegeleiding systematisch groter te zijn dan de gewasgeleiding. Dit duidde op een extra transport van ozon naar de bodem. Dit kon op enkele dagen 25 - 50% van de totale flux

van ozon, gemeten boven het gewas, bedragen. Deze uitwisseling met de bodem was ondermeer afhankelijk van de turbulentie boven het gewas en van de plantarchitectuur.

In hoofdstuk 6 is een overzicht gegeven van de depositie van ozon en de bepalende factoren voor 23 dagen gedurende het groeiseizoen van mais in 1988. De gemiddelde depositie over de gehele dag bedroeg $5 - 50 \text{ mg m}^{-2}$ en vertoonde een duidelijk seizoensverloop. Dit seizoensverloop kon hoofdzakelijk verklaard worden uit het seizoensverloop van de concentratie. Dit werd bevestigd door het feit, dat de dagelijkse depositie van ozon goed beschreven kon worden, alleen gebruikmakend van de daggemiddelde concentratie van ozon. De beste schatting van deze depositie werd verkregen met het produkt van de daggemiddelde concentratie en -depositiesnelheid en de tijd waarover deze gemiddeld waren.

De opname van ozon door het gewas varieerde tussen $2.8 - 25.2 \text{ mg m}^{-2}$ met een gemiddelde van 12.8 mg m^{-2} . Dit vormde op dagbasis 50 - 100% van de dagelijkse depositie. Voor het hele seizoen bedroeg de opname van het gewas 86% van de dagelijkse depositie van ozon. Deze opname kon redelijk goed geschat worden met de dosis aan ozon.

References

- Aalst, R.M. van 1989 Ozone and oxidants in the planetary boundary layer. *In*: T.Schneider et al.(eds.): Atmospheric Ozone research and its policy implications. Studies in Environmental Science 35. Elsevier:573-587.
- Aben,J.M.M. 1990 A system to determine whole-plant exchange rates of ozone, carbon dioxide and water vapour. Kema Scientific and Technical Reports 8: 109-120.
- Al-Kaisi,M., L.J.Brun and J.W.Enz 1989 Transpiration and evapotranspiration from maize as related to leaf area index. *Agricultural and Forest Meteorology* 48: 111-116.
- Asselt, C.J. van, A.F.G. Jacobs, J.H. van Boxel and A.E.Jansen 1991 A simple fast-response thermometer for outdoor use. *In*: Report of the fourth WMO technical conference on instruments and methods of observation (TECIMO-IV). Instruments and Observing Methods Report 35: 129-134.
- Bahe,F.C.,U.Schurath and K.H. Becke 1980 The frequency of NO₂ photolysis at ground level, as recorded by a continuous actinometer. *Atmospheric Environment* 14: 711-718.
- Baldocchi,D.D., B.B.Hicks and P.Camara 1987 A canopy stomatal resistance model for gaseous deposition to vegetated surfaces. *Atmospheric Environment* 21: 91-101.
- Beck, J. 1988 Depositie van ozon op kale grond. Doctoraal verslag, Vakgroep Natuur en Weerkunde, LU Wageningen.
- Berkowicz, R. and L.P. Prahm 1982 Evaluation of the profile method for estimation of surface fluxes of momentum and heat. *Atmospheric Environment* 16:2809-2819.
- Bojkov,R.D. 1988 Ozone changes at the surface and in the free troposphere. *In*: Isaksen (ed.): Tropospheric Ozone. Reidel, Dordrecht: 83-96.
- Boxel, J. van 1986 Heat balance investigations in tidal areas. PhD thesis Free University Amsterdam.
- Boxel, J. van 1987 Verwerkingsprogrammatuur voor de meetwagen. Rapport Vakgroep Natuur en Weerkunde, LU Wageningen.
- Bruin, H.A.R. de, 1982 The energy balance of the earth's surface: a practical approach. KNMI Report 82-1.
- Bruin, W.J. de and J.E.Jaspers 1987 De ontwikkeling van een ozon monitor voor eddy correlatie metingen. Arnhem: NV KEMA Internal Report 51514 87-3157.
- Buck, A. 1976 The variable path Lyman-alpha hygrometer and its operating characteristics. *Bulletin of American Meteorological Society* 57:1113-1118.

Builtjes,P.J.H. 1989 Interaction of planetary boundary layer and free Troposphere. *In*: T.Schneider et al.(eds.): Atmospheric Ozone research and its policy implications - Studies in Environmental Science 35 Elsevier. :605-612.

Busch,N.E. 1973 On the mechanics of atmospheric turbulence. *In*: D.A. Haugen(ed.): Workshop on Micrometeorology. American Meteorological Society(Boston):1-66.

Businger, J.A., J.C. Wyngaard, Y. Izumi and E.F. Bradley, 1971 Flux profile relationships in the atmospheric surface layer. *Journal of Atmospheric Science* 28:181-189.

Businger,J.A. 1973 Turbulent transfer in the atmospheric surface layer. *In*: D.A. Haugen(ed): Workshop on Micrometeorology. American Meteorological Society(Boston):67-100.

Businger,J.A. 1982 Equations and concepts. *In*: F.T.M. Nieuwstadt and H. van Dop (eds.):Atmospheric turbulence and air pollution modelling. - Reidel (Dordrecht): 1-33.

Businger,J.A. 1986 Evaluation of the accuracy with which dry deposition can be measured with current micrometeorological techniques - *Journal of Climate and Applied Meteorology* 25:1100-1124.

CBS 1991 Milieufactetten: cijfers bij de tweede nationale milieuverkenning 1991. *In*: Milieustatistieken CBS, 1991. 's Gravenhage: SDU/uitgeverij.

Chamberlain, A.C. 1953 Aspects of travel and deposition of aerosol and vapor clouds. Report No. AERE HP/R 1261, HMSO, London 29pp.

Chamberlain, A.C. 1966 Transport of gases to and from grass and grass-like surfaces - *Proceedings of the Royal Society of London A* 290:236-265.

Choudhury,B.J. and S.B.Idso 1985 An empirical model for stomatal resistance of field grown wheat. *Journal of Agricultural and Forest Meteorology* 36:65-82.

Choudhury,B.J. and J.L.Monteith 1988 A four-layer model for heat budget of homogeneous land surfaces. *Quarterly Journal of the Royal Meteorological Society* 114: 373-398.

Colbeck,I and R.M.Harrison 1985 Dry deposition of ozone: some measurements of deposition velocity and vertical profiles to 100 metres. *Atmospheric Environment* 19: 1807-1818.

Delany,A.C., D.R.Fitzjarrald, D.H.Lenschow, R.Pearson jr., G.J.Wendel and B.Woodruff 1986 Direct measurements of nitrogen oxides and ozone fluxes over grassland. *Journal of Atmospheric Chemistry* 4: 429-444.

Driedonks, A.G.M. 1981 Dynamics of the well-mixed atmospheric boundary layer. KNMI Scientific report no. 81-2.

Droppo,J.G. Jr. 1985 Concurrent measurements of ozone dry deposition using eddy correlation and profile flux methods. *Journal of Geophysical Research* 90:2111-2118.

Duyzer, J.H. and F.C. Bosveld 1988 Measurements of dry deposition fluxes of O_3 , NO_x , SO_2 and particles over grass/heathland vegetation and the influence of surface inhomogeneity. TNO-KNMI Report R 88/111.

Dyer, A.J. and B.B. Hicks 1970 Flux gradient relationships in the constant flux layer. *Quarterly Journal of the Royal Meteorological Society* 96: 715-721.

Eerden, van der L.J., A.E.G. Tonneijck and J.H.M. Wijnands 1988 Crop loss due to air pollution in the Netherlands. *Environmental Pollution* 53: 365-376.

Finnigan, J.J. 1985 Turbulent transport in flexible plant canopies. *In: B.A. Hutchinson and B.B. Hicks (eds.) The Forest-Atmosphere Interaction: 443-480.*

Fitzjarrald, D.R. and D.H. Lenschow 1983 Mean concentration and flux profiles for chemically reactive species in the atmospheric surface layer. *Atmospheric Environment* 17: 2505-2512.

Fowler, D. 1978 Dry deposition of SO_2 on agricultural crops. *Atmospheric Environment* 12: 369-373.

Fritschen, L.J. and L.W. Gay 1979 Environmental instrumentation. New York: Springer Verlag: 216 pp.

Gash, J.H.C. 1986 A note on estimating the effect of a limited fetch on micrometeorology evaporation measurements *Boundary Layer Meteorology* 35: 409-413.

Galbally, I.E. and C.R. Roy 1980 Destruction of ozone at the earth's surface. *Quarterly Journal of the Royal Meteorological Society* 106: 599-620.

Garland, J.A. and R.G. Derwent 1979 Destruction at the ground and the diurnal cycle of concentration of ozone and other gases. *Quarterly Journal of the Royal Meteorological Society* 105: 169-183.

Garratt, J.R. 1980 Surface influence upon vertical profiles in the atmospheric near-surface layer. *Quarterly Journal of the Royal Meteorological Society* 106: 803-819.

Halbersma, J. and C. Przybyla 1986 Calibration and evaluation of a dielectric soil water content meter. *In: Proceedings International Conference on Hydrological Processes in the Catchment, Krakow, Poland, 8-11 May 1986.*

Harrison, L.P. 1963 Some fundamental considerations regarding psychrometry. *In: Humidity and moisture, vol. I. New York: Reinhold: 165-174.*

Heath, R.L. 1975 Ozone. *In: Responses of plants to air pollution, London/New York: Academic Press: 23-55.*

Heck, W.W., O.C. Taylor, R. Adams, G. Bingham, J. Miller, E. Preston and L. Weinstein 1982 Assessment of crop loss from ozone. *Journal of the Air Pollution Control Association* 32: 353-361.

Heilman,J.L., C.L.Britten and C.M.U.Neale 1989 Fetch requirements for Bowen ratio measurements of latent and sensible heat fluxes. *Agricultural and Forest Meteorology* 44:261-273.

Hicks,B.B. 1986 Measuring dry deposition: a re-assessment of the state of the art. *Water,air and soil pollution* 30: 75-90.

Hicks,B.B.,D.R.Matt and R.T.McMillen 1989 A micrometeorological investigation of surface exchange of trace gases: a case study. NOAA Technical Memorandum ERL ARL-172.

Hicks,B.B, R.P.Hosker Jr., T.P.Meyers and J.D.Womack 1991 Dry deposition inferential measurement techniques-I. Design and tests of a prototype meteorological and chemical system for determining dry deposition. *Atmospheric Environment* 25A:2345-2359.

Holtstag, A.A.M. and H.A.R.de Bruin 1988 Applied modelling of the nighttime surface energy balance over land. *Journal of Applied Meteorology* 22: 689-704.

Jacobs,A.F.G., J.Halbersma and C.Przybyla 1987 Behaviour of the crop resistance of maize during a growing season. *In: Proceedings of workshop: Estimation of Areal Evapotranspiration, Vancouver, Canada IAHS Publ.177:165-173.*

Jacobs,A.F.G. and J.H. van Boxel 1988 Changes of the displacement height and roughness length of maize during a growing season. *Agricultural and Forest Meteorology* 42: 53-62.

Jacobs,A.F.G., W.A.J. van Pul, and A. van Dijken 1990 Similarity moisture dew profiles within a Corn canopy. *Journal of Applied Meteorology* 29:1300-1306.

Jarvis, P.G. 1981 Stomatal conductance, gaseous exchange and transpiration. *In: Plants and their atmospheric environment, J.L. Monteith (ed.):175-204*

Kaimal,J.C. J.C.Wyngaard, Y.Izumi and O.R.Cote 1972 Spectral characteristics of surface-layer turbulence. *Quarterly Journal of the Royal Meteorological Society* 98: 563-589.

Kema-rapport 51514-MOB 89-3323, Jong,M.A. de, Schoofs,M.J., "Analyse van de gemeten stomataire weerstanden van snijmais op proefveld Sinderhoeve gedurende het seizoen 1988".Oktober 1989.

Kema-rapport 82106-MOZ 89-3359, Bestebroer,S.I., Jong,M.A. de, Stortelder,B.J.M., Westen,B.J., "Evaluatie van de porometriemethode toegepast op mais", Januari 1990.

Kramm, G. 1989 A numerical method for determining the dry deposition of atmospheric trace gases. *Boundary Layer Meteorology* 48: 157-175.

Krupa,S.V. and W.J.Manning 1988 Atmospheric ozone: formation and effects on vegetation. *Environmental Pollution* 50:101-137.

Krupa, S.V. and M.Nosal 1989 Effects of ozone on agricultural crops. *In*: T.Schneider et al.(ed): Atmospheric Ozone research and its policy implications. Studies in Environmental Science 35 Elsevier:229-238.

Lenschow,D. and L.Kristensen 1985 Uncorrelated noise in turbulence measurements. *Journal of Atmospheric and Oceanic Technology* 2: 68-81.

Leuning,R., H.H.Neumann and G.W.Thurtell 1979a Ozone uptake by corn: a general approach. *Agricultural Meteorology* 20: 115-135.

Leuning,R., M.H.Unsworth, H.N.Neumann and K.M.King 1979b Ozone fluxes to tobacco and soil under field conditions. *Atmospheric Environment* 13:1155-1163.

Li,Z.J., D.R.Miller and J.D.Lin 1985 A first-order closure scheme to describe counter gradient momentum transport in plant canopies. *Boundary Layer Meteorology* 33: 77-83.

Lindroth,A. 1984 Gradient distributions and flux profile relations above a rough forest. *Quarterly Journal of the Royal Meteorological Society* 110:553-563.

Mandl,R.H., L.H.Weinstein, D.C.McCune and M.Keveny 1973 A cylindrical open-top chamber for the exposure of plants to air pollutants in the field. *Journal of Environmental Quality* 2:371-376.

McBean,G.A. 1972 Instrument requirements for eddy correlation measurements. *Journal of Applied Meteorology* 11:1078-1084.

McLeod,A.R.,J.E.Fackrell and K.Alexander 1985 Open-air fumigation of field crops: criteria and design for a new experimental system. *Atmospheric Environment* 19:1639-1649.

Meyers,T. and K.T.P. U 1987 Modelling the plant canopy micrometeorology with higher-order closure principles. *Agricultural and Forest Meteorology* 41: 143-163.

Meyers,T.P. and B.B.Hicks 1988 Dry deposition of O_3 , SO_2 and HNO_3 to different vegetation in the same exposure environment. *Environmental Pollution* 53:13-25.

Moore,C.J. 1986 Frequency response corrections for eddy correlation systems. *Boundary Layer Meteorology* 37: 17-35.

Monin,A.S. and A.M.Yaglom 1971 Statistical fluid mechanics, mechanics of turbulence, Vol. I Massachusetts: MIT Press.

Monteith,J.L. 1973 Principles of environmental physics. London: Edward Arnold Publ.

Mukammal,E.L. 1965 Ozone as a cause of Tobacco fleck. *Agricultural Meteorology* 2:145-146.

Overgaard Mogenson,V. 1970 The calibration factor of heat flux meters in relation to the thermal conductivity of the surrounding medium. *Agricultural Meteorology* 7: 401-410

Pasquill,F. 1972 Some aspects of boundary-layer description. Quarterly Journal of the Royal Meteorological Society 98: 469-494.

Paulson,C.A. 1970 The mathematical representation of wind speed and temperature profiles in the unstable atmospheric surface layer. Journal of Applied Meteorology 9: 857-861.

Penman,H.L. 1948 Natural evaporation from open water, bare soil and grass. Proceedings Royal Society A 194:120.

Philip,J.R. 1961 The theory of the heat flux meters - Journal of Geophysical Research 66: 571-579.

Philip,J.R. 1963 The damping of a fluctuating concentration by continuous sampling through a tube. Australian Journal of Physics 16: 454-463.

Raupach,M.R. and B.J.Legg 1984 The uses and limitations of flux-gradient relationships in micrometeorology. Agricultural Water Management 8: 119-131.

Raupach,M.R. and A.S.Thom 1981 Turbulence in and above plant canopies. Annual Reviews Fluid Mechanics 13: 97-129.

Raupach,M.R. 1989 Applying Lagrangian fluid mechanics to infer scalar source distributions from concentration profiles in plant canopies. Agricultural and Forest Meteorology 47:85-108.

Rich,S., Waggoner,P.E., and Tomlinson, H. 1970 Ozone uptake by bean leaves. Science 169: 79-80.

Schotanus P., 1982 Turbulente fluxen in inhomogene omstandigheden. Rapport KNMI WR-82-3.

Shaw,R.H. 1985 On diffusive and dispersive fluxes in forest canopies. *In*: B.A.Hutchinson and B.B.Hicks (eds.) The Forest-Atmosphere Interaction:407-419.

Shaw,R.H., G.den Hartog and H.H. Neumann, 1988 Influence of foliar density and thermal stability on profiles of Reynolds stress and turbulence intensity in a deciduous forest. Boundary Layer Meteorology 45:391-409.

Sinclair,T.R., L.H.Allen, Jr. and E.R.Lemon 1975 An analysis of errors in the calculation of energy flux densities above vegetation by a Bowen-ratio profile method. Boundary Layer Meteorology 8: 129-139.

Slooff,W., R.M. van Aalst, E.Heijna-Merkus en R.Thomas (eds.) 1987 Ontwerp Basisdocument Ozon. RIVM report 758474002 (in Dutch).

Smedman, A. and U.Hogstrom 1973 The mastra micrometeorological project. Boundary Layer Meteorology 5:529-573.

Stull, R.B. 1988 An introduction to boundary layer meteorology. Deventer: Kluwer Academic Publ.

Tanner, C.B. and W.A. Jury 1976 Estimating evaporation and transpiration from a row crop during incomplete cover. *Agronomy Journal* 68:239-243.

Tennekes, H. 1973a A model for the dynamics of the inversion above a convective boundary layer. *Journal of the Atmospheric Sciences*, 30:558-567.

Tennekes, H. 1973b The logarithmic wind profile. *Journal of the Atmospheric Sciences* 30: 234-238.

Tingey, D.T. and G.E. Taylor 1982 Variation in plant response to ozone: a conceptual model of physiological events. In: M.H. Unsworth and D.P. Ormrod (eds.): *Effects of gaseous air pollution in agriculture and horticulture*. Butterworths Scientific (London):43-63.

Thom, A.S. 1975 Momentum, mass and heat exchange of plant communities. In: J.L. Monteith (ed.): *Vegetation and the atmosphere*, Vol. 1. Academic Press (London):57-109.

Thomson, W.W., W.M. Dugger, and R.L. Palmer 1966 Effects of ozone on the fine structure of the palisade parenchyma cells of bean leaves. *Canadian Journal of Botany* 44:1677-1682.

Tonneijck A.E.G. 1988 Evaluation of ozone effects on vegetation in the Netherlands. In: T. Schneider et al. (eds.): *Atmospheric Ozone research and its policy implications*. *Studies in Environmental Science* 35. Elsevier:251-260.

Turner, N.C., P.E. Waggoner and S. Rich 1973 Removal of ozone by soil. *Journal of Environmental Quality* 2:259-264.

Turner, N.C., P.E. Waggoner and S. Rich 1974 Removal of ozone from the atmosphere by soil and vegetation. *Nature* 250:486-489.

Vilà-Guerau de Arellano, J., P.G. Duynkerke and P. Builtjes (1992) The divergence of the turbulent diffusion flux due to chemical reactions in the surface layer. *Journal of Geophysical Research*. Submitted for publication.

Webb, E.K., G.I. Pearman and R. Leuning 1980 Correction of flux measurements for density effects due to heat and water vapour transfer. *Quarterly Journal of the Royal Meteorological Society* 106: 85-100.

Wesely, M.L., J.A. Eastman, D.R. Cook and B.B. Hicks 1978 Daytime variations of ozone eddy fluxes to maize. *Boundary Layer Meteorology* 15:361-373.

Wesely, M.L., D.R. Cook and R.M. Williams 1981 Field measurements of small ozone fluxes to snow, wet bare soil, and lake water. *Boundary Layer Meteorology* 20: 459-471.

Wesely, M.L. 1983 Turbulent transport of ozone to surfaces common in the eastern half of the United States. *In: S.E. Schwartz (ed.), Trace Atmospheric Constituents: Properties, Transformations and Fates.* London: Wiley & Sons.: 346-370.

Wesely, M.L. 1989 Parameterization of surface resistances to gaseous dry deposition in regional-scale numerical models. *Atmospheric Environment* 23:1293-1304.

Wieringa, J. 1980 A revaluation of the Kansas mast influence on measurements of stress and cupanemometer overspeeding. *Boundary Layer Meteorology* 18:411-430.

Wijk van, W.R. and D.A. de Vries 1963 Periodic temperature variations. *In: van Wijk W.R. (ed.) Physics of plant environment.* North Holland Publ. Co. Amsterdam.

Wyngaard, J.C. 1973 On surface layer turbulence. *In: D.A. Haugen (ed.): Workshop on Micrometeorology.* American Meteorological Society (Boston): 101-149.

Wyngaard, J.C. 1981 The effects of probe-induced flow distortion on atmospheric turbulence measurements. *Journal of Applied Meteorology* 20: 784-794.

Wyngaard, J.C. 1982 Boundary layer modelling. *In: F.T.M. Nieuwstadt and H. van Dop (eds.): Atmospheric turbulence and air pollution modelling.* - Reidel (Dordrecht): 53-83.

Wyngaard, J.C. 1984 Toward convective boundary layer parameterization: A scalar transport module. *Journal of the Atmospheric Sciences* 41:1959-1969.

Wyngaard, J.C. 1988 Flow-distortion effects on scalar flux measurements in the surface layer: implication for sensor design. *Boundary Layer Meteorology* 42: 19-26.

Zeller, K., W. Massman, D. Stocker, D.G. Fox, D. Stedman and D. Hazlett 1989 Initial results from the Pawnee eddy correlation system for dry acid deposition research. USDA Forest Service Research Paper RM-282.

Appendix A Stability functions used in the flux profile relationships

The Ψ functions used in equation 2.3.14 were taken from Paulson (1970) in unstable stratification, i.e. $L < 0$:

for wind speed profile or momentum;

$$\Psi_m = 2 \ln\left(\frac{1+X}{2}\right) + \ln\left(\frac{1+X^2}{2}\right) - 2 \arctan(X) + \frac{\pi}{2} , \quad A1$$

where:

$$X = \left(1 - \alpha_1 \frac{z}{L}\right)^{1/4}$$

for a scalar quantity;

$$\Psi_s = 2 \ln\left(\frac{1 + Y^2}{2}\right) , \quad A2$$

where:

$$Y = \left(1 - \alpha_2 \frac{z}{L}\right)^{1/4}.$$

Here we have used for $\alpha_1 = 22$ and $\alpha_2 = 13$ (Wieringa, 1980).

For stable stratification i.e. $L > 0$ the function given by Holtslag and De Bruin, (1988) were used:

for all quantities;

$$-\Psi = a \frac{z}{L} + b \left(\frac{z}{L} - \frac{c}{d} \right) \exp\left(-d \frac{z}{L}\right) + \frac{bc}{d} , \quad A3$$

with the constants, $a = 0.7$, $b = 0.75$, $c = 5$ and $d = 0.35$.

Appendix B Estimates and corrections of some terms in the energy balance of a maize crop and the underlying soil

The energy balance of a maize crop and the underlying soil during daytime (as given in equation 2.3.19) needs some more specification. Though the separate adjustments on terms in this balance are small, they in total account for about 10% of the net radiation and consequently should be used in making a correct energy balance. The assessments of the corrections were made by using days with a net radiation of about 300-600 W m⁻² around 1200 GMT. The sensible and latent heat storage terms of the in-canopy air were neglected, since these terms are each smaller than 1 W m⁻².

Heat storage in the soil

Because the soil heat flux is measured at a certain depth, the heat storage, G_s , in the layer above this measurement level should be taken into account. This G_s can be estimated with:

$$G_s = \rho_s d c_s \frac{\partial \langle T_s \rangle}{\partial t} \quad \text{B1}$$

where ρ_s is the density of the soil; here we took 1800 kg m⁻³ for sandy soil with 20% water content, Van Wijk and De Vries (1963),

c_s is the heat capacity of the soil i.e. 1180 J kg⁻¹ K⁻¹ (Van Wijk and De Vries, 1963),

d = depth of the heat flux measurement : 5 cm,

$\langle T_s \rangle$ is the depth averaged soil temperature.

On a sunny day the soil temperature change under a canopy with a LAI of about 3 can easily be 1 K in three hours. If we use this in B1 the G_s is 10 W m⁻², this is about 2-3% of the net radiation.

Heat storage in the biomass S_b

The heat storage term in the biomass S_b can be written as:

$$S_b = n M_p c_w \frac{\partial \langle T_b \rangle}{\partial t}$$

where n is the number of plants per m^2 , here 10 m^2 ,

M_p is the mass per plant, here taken as 0.5 kg per plant,

c_w is the heat capacity of water, i.e. $4200 \text{ J K}^{-1} \text{ kg}^{-1}$,

$\langle T_b \rangle$ is the averaged bio mass temperature.

From the temperature measured in the crop, used as an indicator of the temperature of the biomass and the infra-red measurements (Heiman radiometer) of the canopy foliage, the biomass temperature change was estimated at about 1 K per hour. The S_b then would be about 6 W m^{-2} or about 1-2% of the net radiation.

Energy used in the photosynthesis, Ph

The energy stored in the photosynthesis, Ph, can be estimated as a function of the flux of CO_2 , namely 3.2 W m^{-2} per $\text{g m}^{-2} \text{ h}^{-1} \text{ CO}_2$ (Thom, 1975). Our measurements showed a flux of CO_2 in the growing stage of the crop of about $7 \text{ g m}^{-2} \text{ h}^{-1}$ as a daytime value between 700-1600 UTC. This will use an energy of about 20 W m^{-2} , i.e. about 3-6% of the net radiation.

Appendix C The damping of the concentration fluctuations due to sampling through a tube

The measurements of the fluctuations of the ozone concentration are damped during the transport along the sampling tube before detection by the monitor. Philip (1963) gives an extensive discussion on this matter. We will give here only a brief summary with the practical formulations given in his paper.

The modification function, β , is defined as:

$$\beta(\omega) = \frac{N_x(\omega)}{N_0(\omega)} \quad \text{C1}$$

where ω is the frequency of the fluctuations in rad.s^{-1} ,

x is the distance in the tube from the inlet,

$N_0(\omega)$ the spectral density function of the variance of the concentration at the inlet,

$N_x(\omega)$ the same function as the latter but at point x .

So β gives the attenuation of the variance of the concentration at point x dependent on the frequency of the concentration fluctuation.

β can be approximated by :

$$\beta = \exp \left[\frac{-0.021 \omega^2 a^2}{D U} \right] \quad \text{C2}$$

for $\text{Re} < 1600$ (laminar flow), $\phi \gg Y/10$ and $\Pi < 10$,

where D is the molecular diffusivity for ozone,

U is the mean flow velocity

a is the tube radius

and the dimensionless parameters:

$$\phi = x/a$$

$$Y = U a / D$$

$$\Pi = \omega^2 a^2 / D$$

In our case: $a = 4.35 \text{ mm}$, $x = 1 \text{ m}$, $D = 1.4 \cdot 10^{-6} \text{ m}^2 \text{ s}^{-1}$,

$U = 3.53 \text{ m s}^{-1}$; this leads to

$$\phi = 459, Y = 549, \text{ Re} = 1000.$$

Because we have to deal with the influence of this damping on the flux of ozone or the fluctuations of ozone, the square root of β has to be taken. The square root of β as a function of the natural frequency, n , is plotted in figure C1. This damping causes a loss of fluctuations at high frequencies ($n > 2$ Hz). This would give a few percent decrease in the flux of a scalar using a normalized spectral density function of the flux of a scalar in unstable atmospheric conditions (taken from Kaimal et al. 1972).

Because this part of the spectrum would be filtered out due to the limited frequency response caused by the time constant of the monitor, the influence of the damping on the measured flux is nihil.

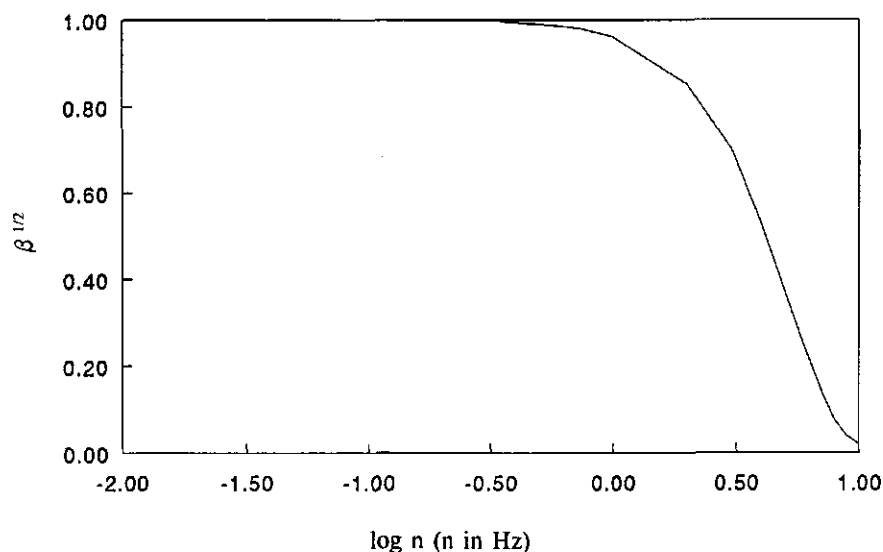


Figure C1 The damping of the fluctuations of ozone given by $\beta^{1/2}$, as a function of the logarithm of the frequency, n , of the fluctuations.

Appendix D Laboratory experiments on the soil resistance to ozone

A laboratory experiment was carried out to determine the soil resistance to ozone. The soil was put into a rectangular dish of 30x20 cm² and placed in a so-called gas exchange chamber. This is a well-ventilated chamber where, for instance the exchange of ozone and carbon dioxide with plants can be studied. A description of the chambers used can be found elsewhere, Aben (1990). The resistance as a function of the soil water content of the experiments carried out in two different chambers are depicted in figure D1. The soil resistance was about 100 s m⁻¹ at 15% soil water content. The resistance decreased to 75 s m⁻¹ at a 10% soil water content. From then on a more-or-less constant value was found.

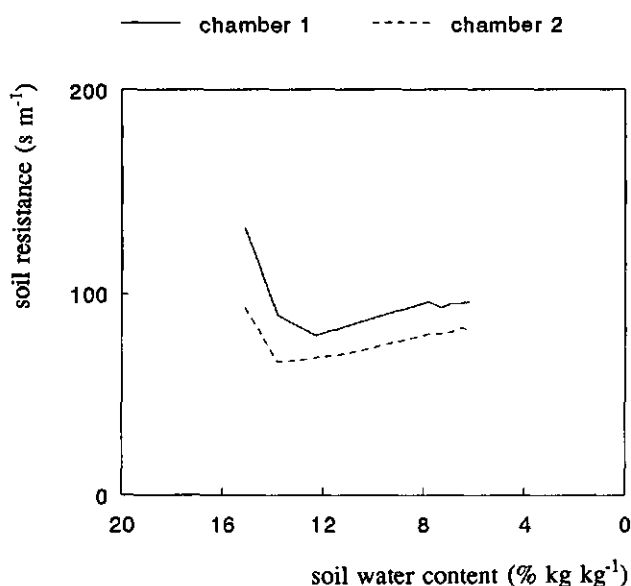


Figure D1 The soil resistance to ozone as a function of the soil wetness.

Appendix E The influence of chemical reactions on the flux of ozone

As was pointed out in section 2.1 a divergence of the flux of ozone can be induced due to the chemical reactions which produce or destroy ozone. No restrictions can be given *a priori* about the concentration levels of the three components to determine whether the flux of ozone is affected by chemical reactions.

The equations which describe the divergence of the fluxes of O_3 , NO_2 and NO under horizontally homogeneous and stationary conditions and with neglecting molecular diffusion read:

$$\frac{\partial \overline{w'O_3'}}{\partial z} = \frac{\overline{[NO_2]}}{\tau_a} - \frac{\overline{[NO]} \overline{[O_3]}}{\lambda} - \frac{\overline{[NO]'}[O_3]'}}{\lambda} \quad E.1a$$

$$\frac{\partial \overline{w'NO_2'}}{\partial z} = -\frac{\overline{[NO_2]}}{\tau_a} + \frac{\overline{[NO]} \overline{[O_3]}}{\lambda} + \frac{\overline{[NO]'}[O_3]'}}{\lambda} \quad E.1b$$

$$\frac{\partial \overline{w'NO'}}{\partial z} = \frac{\overline{[NO_2]}}{\tau_a} - \frac{\overline{[NO]} \overline{[O_3]}}{\lambda} - \frac{\overline{[NO]'}[O_3]'}}{\lambda} \quad E.1c$$

These equations can be closed by rewriting the fluxes with the use of gradient theory (see section 2.3.2). Then the equations E1 can be rewritten into a set of second-order differential equations and solved numerically (Fitzgerald and Lenchow, 1983; Kramm, 1989; Vilà-Guerau de Arellano et al., 1992).

Some runs were made with the model of Vilà-Guerau de Arellano et al., (1992) for half-hourly values on June 30 and September 22. The six boundary conditions used for these runs were the concentrations of O_3 , NO_2 and NO at 2.5 and 6.5 m respectively. The photodissociation constant, τ_a , was calculated as a function of the global radiation according to Bahe (1980). In figure E1a and b the ratio between the flux of ozone at 6.5 m and 2.5 m, $F_{S_1}(6.5m)/F_{S_1}(2.5m)$, is given. On June 30 this ratio varied around 0.95 with a range of 0.84-1.23. For September 22 this was 0.83, with a range of 0.63-1.02.

This means that a systematic deviation of 5-15% was present between the flux of ozone at 6.5 m and at 2.5 m. On a half-hourly basis these deviations can be much larger, i.e. up to 40%.

The influence of the chemical reactions is much smaller if the fluxes are determined with the gradient or modified Bowen ratio technique, because the lower concentration measurement is less affected by the chemical reactions. The fluxes derived with the profile techniques were determined at the geometrical height, which was about 3.9 m. This means that the deviation between the flux at the geometrical height and at 2.5 m was less than half of that depicted in figures E1a and b.

No systematic differences were found between the fluxes of ozone derived with the modified Bowen ratio technique and the eddy correlation technique, as pointed out in section 4.3. This as well indicated that chemical reactions did not severely influence the measurements of the flux of ozone, though the measurements were made at different heights: $z_m(\text{Bowen})=3.9$ m and $z_m(\text{eddy})=6$ m.

In figures E2a and b, the photostationary ratio, R, defined by:

$$R = \frac{1/\lambda \overline{[NO]} \overline{[O_3]}}{1/\tau_a \overline{[NO_2]}} \quad \text{E2}$$

is depicted for these runs. In equation E2 the covariance term $\overline{NO \cdot O_3}$ is neglected. If the triad of O_3 , NO_2 and NO is in equilibrium the value of R should be unity. From figures E2a and b it can be seen that this value varied around 0.8 with a range of 0.5-1. This indicates that no photostationary equilibrium existed and is shifted towards the production of ozone. A part of this deviation from the equilibrium can be explained by uncertainties in the reaction constants and the concentration measurements. But this systematic low value of R mainly indicated the influence of other chemical reactions; especially the reactions of hydrocarbons with NO leads to lower values in the numerator of this ratio. Generally, the ratio R at the top is larger than the R at the bottom. This indicates that when the triad of gases was transported downwardly it deviated more from the photostationary equilibrium.

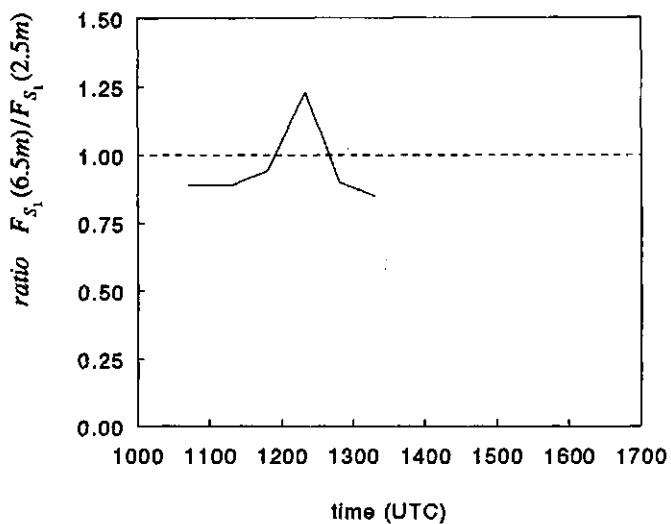


Figure E1a The ratio between the flux of ozone at 6.5 m and 2.5m as a function of time on June 30.

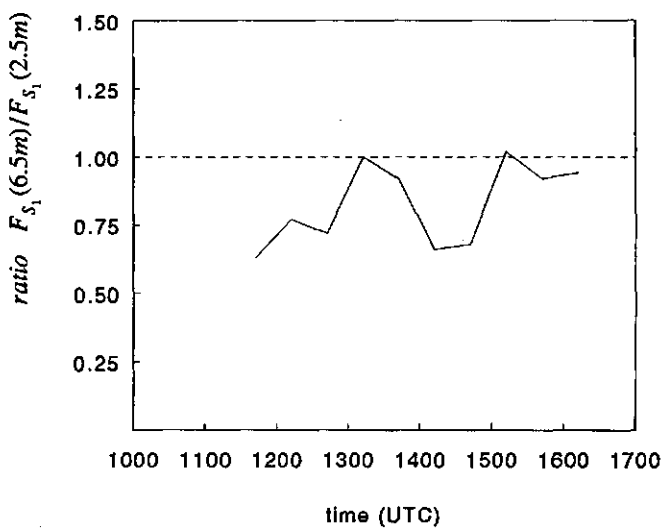


Figure E1b as a) but for September 22.

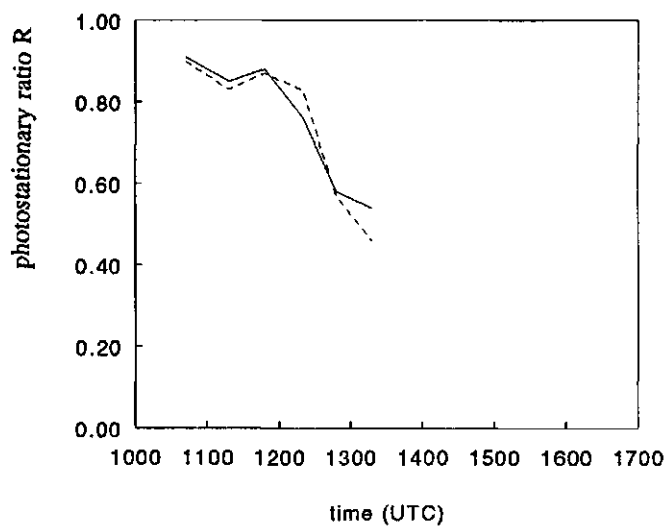


Figure E2a The photostationary state relation at 6.5 m and 2.5 m as a function of time, on June 30.

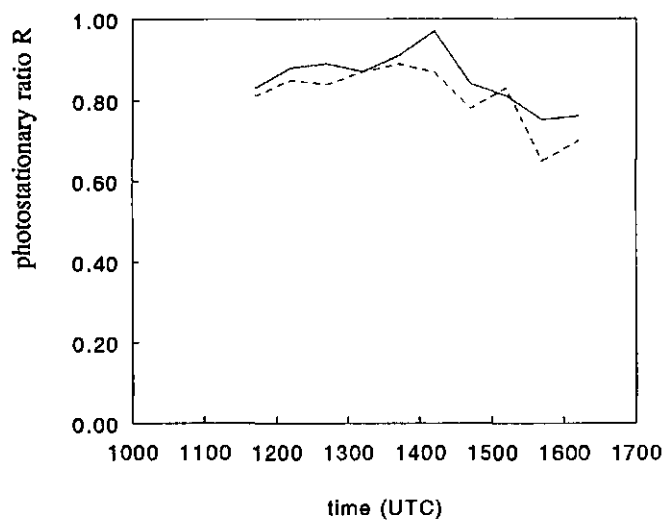


Figure E2b as a) but for September 22.

Appendix F The probable error method

The probable error method is based on the idea that errors in the variables are normally distributed and that there is some probability that errors in the different variables will compensate each other to limited degree (Fritschen and Gay, 1979).

In the application of the method, one has to differentiate the formula or model in question with respect to the separate variables and multiply each different differential by the error in the variable and take the square root of the sum of the squared products.

The error in the flux of ozone, F_{s_1} , derived with the profile technique (equation 2.3.9), can be estimated with:

$$\frac{\delta F_{s_1}}{F_{s_1}} = \left[\left(\frac{\delta u_*}{u_*} \right)^2 + \left(\frac{\delta s_{1*}}{s_{1*}} \right)^2 \right]^{1/2}, \quad \text{F1}$$

where δ is the absolute error in the variable.

The error in u_* and s_{1*} are estimated with (equations 2.3.14a and b):

$$\frac{\delta u_*}{u_*} = \left[\left(\frac{\delta \Delta U}{\Delta U} \right)^2 + \left(\frac{\delta \left(-\psi_m \left(\frac{z_2}{L} \right) + \psi_m \left(\frac{z_1}{L} \right) \right)}{\ln \frac{z_2 - d}{z_1 - d} - \psi_m \left(\frac{z_2}{L} \right) + \psi_m \left(\frac{z_1}{L} \right)} \right)^2 \right]^{1/2} \quad \text{F2}$$

$$\frac{\delta s_{1*}}{s_{1*}} = \left[\left(\frac{\delta \Delta S_1}{\Delta S_1} \right)^2 + \left(\frac{\delta \left(-\psi_s \left(\frac{z_2}{L} \right) + \psi_s \left(\frac{z_1}{L} \right) \right)}{\ln \frac{z_2 - d}{z_1 - d} - \psi_s \left(\frac{z_2}{L} \right) + \psi_s \left(\frac{z_1}{L} \right)} \right)^2 \right]^{1/2} \quad \text{F3}$$

The uncertainty in the above estimates caused by the uncertainty in d and κ are neglected because these uncertainties are systematic.

The error in the flux of ozone derived with the modified Bowen ratio technique (equation 2.3.23) can be estimated with:

$$\frac{\delta F_{S_1}}{F_{S_1}} = \left[\left(\frac{\delta \Delta S_1}{\Delta S_1} \right)^2 + \left(\frac{\delta (\Delta \rho_v + \alpha \Delta T)}{(\Delta \rho_v + \alpha \Delta T)} \right)^2 + \left(\frac{\delta A}{A} \right)^2 \right]^{1/2} \quad \text{F4}$$

In the calculations for table 4.2 it was used that the error in the stability functions due to an error in the Obukhov length was 5%. Along with the estimates on the errors in the differences from table 4.1 and an error in the available energy of 5%. If more than two measurement levels were used (such as for wind speed, temperature and humidity), the accuracies were increased by a factor of $(n-1)^{-1/2}$ where n is the number of levels.

The error in u_* and s_{*1} were 10-14% and 14-51%, respectively. This resulted in a total error of the flux of ozone determined with the profile technique of 20-53%.

The error in the flux of ozone determined with the modified Bowen ratio technique was 13-58%.

(The error in the sensible heat flux, H_s , and latent heat flux, LE, were estimated both at 9-28%, following the same approach).

Appendix G Estimates of the daytime deposition of ozone using idealized daytime patterns of deposition velocity and concentration

The daytime deposition of ozone, I_d , (defined in section 6.1), can also be written as:

$$I_d = \int_{t_1}^{t_2} V_d(t) S_1(t) dt \quad . \quad G1$$

Generally the V_d and S_1 show typical daily patterns with low values during night-time and maximum values around noon or somewhat later (see section 2.1 and 5.3.3 for typical concentration and surface conductance patterns). As an approximation these patterns can be represented in a very simplified way by, valid between sunrise t_1 and sunset t_2 :

$$V_d(t) = V_d(0) + V_d(\max) \sin \psi t \quad , \quad S_1(t) = S_1(0) + S_1(\max) \sin \psi t \quad , \quad G2$$

where the 0 denotes a initial value, for instance the night-time value, max denotes the maximum daily value and $\Psi = \pi/T$ with T daylight period of 12 hours. As a first approximation we assume that both variables have the same periodicity.

If these functions are used in equation G2, I_d becomes:

$$I_d = V_d(0) S_1(0) T + 2 V_d(0) S_1(\max) \frac{T}{\pi} + 2 V_d(\max) S_1(0) \frac{T}{\pi} + V_d(\max) S_1(\max) \frac{T}{2} \quad . \quad G3$$

The means of V_d and S_1 over period T are:

$$\bar{V}_d = V_d(0) + \frac{2}{\pi} V_d(\max) \quad , \quad \bar{S}_1 = S_1(0) + \frac{2}{\pi} S_1(\max) \quad . \quad G4$$

The $I_d(\text{est})$ calculated with equation 6.4 can be rewritten in:

$$I_d(\text{est}) = V_d(0) S_1(0) T + 2 V_d(0) S_1(\max) \frac{T}{\pi} + 2 V_d(\max) S_1(0) \frac{T}{\pi} + 4 V_d(\max) S_1(\max) \frac{T}{\pi^2} \quad .$$

G5

The difference between I_d and $I_d(\text{est})$ is:

$$I_d - I_d(est) = V_d(max) S_1(max) T \left(\frac{1}{2} - \frac{4}{\pi^2} \right) . \quad G6$$

As a first approximation for ozone we assume that the initial values $V_d(0)$ and $S_1(0)$ are zero (which is not a bad assumption for during the night), the ratio $I_d(est)/I_d = 0.8$. This means that an underestimate of the daily deposition of ozone is made by $I_d(est)$ due to loss in correlation between the deposition velocity and the concentration of ozone. If this correlation is 1 this loss is maximal 20%. This underestimate is smaller if the initial values, $V_d(0)$ and $S_1(0)$, are greater than zero.

Curriculum vitae

Wilhelmus Adrianus Johannes van Pul werd geboren op 22 september 1958 te Amstelveen. De lagere school doorliep hij eerst in Amstelveen en later in Voerendaal. Het Atheneum B-diploma werd behaald in 1976 aan de Scholengemeenschap Sintermeerten te Heerlen. In 1977 werd begonnen met een studie Milieuhygiëne, met als specialisatie Luchthygiëne en -verontreiniging, aan de Landbouw Universiteit te Wageningen. De doctorale fase bestond uit twee hoofdvakken: Luchthygiëne en -verontreiniging en Meteorologie. Dit laatste vak werd gedaan op het KNMI. In september 1984 behaalde hij het doctoraaldiploma.

Van november 1984 tot en met maart 1986 was hij werkzaam bij de firma Geosens als meteorologisch medewerker. In die functie zorgde hij voor meteorologische ondersteuning van de meetvluchten en verrichtte onderzoek in samenwerking met KNMI, RIVM en KEMA. Van april 1986 tot en met maart 1990 voerde hij het promotieonderzoek uit, waarvan hier verslag gedaan is.

Vanaf september 1990 is hij werkzaam bij het RIVM te Bilthoven als wetenschappelijk medewerker bij de afdeling Atmosferische Proces Studies (APS) van het Laboratorium voor Luchtonderzoek (LLO).